University of California, Irvine

CLLP the Wings of Inflammation:

An Investigation of Immunomodulatory Collagen-mimetic LAIR-1 Ligand Peptides

DISSERTATION

submitted in partial satisfaction of the requirements for the degree of

DOCTOR OF PHILOSOPHY

in Chemical and Biomolecular Engineering

by

Andrew T. Rowley

Dissertation Committee:

Professor Szu-Wen Wang, Co-Chair

Professor Wendy Liu, Co-Chair

Professor Elliot Botvinick

2022

Copyright Page

Dedication

To my incredible Parents; without your unending love and support, none of this would have been possible. Thank you both.

Table of Contents

List of Figures

List of Abbreviations

CLLP	collagen-mimetic LAIR-1 ligand peptide
LAIR-1	leukocyte-associated immunoglobulin-like receptor-1
BMDM	bone marrow derived macrophages
DC	dendritic cell
BMDC	bone marrow derived dendritic cells
ECM	extracellular matrix
ITIMs	immune receptor tyrosine-based inhibitory motifs
C1q	complement component 1q
SLE	Systemic Lupus Erythematosus
SH2	Src Homology 2
SHP-1/2	H2 domain-containing protein tyrosine phosphatase-1/2
Csk	C-terminal Src kinase
TLRs	toll like receptors
Arg	arginine
Glu	glutamic acid
Trp	Tryptophan
GPP	Glycine-Proline-Proline
LPS	lipopolysaccharide
IFN γ	interferon gamma
IL-13	interleukin 13
IL-4	interleukin 4

TNFα	tumor necrosis factor alpha
KD	knockdown
NT	non-targeted
siRNA	small interfering or silencing ribonucleic acid
PLGA	poly(lactic-co-glycolic acid)
MP	microparticles
NP	nanoparticles
E2	protein nanoparticle derived from E2 subunit of pyruvate dehydrogenase
SRA-1	scavenger receptor class A – 1
MHC I	major histocompatibility complex class I
MHC II	major histocompatibility complex class II
SIINFEKL	peptide epitope in ovalbumin antigen
FITC	fluorescein isothiocyanate
PE	phycoerythrin
PECy7	phycoerythrin cyanine (tandem fluorophore)
APC	Allophycocyanin
AF488	Alexa Fluor 488

Acknowledgements

This work was supported by the National Institutes of Health (R21EB022240 and R01EB027797) and an NSF Graduate Fellowship awarded to Andrew T. Rowley

Thank you to Dr. Wang and Dr. Liu for mentoring and educating me throughout my PhD experience

Thank you to my friends and colleagues for the support, help and good times.
Especially: Bryce Wilson, Aaron Ramirez, Enya Li, Natalie Wu-Woods, Dr. Vijaykumar Meli, Dr. Praveen Veerasubramanian, Dr. Raji Nagalla, Dr. Esther Chen

Thank you to the love of my life Jade Talley for keeping my mental health afloat and building a home with me here in California

Vita

Education:

University of California, Irvine Irvine, Ca 2017 – 2022
PhD in Chemical and Biomolecular Engineering:
Master's in Chemical and Biomolecular Engineering: December 2018
Maintained a 3.9 GPA average

University of Illinois Champaign, IL 2012 – 2016
Bachelor's in Chemical Engineering:
Maintained a 3.4 GPA average

Publications & Awards:

Wang & Liu Research Groups 2/18-current

- Co-Author Publication: V.S. Meli, A. T. Rowley, P.K. Veerasubramanian, S.E. Heedy, A.F. Yee, W.F. Liu, and S-W Wang, Role of Substrate Stiffness and Collagen Interactions in Macrophage Immunomodulation, in preparations for *Biomaterials Science.,* 2022

- First author publication: Rowley, A. T., Vijaykumar M. S., Wu-woods N.J., Chen E. Y., Liu W. F., Wang S.W., Effects of Surface-Bound Collagen-Mimetic Peptides on Macrophage Uptake and Immunomodulation., *Front. in Bioeng. and Biotec.*, 2020. https://doi.org/10.1021/acscatal.6b02475

- Awarded the NSF Graduate Research Fellowship based on original immunotherapy drug delivery proposal

- Published Review article as first author for a special issue journal: A. T. Rowley, R. R. Nagalla, S.-W. Wang, W. F. Liu, "Extracellular Matrix-Based Strategies for Immunomodulatory Biomaterials Engineering", Adv. Healthcare Mater. 2019, 1801578. https://doi.org/10.1002/adhm.201801578

Li Research Group 9/17-1/18

- Co-author Publication: Black WB, King E, Wang Y, Jenic A, Rowley AT, Seki K, Luo R, Li H, Engineering a Coenzyme A detour to expand the product scope and enhance the selectivity of the Ehrlich pathway.*ACS Synth. Biol.* 2018.

Flaherty Research Group 8/15-12/16

- Co-author Publication: Moteki, T.; Rowley, A.; Flaherty, D. Self-Terminated Cascade Reactions That Produce Methylbenzaldehydes From Ethanol. *ACS Catalysis* 2016, *6*, 7278-7282.

- Co-author Publication: Moteki, T., Rowley, A. T., Bregante, D. T. and Flaherty, D. W. (2017), Formation Pathways toward 2- and 4-Methylbenzaldehyde via Sequential Reactions from Acetaldehyde over Hydroxyapatite Catalyst. ChemCatChem. doi:10.1002/cctc.201700151

ABSTRACT OF THE DISSERTATION

CLLP the Wings of Inflammation:
An Investigation of Immunomodulatory Collagen-mimetic LAIR1 Ligand Peptides

By
Andrew T. Rowley

Doctor of Philosophy in Chemical and Biomolecular Engineering

University of California, Irvine, 2022
Professor Szu-Wen Wang, Co-Chair
Professor Wendy Liu, Co-Chair

Persistent inflammatory stimuli can result in chronic inflammation and ultimately disease states such as, rheumatoid arthritis and Alzheimer's Disease. Typical therapeutic approaches have failed to resolve chronic inflammation in patients. Therefore, this proposal will investigate an alternative strategy of immunomodulatory biomaterials, specifically a deliverable collagen-mimetic peptide that has been engineered as a high affinity ligand for the inhibitory immune receptor LAIR-1, named Collagen-mimetic LAIR-1 Ligand Peptide (CLLP). The hypothesis of this research is that interactions between CLLP and LAIR-1 expressing immune cells, be it through functionalized biomaterials or particle delivery vehicles, will result in suppressed inflammatory activation, furthermore phagocytes seeded on CLLP surfaces will experience increased uptake (dictated in part by the extent of LAIR-1 expression). When investigating CLLP's effect on inflammatory activation of macrophages and dendritic cells it was observed that LAIR-1 expressing cells were significantly inhibited in their inflammatory activation when seeded onto CLLP surfaces. In contrast, when investigating cells that had naturally low LAIR-1 expression or cells with significantly reduced LAIR-1 expression, via siRNA knockdown, CLLP failed to reduce inflammatory activation. Furthermore, both macrophages and dendritic cells experienced increases in uptake on CLLP functionalized surfaces. The results of these uptake

experiments also strongly suggest that LAIR-1 is inhibitory to uptake and the observed CLLP induced increases in uptake are not due to LAIR-1 signaling. When dendritic cells are seeded on CLLP surfaces and stimulated with antigen functionalized nanoparticles, the cells exhibit increased antigen presentation. When CLLP was delivered to cells via nanoparticles it successfully inhibited macrophage activation. Interestingly functionalizing nanoparticles with CLLP significantly reduced the uptake of said particles by LAIR-1 expressing phagocytes. The immunomodulatory strategy of CLLP functionalization could potentially be broadly applied, for example toward the development of device coatings, anti-inflammatory particle-based therapeutics, and/or integrated biomaterials.

Chapter 1: Introduction

Scope of Chapter 1: Background information covering the Inflammatory response, key cellular players in the development of chronic inflammation, and a potential therapeutic strategy utilizing an inhibitory receptor and its collagen ligands.

Chapter 1.1: Inflammatory Response

Chapter 1.2: Chronic Inflammation & Key Immune Cells

Chapter 1.3: Leukocyte Associated Immunoglobulin-like Receptor 1

Chapter 1.4: Collagen the LAIR-1 Ligand

Chapter 1.5: CLLP

Portions of this introduction have been slightly modified and published as: A.T. Rowley, R.R. Nagalla, S.W. Wang, W.F. Liu, Extracellular Matrix-Based Strategies for Immunomodulatory Biomaterials Engineering, Advanced Healthcare Materials 8(8) (2019).

Chapter 1.1: Inflammatory Response

Innate immunity plays a predominant role in the development and resolution of inflammation. Normally the first facet of host immunity to begin immediately after an inflammatory event is the cascade of complement proteins. Activation of complement leads to robust and efficient proteolytic cascades, which terminate in opsonization and lysis of the pathogen as well as in the generation of the classical inflammatory response through the production of potent proinflammatory molecules and further subsequent activation of innate immune cells [1]. Simultaneously resident innate immune cells, predominantly resident macrophages and monocytes respond to the inflammatory event by producing and emitting pro-inflammatory cytokines and chemokines into the microenvironment. Damaged epithelial and endothelial cells, at sites of tissue injury, can also release factors that trigger complement cascade, along with chemokines and growth factors[2]. These inflammatory constituents in conjunction with the pro-inflammatory cytokines/chemokines released by resident innate immune cells cause the recruitment, invasion, and pro-inflammatory activation of reinforcement immune cells. The first cells that are attracted via chemokines are neutrophils, followed by monocytes, and then lymphocytes (natural killer cells [NK cells], T cells, and B cells), and finally mast cells[2]. Monocytes can further differentiate into macrophages and dendritic cells once recruited via chemotaxis into damaged tissues. Alterations in healthy inflammation-mediated immune cell functions are associated with many diseases, including cancer, chronic inflammatory diseases, and autoimmune and degenerative diseases[3].

The period between peak inflammatory cell influx and the clearance of these cells from the tissue site and the restoration of functional homeostasis is classically defined as resolution. Resolution is a complex, regulated cascade of processes that begins when the danger signals that

triggered the inflammatory response are neutralized. Subsequently, the synthesis of pro-inflammatory mediators is suspended, and any such mediators/chemokine gradients that still remain are catabolized and/or diluted over time, stopping further cellular recruitment. After recruitment is stopped and pro-inflammatory mediators are neutralized, previously recruited immune cells are cleared from the tissue. Some recruited immune cells do re-enter systemic circulation, but many of the infiltrated immune cells undergo local apoptosis or necrosis, followed by efferocytosis (uptake) by recruited monocyte-derived macrophages. Once the uptake of dead and/or apoptosed cells is completed, macrophages can leave the previous site of inflammation by lymphatic drainage[4].

Chapter 1.2: Chronic Inflammation & Key Immune Cells

Typically, the process of acute inflammation and resolution occurs anywhere between a few hours and several days depending on the inflammatory event. However, dysregulation of either the acute inflammatory response and/or the resolution process, can lead to uncontrolled chronic inflammation that can last weeks or even years. Acute inflammation is more uniform histologically than chronic inflammation. In general, chronic inflammation can be characterized by the sustained recruitment, infiltration and activation of predominantly monocytes as well as lymphocytes, during the resolution process (e.g. the proliferation of fibroblasts, blood vessels and connective tissues after injury). Essentially chronic inflammation is the simultaneous destruction and healing of the local tissue. However, with an uncontrolled inflammatory response, tissue destruction occurs faster than cellular regeneration, causing pathological fibrosis. Eventually, the tissue's function is reduced or even lost completely. Chronic inflammation plays a key role in the development and progression of many chronic diseases

including, but not limited to, autoimmune diseases, metabolic disorders such as atherosclerosis and obesity, fibrosis, arthritis, Alzheimer's and cancer[5-8].

Macrophages are monocyte derived cells are critical cellular components in the initiation and development of chronic inflammatory responses. Distinct phenotypic populations of macrophages (e.g. previously referred to as M0, M1 and M2) regulate the chronic inflammatory environment through the production of an immense number of soluble factors (known as cytokines and chemokines) that modulate and direct cellular behavior in the local microenvironment[9, 10]. When trying to induce resolution of an inflammatory event it is important to transition macrophages away from inflammatory phenotypes (e.g. M1) and towards healing phenotypes (e.g. M2) in order direct surrounding cells towards healing behaviors. Macrophages are also the main driving force in the clearance phase of acute inflammation that helps facilitate the transition towards resolution. Generally, when trying to quell inflammation it is desirable to reduce the inflammatory activation of macrophages while directing their behavior towards increased uptake [10].

Another monocyte derived phagocyte critical to the development of resolution is the dendritic cell (DC). DCs initiates and directs the adaptive immune response to chronic inflammatory events and/or inflammatory materials. Previous research has provided evidence that DC activation is critical to the resolution of chronic inflammation[11-16]. After activation, DCs uptake antigenic materials, transgress to the lymph nodes from the site of inflammation and communicate with the adaptive immune system (T cells and B cell) in order to facilitate sustained adaptive immunity[17]. Therefore, both inflammatory activation and uptake by DCs is critical to the development of sustained immunity and ultimately resolution of the inflammatory event.

Successful therapeutics would target innate immune cell phagocyte activation and phenotype modulation with the goal of promoting resolution-based phenotypes and cellular behaviors (such as uptake). One method to achieve these goals would be to target Inhibitory Immune Receptors (IIRs) which naturally function in conjunction with their ligands to tightly regulate the inflammatory response. IIRs are well-established negative regulators of the immune response, with the inhibitory signal typically transduced through immunoreceptor tyrosine-based inhibitory motifs (ITIMs) located in the intracellular tail of the receptor with the consensus sequence V/L/I/SxYxxV/L/I [18]. An accumulating number of inhibitory receptors have been identified on phagocytes, and emerging evidence suggests that they play an important regulatory role in the activation and functionality of these leukocyte populations[19, 20]. The ideal therapeutic IIR target would be a receptor that is highly expressed on target immune cell types, particularly macrophages, which inhibits inflammatory activation, with a unique deliverable ligand. Using these criteria, therapeutic IIR targets were narrowed down to one highly and unanimously expressed inhibitory receptor, known as the Leukocyte Associated Immunoglobulin-like Receptor 1 (LAIR-1).

Chapter 1.3: Leukocyte Associated Immunoglobulin-like Receptor 1

LAIR-1 is a transmembrane glycoprotein with a cytoplasmic tail containing two immune receptor tyrosine-based inhibitory motifs (ITIMs) and is expressed in both mice and humans on a majority of immune cell types, including natural killer cells, T cells, B cells, monocytes/macrophages, some dendritic cell types, eosinophils, basophils, and mast cells[21]. Upon LAIR-1 binding and activation, the ITIMs in the cytoplasmic tail recruit two protein tyrosine phosphatases, SHP-1 and SHP-2 (but not SHIP), as well as C-terminal Src kinase, all of which interacted with the ITIMs of LAIR-1 via a SH2 domain [21-23]. SHP-1 and SHP-2

themselves have been implicated in playing a regulatory role for a wide range of immune cell functions. For example, in phagocytic cells, SHP-1 and SHP-2 and have been shown to directly affect cellular signaling pathways, such as the signaling pathways initiated by Fc receptors, TLRs, cytokine receptors, chemokine receptors and integrins [20]. While SHP-1 is widely accepted as a negative regulator of signaling events, SHP-2 is thought to also positively promote signaling as well as inhibit it [24]. Specifically, researchers have observed that mice with SHP-2 deficiencies in the T-cell lineage clearly show decreases in TCR/CD3-driven proliferation and IL-2 production as well as decreased induction of the activation markers CD69 and CD25 [25]. LAIR-1 signaling/inhibition can also occur independently of phosphatases through SH2 containing C-terminal Src kinase (Csk). It has been shown that LAIR-1 still had an inhibitory effect on BCR-induced calcium mobilization in phosphatase-deficient DT40 cells and that LAIR-1intracellular ITIMs bound Csk in a phosphorylation dependent manner [23]. Overexpression of Csk negatively regulates the signaling of both TCR and FcεRI, while down-regulation of Csk lowers the threshold of TCR signaling [26-28]. Mice in which the Csk gene is deleted in granulocytes develop multifocal inflammation and are hyperresponsive to LPS, indicating an essential role for Csk in setting an activation threshold in granulocytes [29]. The complex and varied regulatory roles of SHP-1, SHP-2, and Csk, which are recruited by the ITIMs of the intracellular domain of LAIR-1, imply that the biological role of LAIR-1 and its effects on immune cell behaviors is complex and multifaceted.

It has been shown that the binding of LAIR-1 inhibits the activation of immune cells including, T-cells, B-cells, NK cells, dendritic cells and monocytes/macrophages, although interestingly there is also evidence showing LAIR-1 is required in activation of Th17 T cell response [21, 30-35]. LAIR-1 and the complement protein C1q are also implemented in self-

tolerance and the development of autoimmune responses, particularly when it comes to the clearance of apoptotic cells. Apoptosis is a mechanism for programmed cell death that results in the surface display of normally internalized proteins, which signals the immune system to initiate uptake. Besides uptake signal proteins, apoptotic cell surfaces have autoantigens, which induce an immune response that can be harmful to healthy tissue if they accumulate to high concentrations[36]. Low apoptotic cell clearance has been linked to autoimmune diseases such as Systemic Lupus Erythematosus (SLE) [37, 38]. Complement protein C1q plays a pivotal role in the uptake of apoptotic cells. C1q globular head regions bind to apoptotic cell membranes, tagging apoptotic cells for uptake, while C1q's collagen-domain-containing tails bind receptors on the surface of innate immune cells. The multiple C1q tails can simultaneously bind more than one receptor on immune cells (such as LAIR-1) eliciting a dynamic immune response [39-43]. Apoptotic bodies have been demonstrated to elicit anti-inflammatory effects on macrophages, with LAIR-1 being implicated in the mechanisms driving these inhibitory results [39, 44-48]. Furthermore, using LAIR-1 knockout mice and/or cells, along with LAIR-1 antibodies, it has been shown that LAIR-1 expression and/or engagement significantly affects immune cell phenotype and function, particularly in regards to inflammatory responses, which varies depending on immune cell type and phenotypic state [49, 50].

Given its expression on most immune cells, its inhibitory properties and regulatory role, LAIR-1 is thought to be a potential therapeutic target for inflammatory diseases such as fibrosis and arthritis, as well as diseases such as acute myeloid leukemia and other cancers [35, 51-53]. For example, Kang et al. suggested that intervention in LAIR-1 signaling may lead to successful treatment of acute myeloid leukemia, as their data showed LAIR-1 knockdown abolishes leukemia development but does not affect normal hematopoiesis of stem cells. It has also been

shown that LAIR-1 antibodies significantly reduce collagen induced autoimmune arthritis when compared to Ig and no treatment controls in mice [54]. Furthermore, as mentioned previously, LAIR-1 plays a role in self-tolerance and the clearance of apoptotic cells and is thought to be a potential therapeutic target in treatment of systemic lupus erythematosus (SLE). It has been observed by Bonaccorsi et al, that Plasmacytoid dendritic cells (pDCs) isolated from peripheral blood of systemic lupus erithematosus (SLE) patients express lower levels of LAIR-1 than pDCs from healthy donors [55].

Chapter 1.4: Collagen the LAIR-1 Ligand

LAIR-1 recognizes ligands that, in part, contain the triple helical regions of collagen-like domains, characterized by the repeating glycine-proline-hydroxyproline sequences but not glycine-proline-proline sequences [33, 56]. The mechanism of LAIR-1 binding to human collagen III is likely conserved in humans and mice. Structure and mutagenesis studies have shown that the amino acids of the LAIR-1 receptor that bind collagen (Arg59, Glu61, and Trp109) are conserved in over 9 different species, including the human and mouse homologues [57], and translates to nearly identical binding affinities with human collagen III [31, 32]. The unique role of LAIR-1 and collagen in immune regulation is thought to influence multiple physiological processes including inflammation, wound healing, as well as progression of cancer and other disease states [19, 21, 58, 59].

The extracellular matrix protein collagen plays a complex multifaceted role in regulating cells in the immune system and maintaining homeostasis. It is the most abundant protein in the human body and comes in 29 different varieties, all containing the conserved triple helix suprastructure stabilized by repeated amino acid sequences of glycine-X-Y, where X and Y can

be any amino acid but are often proline and hydroxyproline, respectively [60]. Specific regions of collagen are recognized as ligands by different receptors expressed by immune cells; these receptors include integrins, discoid domain receptors, immunoglobulin-like receptors, and mannose receptors, resulting in diverse immunomodulatory responses [61, 62]. Interaction with natural collagen matrices, reconstituted collagen hydrogels, and/or collagen peptides has been shown to increase cellular adhesion and integrin expression in both adaptive and innate immune cells, as well as actively modulate the phenotype of immune cells in a variety of ways, affecting a range of immune cell functions [63-66]. More specifically, adhesion to collagen generally reduces the inflammatory response of macrophages and is thought to have a critical regulatory role in setting the threshold for innate immune responses in tissue [59]. Furthermore, it has been observed that tumor cells upregulate the deposition of collagen in the tumor-microenvironment, and it has been hypothesized that this increase collagen deposition is a mechanism used by tumor cells to suppress and evade immune cell detection via collagen induced LAIR-1 inhibitory signaling [59, 67].

Chapter 1.5: CLLP

To improve receptor targeting, several studies have identified high LAIR-1 affinity collagen segments (and/or peptides) and characterized their role in T-cell activation and cellular adhesion [33]. A collagen III peptide, referred to here as LAIR-1 ligand peptide (CLLP), in particular has high affinity for LAIR-1, exemplified by the greatest inhibition of CD3-induced T cell activation as well as significant inhibition of FcεR1-induced degranulation of mast cells [33]. The sequence of CLLP is C(GPP)5GAOGLRGGAGPOGPEGGKGAA GPOGPO(GPP)5-NH2 (where “O” is hydroxyproline). The CLLP sequence includes the collagen III synthetic peptide III-30 sequence known to bind LAIR-1, two (GPP)5 flanking regions to ensure triple

helical conformation. CLLP interaction with LAIR-1 requires a trimeric structure of the peptide[57] and the triple-helical folding of the CLLP peptides were confirmed via circular dichroism. A N-terminal cysteine for surface functionalization, using thiol chemistries, has also been synthesized into the peptide. This engineered cysteine handle allows the CLLP peptide to be utilized as a deliverable therapy on micro- and nanoparticles, as well as functionally incorporated into/onto biomaterials for engineered immunomodulatory purposes.

Although LAIR-1 has been identified as an inhibitory membrane-bound receptor in the regulation of the immune system, the application of its ligands in biomaterial design has not been previously investigated. This dissertation will therefore provide evidence towards the feasibility of using collagen mimetic LAIR-1 ligand peptides (CLLPs) to decrease inflammatory activation, increase uptake and promote resolution, as well as demonstrate other potentially beneficial biomedical applications of the immunomodulatory biomaterial CLLP.

Chapter 2: Effect of CLLP Functionalized Surfaces on Inflammatory Activation

Scope of Chapter 2: The effects of CLLP (a LAIR-1 targeting, collagen mimetic peptide) on bone-marrow-derived-monocyte-differentiated macrophage/dendritic cell, inflammatory activation and the importance of LAIR-1 in facilitating these effects.

Chapter 2.1: In vitro experimental system design and characterization of LAIR-1 expression in bone marrow monocyte-derived cell culture populations.

Chapter 2.2: Study the effects of CLLP on LPS induced proinflammatory cytokine emission by BMDMs and determine the role of LAIR-1 using siRNA knockdown

Chapter 2.3: Study the effects of CLLP on LPS induced expression of proinflammatory surface markers by BMDCs and determine the role of LAIR-1 using siRNA knockdown

Chapter 2.4: Chapter 2 conclusion

Portions of this chapter have been slightly modified and published as: A.T. Rowley, V.S. Meli, N.J. Wu-Woods, E.Y. Chen, W.F. Liu, S.W. Wang, Effects of Surface-Bound Collagen-Mimetic Peptides on Macrophage Uptake and Immunomodulation, Front Bioeng Biotechnol 8 (2020) 747.

Chapter 2.1: **In Vitro Experimental System Design**

In order to investigate the immunomodulatory potential of CLLP an in vitro model was developed that ensured cell-peptide interactions in a controlled, consistent, reproducible manner. Therefore, CLLP functionalized culture well surfaces via maleimide - cysteine thiol chemistry, were used. Specifically, maleimide activated clear 8-well strip plates (purchased from Pierce™) were functionalized with either cysteine or CLLP (A.1.0.1).

All functionalization chemistry was performed under sterile conditions. CLLP size and structure was confirmed using Mass Spectroscopy and Circular Dichroism (A.1.0.2), respectively, for each lot of peptides purchased before beginning experiments. A CLLP peptide biotinylated at the C-terminus was used to quantify the extent of surface functionalization (A.1.0.3). This CLLP surface saturation concentration was further supported with a functional inhibition assay described in the appendix (A.1.0.4) (A.1.0.5)

This dissertation focuses on two cell types, Macrophages and Dendritic Cells. It was decided that the most physiologically relevant way to study these two cell types in vitro would be to differentiate them from bone marrow derived monocytes. The procedure for both cell types (i.e. bone-marrow derived macrophages/ dendritic cells or BMDMs / BMDCs) are described in the appendix (A.1.0.6). Before beginning experiments, I investigated expression of LAIR-1 on both BMDMs and BMDCs. It has been shown that BMDMs are a high LAIR-1 expressing homogenous cell population [50]. In contrast, others have reported that BMDCs have two subpopulations with heterogeneous LAIR-1 expression; BMDCs that do not express F4/80 show little or variable LAIR-1 expression, and BMDCs that do express F4/80 demonstrate significantly greater LAIR-1 expression [50, 68, 69]. My data is also consistent with these

finding (Figure 1A), showing a significantly greater positive expression for LAIR-1 by BMDMs than BMDCs and describing a positive correlation between F4/80 expression and LAIR-1 expression by BMDCs. F4/80+ BMDCs strongly express LAIR-1 (4.75x104 ± 4.77x103 MFI of LAIR-1 signal), whereas F4/80- BMDCs had significantly lower LAIR-1 expression ($1.6x10^4$ ± $7.31x10^3$ MFI of LAIR-1 signal) (Figure 1B). The response of both BMDMs and BMDCs on experimental surfaces (with and without LAIR-1 ligand, CLLP) was then subsequently investigated using cells that showed both high (F4/80+ & BMDMs) and low (F4/80-) expression levels of LAIR-1 (Figure 1C). It is important to note that F4/80 is known as a macrophage marker and F4/80+ BMDCs are more macrophage-like cells than classical dendritic cells, whereas F4/80- BMDCs are more representative of classical dendritic cells in vivo [70, 71]. The BMDM population did not require subpopulation analysis due to its homogenous expression of LAIR-1.

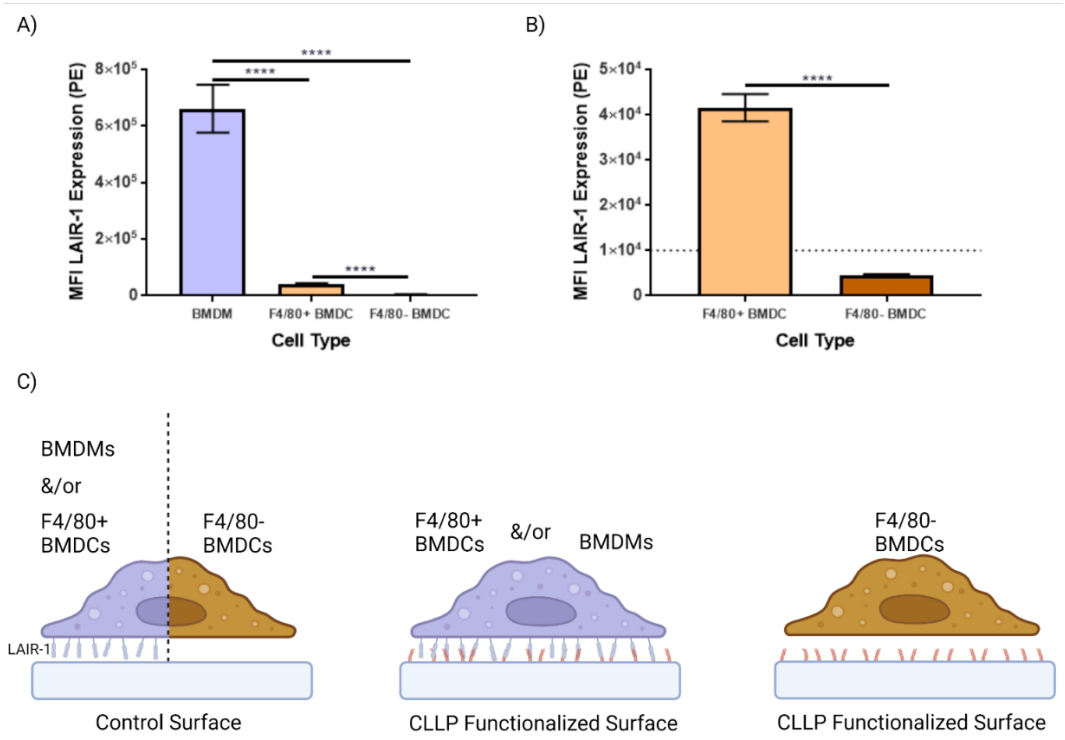

Figure 1: LAIR-1 expression of cells of interest and in vitro experimental system (A) Quantitative analysis of compiled flow data describing the extent of LAIR-1 expression by BMDMs and each BMDC F4/80 subpopulation N≥3. (B) Focused quantitative analysis of compiled flow data describing the extent of LAIR-1 expression by BMDC F4/80 subpopulation N≥3. The antibody panel was as follows: CD11c (FITC), MHCII (PE-Cy7), LAIR-1 (PE), F4/80 (APC). 10^4 is roughly the baseline fluorescent intensity for the LAIR-1 (PE) gates, meaning if the intensity is sufficiently greater than this value it is considered positive for expression, fluorescent intensities at this value or lower are considered negative for the expression of the intended marker. (C) Graphic representing general experimental systems, showing both BMDMs and BMDCs seeded on CLLP functionalized surfaces and/or control surfaces (Cysteine functionalized surfaces, and unfunctionalized maleimide surfaces), depicting hypothesized LAIR-1 engagement.

The initial experiments done with CLLP functionalized surfaces were designed to answer the questions proposed in chapter 2, namely, confirm the hypothesized anti-inflammatory effects of CLLP on LPS driven activation of both macrophages and dendritic cells. Furthermore, we aimed to investigate the specific role that LAIR-1 plays in the observed immunomodulatory effect of the engineered peptide on LPS activation. As mentioned above there are numerous literary sources describing the inhibitory effect of LAIR-1 on immune cell activation, therefore it was hypothesized that LAIR-1 : CLLP interactions would result in inhibition of LPS activation in by LAIR-1 expressing BMDMs and BMDCs.

Chapter 2.2: **CLLP Functionalized Surfaces Reduce the Production of Pro-Inflammatory Cytokines by Activated BMDMs via the Target Receptor LAIR-1**

I first investigated CLLP modulated LPS activation in macrophages. As described earlier, one of the main functions of macrophages in vivo is cytokine/chemokine production and macrophages play a predominant role in initiating and maintaining inflammatory microenvironment in the tissue via cytokine production. Therefore, it was decided that inflammatory cytokines, such as TNF-α, were to be the marker used to quantify BMDM activation. The experimental system/protocol used to study the effects of CLLP on LPS stimulated activation of macrophages is described in the appendix (A.1.0.5). The results of these experiments showed significant reduction in TNF-α emission on CLLP surfaces when compared to control surfaces (Figure 2). CLLPs effect on other proinflammatory markers such as RANTES (regulated upon activation, normal T-cell expressed, and secreted; CCL-5), MIG (monokine induced by gamma interferon; CXCL-9), MIP-1α (macrophage inflammatory protein-1α; CCL-3), MIP-1β (CCL-4), and MIP-2 (CXCL-2), were investigated by Yoon et al, and found to share a similar trend with TNF-α, significantly decreased production on CLLP surfaces when compared to control surfaces [72]. This prior investigation had also showed that an irrelevant control peptide (e.g., an ovalbumin epitope) that was conjugated to the surface elicited similar TNFα levels as those observed for maleimide and cysteine-conjugated control surfaces [72]. The results of these experiments clearly showed that CLLP functionalized surfaces decreased the activation of macrophages confirming the hypothesized inhibitory effects of the engineered peptide.

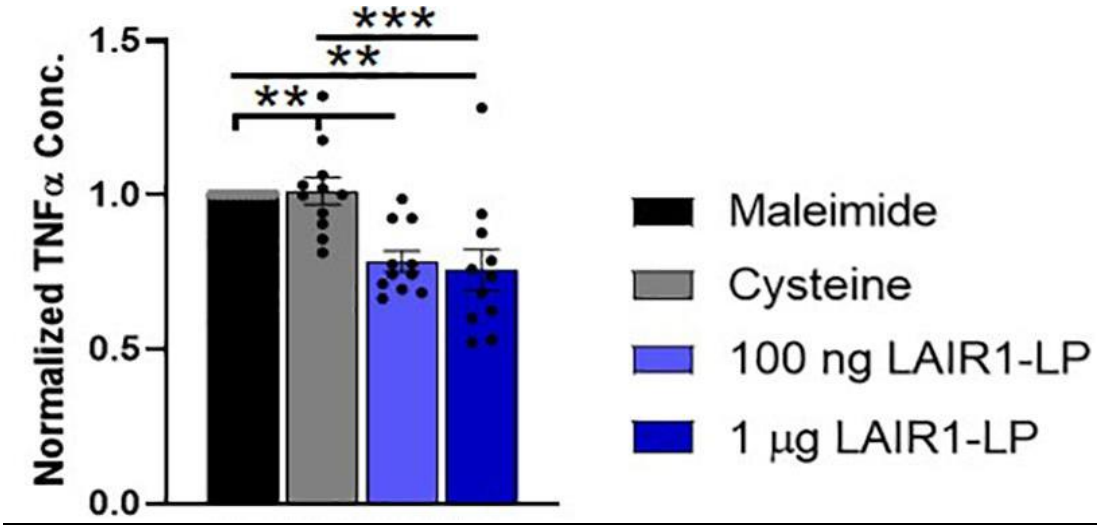

Figure 2: Normalized TNFα concentration, determined via ELISA, produced by BMDMs seeded on CLLP surfaces, compared to control surfaces, when stimulated with 0.3 ng/mL LPS and 0.3 ng/mL IFNy. Values reported are average ± S.E.M., with N=11 independent biological replicates, and the dots are individual data points. Statistical significance was determined by one-way ANOVA with Tukey's post hoc test (*$p < 0.05$, **$p < 0.01$, ***$p < 0.001$)

Next, we wanted to confirm that the observed anti-inflammatory effects of CLLP on LPS stimulated BMDMs was a result of the targeted LAIR-1 : CLLP interaction. In order to confirm that LAIR-1 engagement was responsible for the observed inhibition of macrophage activation on CLLP functionalized surfaces, LAIR-1 knockdown experiments were conducted. Knockdown of LAIR-1 gene was performed by nucleofection (4D-Nucleofector system, Lonza) using siRNAs (siGENOME siRNAs, Dharmacon) (A.1.1.0). Extent of LAIR-1 knockdown as well as LAIR-1 expression on the various surfaces was determined via qRT-PCR gene expression analysis. RNA was isolated from the BMDMs using TRI Reagent (Sigma T9424) following the manufacturer's protocol (A.1.1.1)(A.1.1.2)(A.1.1.3).

LAIR-1 knockdown (KD) was effective and decreased LAIR-1 gene expression by 90% when compared to the non-target (NT) control (A.1.1.3). After sufficient knockdown of LAIR-1 experiments were repeated as previously described using these LAIR-1 knockdown BMDMs (A.1.0.5). The results of the experiments showed that when LAIR-1 is knocked-down the previously observed decreases in TNFa on CLLP functionalized surfaces was lost and no difference in TNFa was observed between cysteine and CLLP surfaces. While the NT control cells on CLLP functionalized surfaces still exhibited the previously observed decreases in TNFa emission when compared to control surfaces (Figure 3). The results of the LAIR-1 KD activation experiment clearly demonstrated that the decreased TNFa emission by LPS stimulated BMDMs observed on CLLP functionalized surfaces was indeed a result of LAIR-1 engagement. It was concluded that the observed anti-inflammatory effects of CLLP on LPS stimulated BMDMs results from the binding of the collagen-mimetic ligand peptide by LAIR-1.

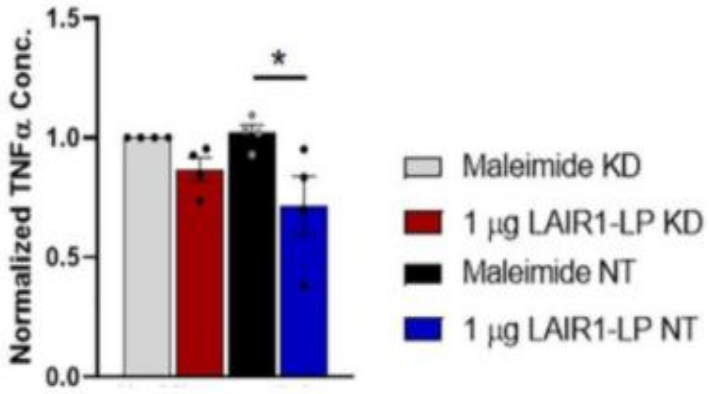

Figure 3: Normalized ELISA data depicting the average TNFα concentration of LPS/IFNγ stimulated BMDMs (with LAIR-1 KD and NT) on surfaces with and without CLLP. Values reported are average ± S.E.M., with N=4 independent biological replicates, and the dots are individual data points. Statistical significance was determined by one-way ANOVA with Tukey's post hoc test (*$p < 0.05$)

<u>Chapter 2.3</u>: CLLP Surfaces Selectively Decrease the Inflammatory Activation of Only F4/80+ BMDCs, via the Target Receptor LAIR-1

To test the effects of CLLP surfaces on inflammatory activation of dendritic cells, we cultured BMDCs on CLLP-coated surfaces and measured the expression of the inflammatory marker CD86 in response to LPS (Figure 4A)(A.1.0.5). We observed that F4/80+ BMDCs showed an average decrease of ~15% in CD86 expression in response to 100 ng/mL stimulation of LPS on CLLP surfaces (Figure 4B). Conversely, the CD86 response to LPS by F4/80- BMDCs, was unaffected by CLLP surfaces (Figure 4C). Given the high correlation of F4/80 expression with LAIR-1, these data suggest that the incorporation of LAIR-1 ligands onto the substrate surface can decrease the inflammatory activation of LAIR-1. We therefore examined the effects of decreasing LAIR-1 expression.

To confirm this, we performed studies with BMDCs in which the LAIR-1 gene was knocked down using siRNA (A.1.1.0). Experiments were repeated as previously described, although cell seeding on experimental surfaces was for 36 hours to ensure sufficient knockdown (Figure 4A) (A.1.2.0). We examined CD86 expression response, with and without LPS activation, in LAIR-1 knockdown (KD) and non-target (NT) control cells. The results show that knockdown of LAIR-1 expression abrogates the CLLP-induced decrease in activation (i.e., CD86 expression) of F4/80+ BMDCs (Figure 4D) but had no observable effect on the expression of CD86 of F4/80- cells (Figure 4E). Specifically, non-target F4/80+ BMDCs experienced ~60% decrease in CD86 expression on CLLP surfaces when stimulated with LPS, while LAIR-1 KD cells showed no differences (Figure 4D&E). However, for F4/80- BMDCs, in both LAIR-1 KD and non-target conditions there were no observable differences in CD86 expression either on CLLP or control surfaces (Figure 4E).

The results of this study strongly suggest that the ability of CLLP surfaces to inhibit dendritic cell activation (i.e., CD86 expression) is facilitated by LAIR-1. These inhibitory effects are only observed in high LAIR-1 expressing F4/80+ BMDCs; they are not observed when LAIR-1 is knocked down, nor are they observed for F4/80- BMDCs that naturally have variable LAIR-1. The observation that F4/80- BMDCs were unaffected by LAIR-1 ligands is consistent with recent findings by Carvalheiro et al., that showed LAIR-1 activating antibodies were unable to inhibit low LAIR-1 expressing dendritic cells [50]. Furthermore, multiple literature sources have reported that collagen-based materials do not decrease the inflammatory activation of F4/80- dendritic cells [73-75]. The ability of CLLP surfaces to decrease the inflammatory activation of F4/80+ BMDCs via LAIR-1 engagement is consistent with my previously published evidence [72, 76] and others [31-33] that showed LAIR-1 expressing cells are inhibited by LAIR-1 ligands.

Overall, the results of the experiments described in Figure 4 provide evidence that culture of F4/80+ dendritic cells on biomaterials displaying the LAIR-1 ligand CLLP leads to inhibition of their inflammatory response, while the activation of F4/80- dendritic cells that exhibit little to no LAIR-1 expression is unaffected. There is evidence to show that maintained activation of F4/80- dendritic cell in vitro and classical dendritic cells in vivo (cells more accurately represented by F4/80- BMDCs), may be advantageous towards sustained immunity and effective resolution of inflammatory events [11-16]. For example, Yamashita et al, reported that dendritic cell activation in combination with pro-inflammatory chemokines CCL21 and CCl19 was critical in the resolution of airway inflammation [15]. Incorporating LAIR-1 ligands into collagen-mimetic peptides effectively elicits control over inflammatory activation of BMDC

subpopulations with significant LAIR-1 expression, which may ultimately lead to greater resolution in vivo compared to indiscriminate inhibition of inflammatory activation of all cells.

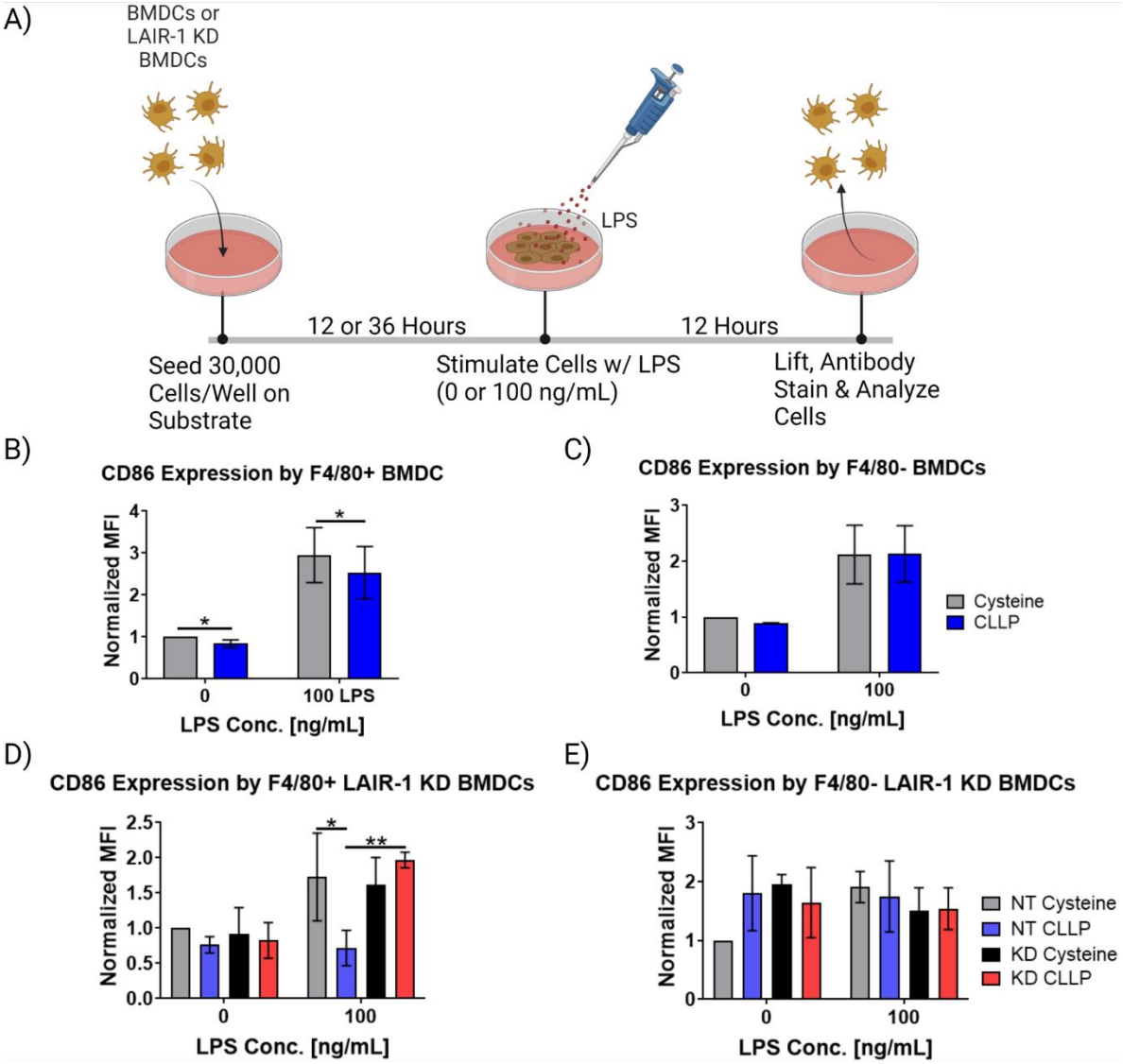

Figure 4: CLLP surfaces inhibit F4/80+ BMDC activation A) Experimental protocol designed to study the effect of CLLP functionalized surfaces on the LPS response of BMDCs and LAIR-1 KD BMDCs. B) Normalized MFI for CD86 expression of F4/80+ BMDCs, determined via flow cytometry, on both CLLP-conjugated and Cysteine-conjugated control surfaces with or without LPS. C) Normalized MFI for CD86 expression of F4/80- BMDCs with little to no LAIR-1

expression. D) Normalized MFI for CD86 expression by both LAIR-1 KD F4/80+ BMDCs and NT F4/80+ BMDC control cells, seeded on both CLLP and control surfaces, with and without LPS stimulation. E) Normalized MFI for CD86 expression by both LAIR-1 KD F4/80- BMDCs and NT F4/80- BMDC control cells. Values reported are average ± S.E.M., with N = 3 independent biological replicates. Statistical significance was determined by two-way ANOVA with Bonferroni's post hoc test (*$p < 0.05$).

Chapter 2.4: Conclusion

It was observed that CLLP functionalized surfaces inhibit pro-inflammatory activation of LAIR-1 expressing BMDMs and BMDCs, via engagement with target receptor LAIR-1. Cells that did not express LAIR-1, either naturally or artificially via siRNA, experienced no inhibition of pro-inflammatory activation on CLLP surfaces. Figure 5 is a graphical representation of the conclusion determined from the activation experiments performed in chapter 2.

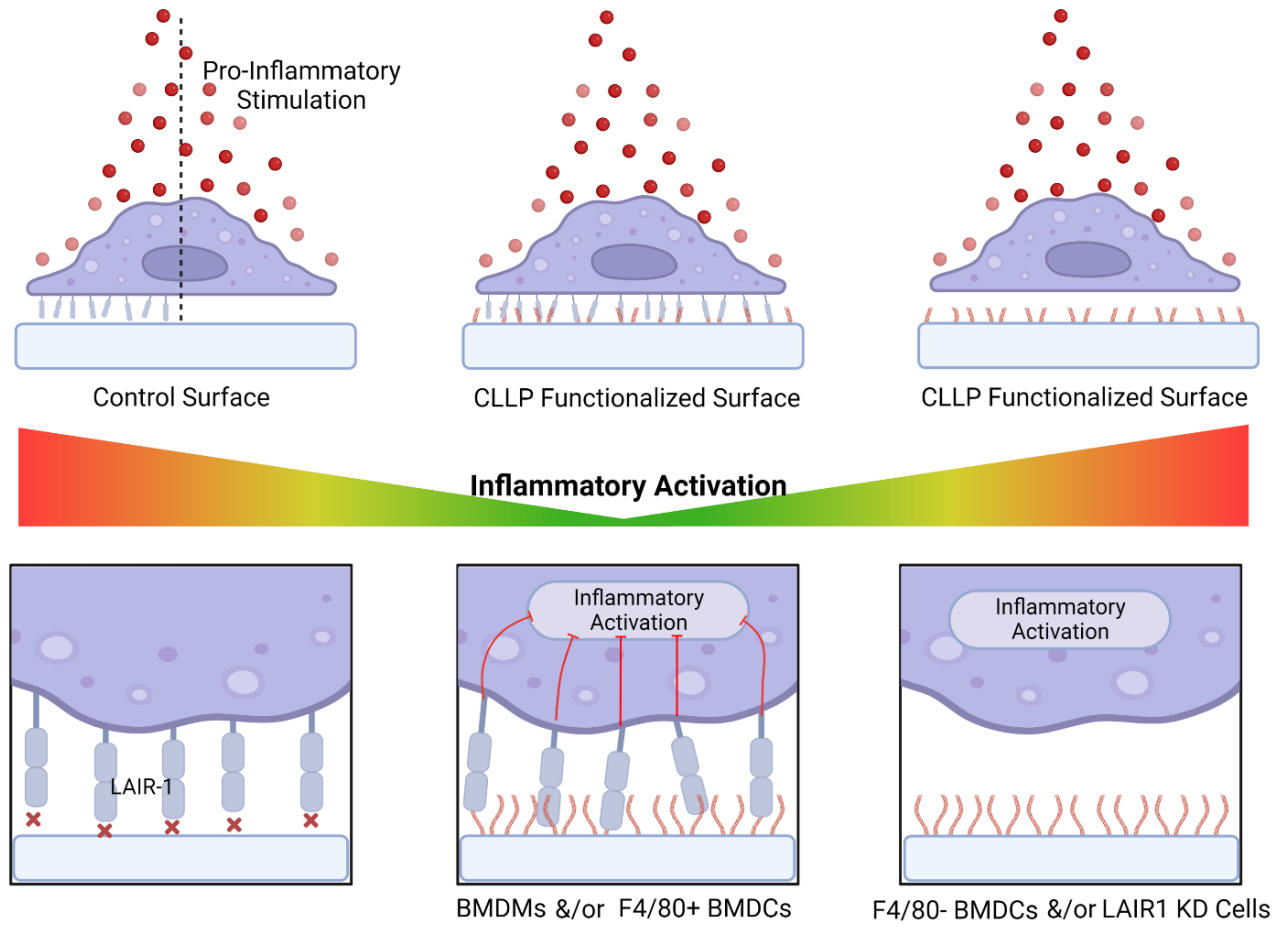

Figure 5: Graphical abstract summarizing the conclusions of chapter two, functionalizing cell culture surfaces with collagen mimetic high affinity LAIR-1 ligand peptides (CLLPs) reduces the extent of LPS induced activation in LAIR-1 expressing murine bone marrow monocyte derived macrophages and dendritic cells.

Chapter 3: **Effects of CLLP Functionalized Surfaces on Uptake**

Scope of Chapter 3: The study on the effects of LAIR-1 targeting collagen mimetic peptide (CLLP) functionalized surfaces on the critical innate immune behaviors of, uptake by and antigen display by monocyte-derived cells. Additionally, this aim will investigate the contribution of the surface receptor LAIR-1 to the observed CLLP surface effect.

- **Chapter 3.1**: Study the effects of CLLP functionalized surfaces on uptake by BMDMs and using siRNA KD provide evidence on the role of LAIR-1.
  - 3.1a: BMDMs Uptake
    - PLGA microparticles
    - PLGA nanoparticles
    - Apoptotic 3T3 fibroblasts
  - 3.1b: LAIR-1 KD BMDM Uptake
    - PLGA Microparticles
    - Uptake Receptor Expression
- **Chapter 3.2**: Study the effects of CLLP functionalized surfaces on uptake and antigen display by BMDCs and determine the role of LAIR-1 using KD.
  - 3.2a: BMDC Uptake
    - PLGA microparticles
    - E2 nanoparticles
  - 3.2b: LAIR-1 KD BMDC Uptake
    - PLGA microparticles
    - E2 nanoparticles
  - 3.2c: BMDC Antigen Display
    - Soluble SIINFEKL
    - E2 nanoparticle delivered SIINFEKL
  - 3.2d: LAIR-1 KD BMDC Antigen Display
    - E2 nanoparticle delivered SIINFEKL
- **Chapter 3.3:** Chapter 3 Conclusion

Portions of this chapter have been slightly modified and published as: A.T. Rowley, V.S. Meli, N.J. Wu-Woods, E.Y. Chen, W.F. Liu, S.W. Wang, Effects of Surface-Bound Collagen-Mimetic Peptides on Macrophage Uptake and Immunomodulation, Front Bioeng Biotechnol 8 (2020) 747.

Chapter 3: Effects of CLLP Functionalized Surfaces on Uptake

One critical innate immune function carried out by both macrophages and dendritic cells is uptake/clearance. As described previously, uptake is an innate immune cell function that plays a pivotal role in maintaining homeostasis, self-tolerance, inflammation, wound healing, and is implicated as a factor in the development of various disease states. Therefore, understanding the effects of CLLP on uptake will help determine how and where to effectively apply CLLP.

Chapter 3.1a: Effects of CLLP Surfaces on BMDM Uptake

The first cell type investigated was BMDMs as they are known as playing predominant roles in clearance and/or uptake in vivo. To investigate a more complete picture of macrophage uptake, materials of different sizes and compositions were used. As mentioned earlier material content and size effects which mechanism of uptake is employed by the cell. Additionally, it was desired to study uptake in two contexts, a natural context and a drug delivery context. Therefore, apoptotic cells were used to study BMDM uptake in its natural context, and PLGA particles of both microscopic and nanoscopic size were used to study BMDM uptake in the context of drug delivery. Furthermore, it was important to study the effects of CLLP on macrophage uptake in a range of physiological conditions, meaning BMDMs were stimulated into three different phenotypes. The three BMDM phenotypes are described here as; M0 meaning no stimulation, M1 meaning 0.1 ng/mL LPS and 0.3 ng/mL IFNy, and M2 meaning 3 ng/mL of IL-4/-13. M0 is a phenotype representative of naive macrophages, M1 is representative of activated and/or inflamed macrophages and finally M2 is indicative of a resolution phenotype of macrophages. Although we recognize that the boundaries for classification of the macrophage phenotypes into M0 (resting, non-activated), M1 (classically activated, pro-inflammatory), and M2 (alternatively

activated, pro-healing) are not strictly distinct, for simplicity we will describe BMDMs stimulated with LPS/IFNγ and with IL-4/IL-13 as M1 and M2 conditions, respectively.

Chapter 3.1a.1: PLGA Microparticle Uptake by BMDMs on CLLP Surfaces

The most significant results from my uptake studies came from the PLGA MP system. PLGA is a biodegradable polymer and has been used in several FDA-approved medical devices, for its drug loading capabilities and its potential to improve surface to host cell interactions [77]. PLGA MP uptake is relevant to drug delivery as PLGA has been used as vehicles for hydrophobic drug payloads [78-82]. In the context of implant integration, PLGA MPs can be a model for debris from PLGA-based medical devices/implants[83, 84], which are often plagued with inflammation [85-87]. Microparticles are taken up via phagocytosis and, due to their size, they are slow to be internalized by cells, and easily discerned/measured, which makes for a consistent optimized experimental system.

PLGA MPs were synthesized (A.2.1.0) and characterized via SEM images. ImageJ analysis was used to quantify average diameter and PDI of the PLGA MP population using SEM images. Analysis of these images showed that MPs exhibited an average diameter of 2.5 μm ± 0.75 μm, with a PDI of 0.09, scale bar equals 10 micron (Figure 6B). When investigating PLGA MP uptake, BMDMs were seeded in 96-well maleimide surfaces and surfaces functionalized with cysteine or CLLP as described for 12 h, and then incubated with stimulation solution and PLGA MPs (150,000 particles/well) for an additional 12 h. After 12 h of incubation, cell supernatant was removed for cytokine analysis via ELISA, wells were then washed with PBS, and BMDMs were lifted for flow cytometry analysis (A.2.1.1)(Figure 6A). Imagestream flow cytometry was also done to provide qualitative analysis of MP uptake and internalization. Four

replicate wells were combined for each condition for each n, and the experiment was repeated with cells from multiple mice, $n \geq 3$. ImageStream analyses of images that were obtained at internal focal planes confirmed that the PLGA MPs were successfully taken up by BMDMs, and > 90% of the fluorescent signal which was gated to be positive uptake showed MP that were internalized by cells, scale bar equals 10 micron (Figure 6C). The results of these PLGA MP uptake experiments showed that almost all BMDMs exhibited MP uptake across CLLP and control surfaces. However, CLLP peptide-functionalized surfaces significantly increased the amount of PLGA MPs taken up by BMDMs to approximately two-fold in every stimulated phenotype (i.e., M0, M1, M2), when compared to the effects on cysteine-functionalized (no CLLP) surfaces (Figure 6D). As phagocytosis was increased, the CLLP functionalized surfaces simultaneously resulted in a significant reduction (~40%) in the inflammatory cytokine TNFα by LPS/IFNγ-stimulated BMDMs, when compared to TNFα levels on the non-CLLP control surfaces (Figure 6E). The decrease in TNFα secretion on CLLP surfaces, without the presence of microparticles, is consistent with prior studies[72].

The overall results observed from these experiments are that CLLP surfaces significantly increased the average PLGA MP phagocytosis per BMDM across the M0, M1, and M2 phenotypes and decreased the overall inflammatory response of BMDMs in LPS/INFγ-stimulated condition, when compared to control surfaces (Figure 6D&E). These results are the most significant of the three studies, but all uptake studies confirmed these results in BMDMs.

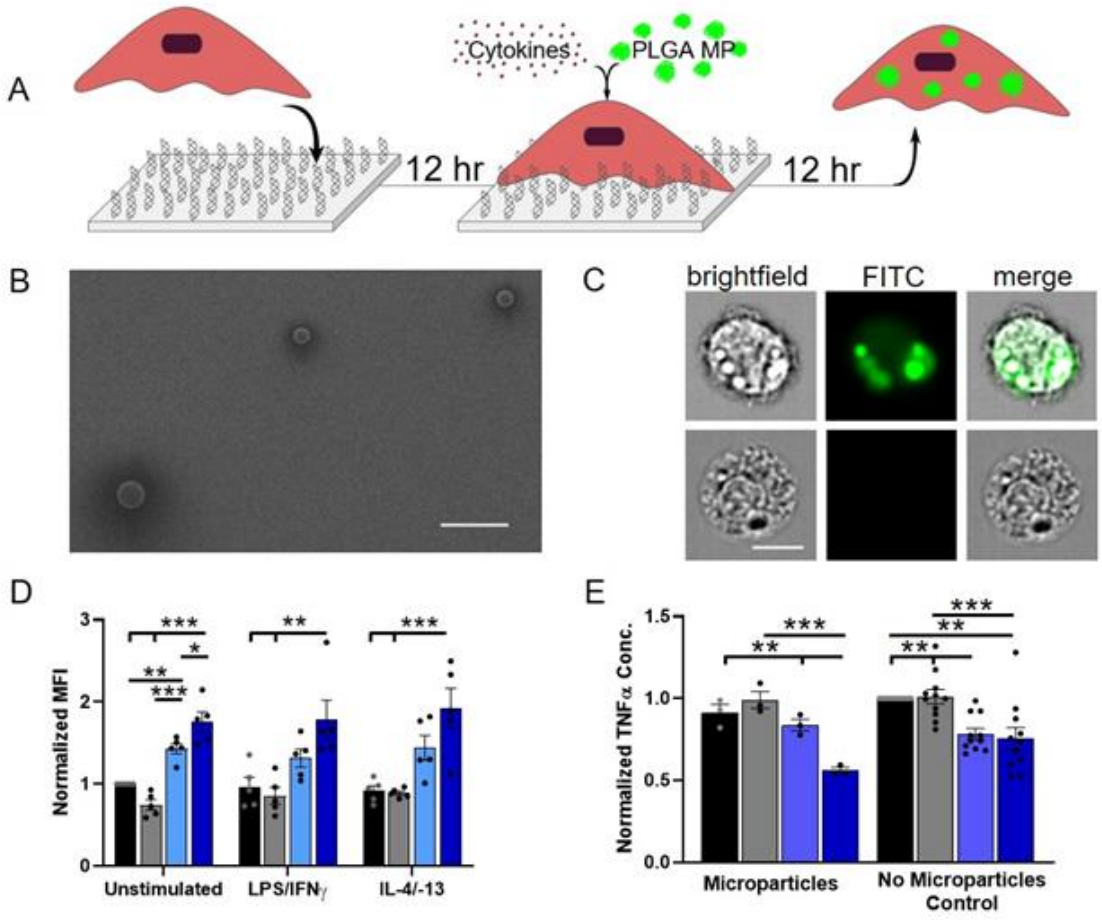

Figure 6: Effects of CLLP-conjugated surfaces on the uptake of PLGA microparticles (MPs) by BMDMs. (A) Diagram depicting experimental conditions and timeline used to investigate CLLP modulated PLGA MP uptake. (B) Representative SEM image of PLGA MPs. Average particle diameter was 2.5 ± 0.75 μm, with a PDI of 0.09 (Scale bar = 10 μm). (C) Representative flow cytometry microscopy images are shown of unstimulated BMDMs, cultured on control (maleimide) surfaces and incubated with BODIPY-labeled PLGA MPs. Columns, from left to right, are images in brightfield, FITC wavelength (BODIPY dye), and combined brightfield/BODIPY (Scale bar = 10 μm). (D) Mean fluorescence intensity of BODIPY-labeled PLGA MPs, in macrophages with internalized particles. Values have been normalized to the

unstimulated BMDMs on maleimide surfaces. (E) Pro-inflammatory TNFα concentrations secreted by BMDMs that were stimulated with LPS/IFNγ, on the different surfaces, with and without PLGA MPs. Values were normalized to the TNFα concentration for the maleimide surface with no microparticles (control). For panels (D,E), values reported are average ± SEM, with $N \geq 3$ independent biological replicates, and the dots are individual data points. Statistical significance was determined by one-way ANOVA with Tukey's post hoc test (*$p < 0.05$, **$p < 0.01$, ***$p < 0.001$).

<u>Chapter 3.1a.2</u>: PLGA Nanoparticle Uptake by BMDMs on CLLP Surfaces

PLGA particles are also relevant on a nanoscopic scale in drug delivery [78, 79, 81, 82, 88, 89], and therefore it was also important that the effects of CLLP on PLGA NP uptake were investigated. After PLGA nanoparticle synthesis (A.2.1.2) dynamic light scattering analysis determined that the average NP size was 214 nm in diameter with an average PDI of 0.035 (A.2.1.3), and TEM images confirmed the shape and size of PLGA NPs (Figure 7B). ImageStream analysis qualitatively confirmed that the PLGA NPs were successfully taken up by BMDMs (Figure 7C). To investigate the effects of CLLP functionalized surfaces on the uptake of nanoparticles (NPs), PLGA NPs were incubated with BMDMs and seeded on surfaces conjugated with and without CLLP (Figure 7A)(A.2.1.4).

I observed again that approximately 90% of BMDM on all surfaces exhibited NP uptake at the time point examined (1 h) (A.2.1.5), but that unstimulated BMDMs (M0) seeded on the CLLP saturated surfaces (1 μg/well) exhibited a significant (~25%) increase in the average total uptake of PLGA NPs per BMDM when compared to both control surfaces without CLLP ($p < 0.05$; Figure 7D). Although the M1 and M2 conditions did not show statistically significant

uptake differences between the macrophages grown on the CLLP vs. no-LAIR-LP surfaces, the trends were similar to those observed for the MPs, and the averages in uptake were higher on CLLP surfaces. Unlike the results for the MPs, there were no significant differences in the pro-inflammatory TNFα secretion between M1-stimulated macrophages which had taken up nanoparticles and were cultured on the different surfaces, although the trends did show a decrease in the average TNFα concentration on CLLP surfaces (Figure 7E). Therefore, while increases in MP uptake is correlated with decreased TNFα secretion on LAIR-LP conjugated surfaces, the relationship between uptake and decreases in TNFα concentrations appear to be less significant for NPs. The effects of CLLP on PLGA NP uptake was less impactful than its effects on PLGA MP phagocytosis (Figure 6D, 7D). One reason may be that unlike NPs, the uptake of MPs is directed more significantly via surface receptors and cell membrane interactions, resulting in increased inflammatory response in macrophages when compared to nanoparticle uptake [90]. This, together with increased activation by MPs (Figures 6E,7E), may account for the more significant effects of CLLP when compared to PLGA NP uptake.

Another possible reason for the larger differences within the MP groups, compared to the NP data, is the different experimental times required to achieve “saturated” uptake (A.2.1.5); NP uptake happens quickly, which experimentally limited NP uptake to a 1-h incubation period, while MP uptake occurs more slowly (12 h). This could explain why similar trends were observed between NP and MP data, but the effects of CLLP may not have been as distinguishable, even after only 1 h of uptake, for the NPs.

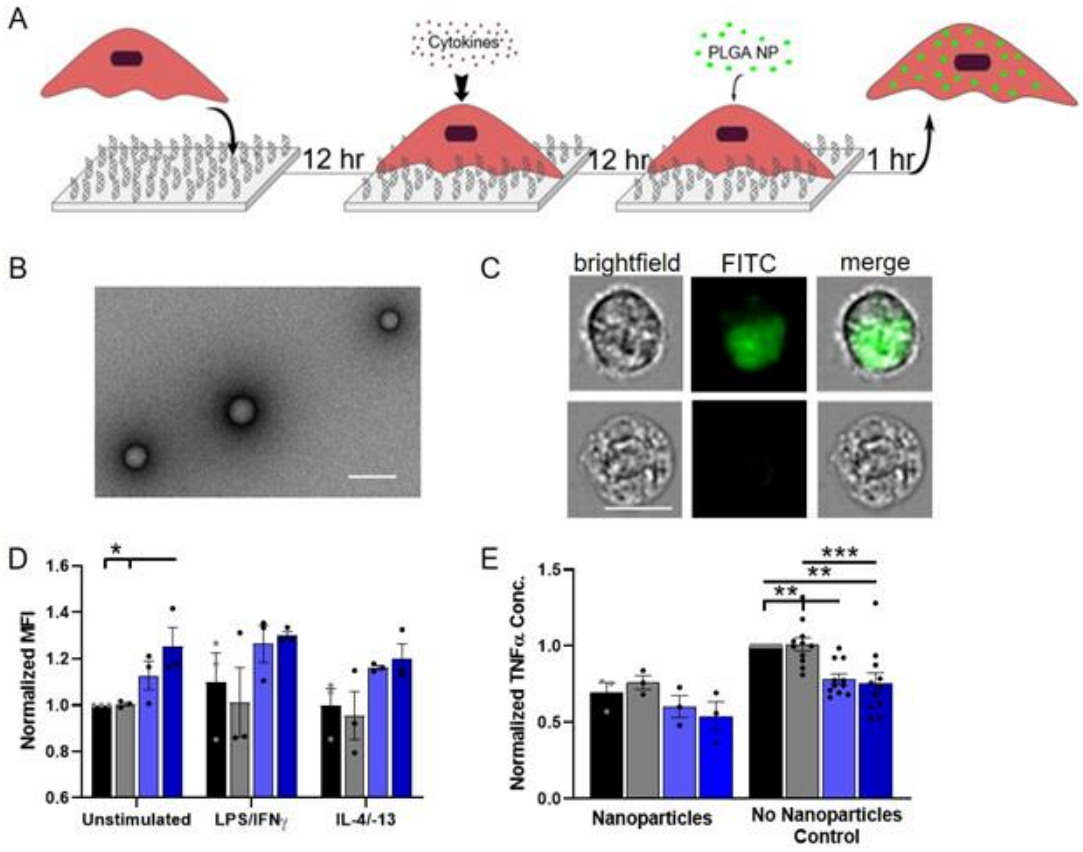

Figure 7: Effects of CLLP-conjugated surfaces on the uptake of PLGA nanoparticles (NPs) by BMDMs. (A) Diagram depicting experimental conditions and timeline used to investigate CLLP modulated PLGA NP uptake. (B) Representative TEM image of PLGA NPs. Average particle diameter was 214 nm with an average PDI of 0.035 by DLS analysis (Scale bar = 500 nm). (C) Representative flow cytometry microscopy images are shown of unstimulated BMDMs, grown on maleimide control surfaces and incubated with BODIPY-labeled PLGA NPs. Columns, from left to right, are images in brightfield, FITC wavelength (BODIPY), and combined brightfield/BODIPY (Scale bar = 10 μm). (D) Mean fluorescence intensity of BODIPY-labeled PLGA NPs, in macrophages with internalized particles. Values have been normalized to the unstimulated BMDMs on maleimide surfaces. (E) Pro-inflammatory TNFα concentrations

secreted by BMDMs that were stimulated with LPS/IFNγ, on the different surfaces, with and without PLGA NPs. Values were normalized to TNFα concentration for the maleimide surface with no nanoparticles (control). For panels (D,E), values reported are average ± S.E.M. with N ≥ 3 independent biological replicates, and the dots are individual data points. Statistical significance was determined by one-way ANOVA with Tukey's post hoc test (*$p < 0.05$, **$p < 0.01$, ***$p < 0.001$).

Chapter 3.1a.3: 3T3 Fibroblast Uptake by BMDMs on CLLP Surfaces

Once the effects of CLLP on PLGA particle uptake were analyzed, it was important to investigate uptake mechanisms with more natural context in vivo, using a more biologically relevant uptake material. Therefore, we decided to study the immunomodulatory effects of CLLP functionalized surfaces on the innate immune cell function of apoptotic cell clearance. Apoptotic clearance is, as previously mentioned, a critical homeostatic function of innate immune phagocytes that has been implicated in the development of autoimmune diseases such as SLE[91]. Not only does studying the effects of CLLP on macrophage apoptotic clearance highlight a potential therapeutic target (LAIR-1) for autoimmune diseases, it also sheds light on the biological roles of LAIR-1 and collagen in directing innate immune responses of macrophages.

Using previously described methods the effect of CLLP functionalized surfaces on apoptotic cell uptake by BMDMs was investigated (A.2.1.6)(A.2.1.7)(Figure 8A) ImageStream images that qualitatively depict the uptake of apoptotic fibroblasts by BMDMs are presented in Figure 8B. Internalization analysis determined that >99% of the cells gated to have positive fluorescent signal showed complete internalization of apoptotic cells by BMDMs. Due to the

tendency of apoptotic bodies to aggregate at high concentrations and lead to heterogenous coverage of BMDMs, the "saturated population" uptake condition that we obtained for MP and NP studies (A.2.1.5) could not be achieved. Saturated uptake is defined as the average percentage of unstimulated BMDMs exhibiting uptake is ≥80% on all surfaces. Therefore, an additional metric describing the percentage of macrophage population exhibiting uptake (Figure 8C) was used in combination with MFI (Figure 8D) to more completely describe the effects of CLLP on macrophage uptake of apoptotic cells.

The data demonstrated CLLP's ability to significantly increase the percentage of unstimulated BMDMs exhibiting uptake of apoptotic 3T3 cells by greater than twice the values obtained on either of the control surfaces (Figure 8C). M2 BMDMs (with IL-4/IL-13) also showed this increasing trend, but the increase was just under statistical significance. These CLLP-induced increases in percentage of BMDMs exhibiting uptake were also conserved for PLGA MPs at unsaturated conditions (A.2.1.8). Interestingly, although CLLP surfaces had no effect on the percentage of M1 (LPS/IFNγ-stimulated) BMDMs exhibiting uptake, the ligand peptide exerted an inhibitory effect on the average total uptake of apoptotic 3T3 fibroblasts by M1-stimulated BMDMs, with a significant ~30% arrest of uptake when compared to uptake on maleimide surfaces (Figure 8D). This trend of decreased average uptake on CLLP surfaces was also observed for M0 and M2 phenotypes but was not determined to be statistically significant.

It was observed that apoptotic cells had an anti-inflammatory effect on M1-stimulated BMDMs. The macrophage TNFα secretion response to apoptotic cells were equivalent on every surface and were at comparable levels as the TNFα of BMDMs seeded on CLLP surfaces but with no apoptotic cells (Figure 8E). We observed a significant ~20% decrease in TNFα secretion between the BMDMs on maleimide and cysteine control surfaces, when apoptotic cells were

present. Apoptotic bodies have been demonstrated to elicit anti-inflammatory effects on macrophages, with LAIR-1 being implicated in the mechanisms driving these results[39, 47, 48, 92, 93]. Thus, additional anti-inflammatory effects of the peptide were not observed, and the expected CLLP-induced decreases in TNFα were not discernable in the presence of apoptotic bodies (Figure 8E).

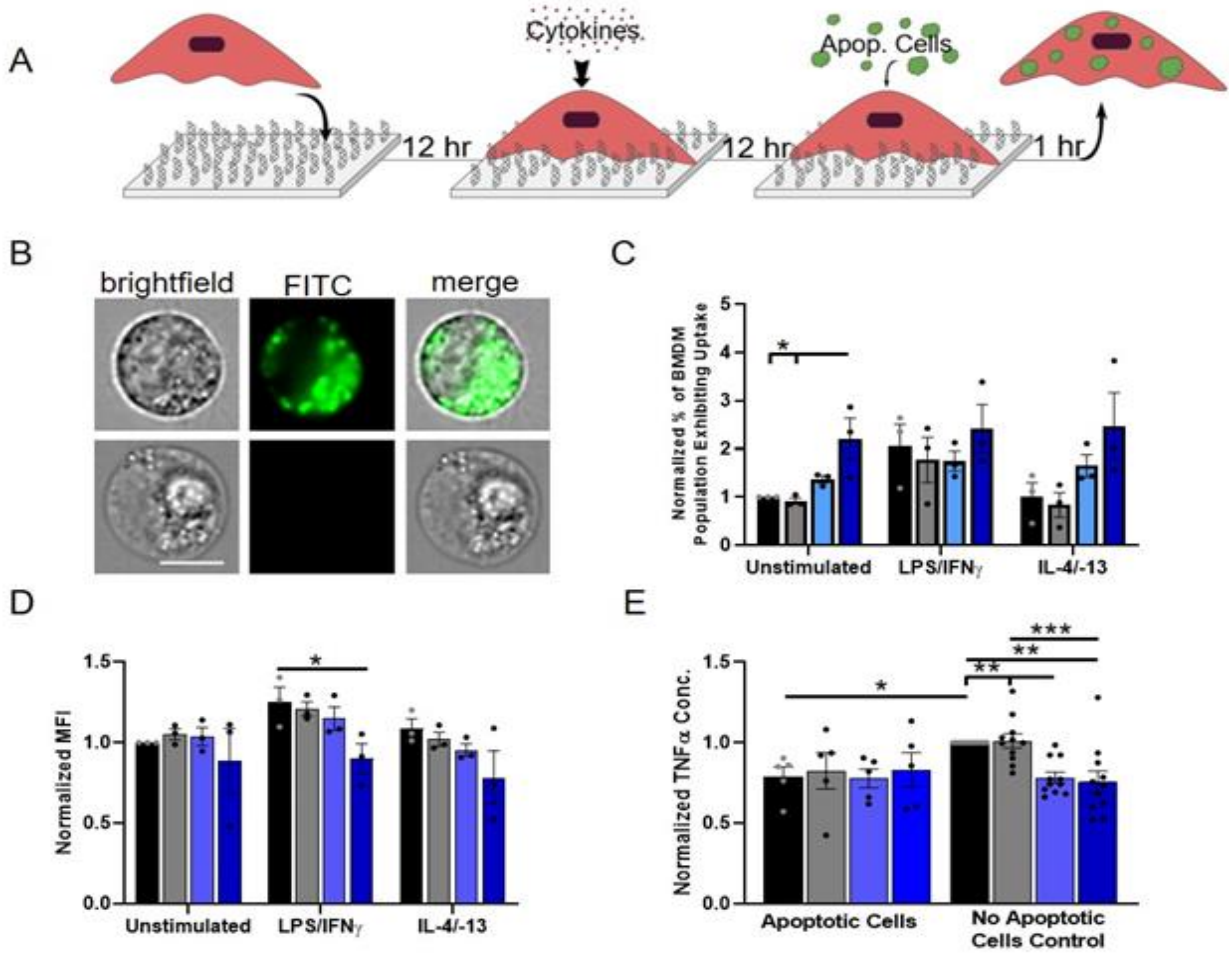

Figure 8: Effects of CLLP-conjugated surfaces on the uptake of apoptotic cells by BMDMs. (A) Diagram depicting experimental conditions and timeline used to investigate CLLP modulated uptake of apoptotic cells. (B) Representative flow cytometry microscopy images are shown of

unstimulated BMDMs grown on maleimide surfaces (control) and incubated with DiO-labeled apoptotic 3T3 fibroblasts. Columns, from left to right, are images in brightfield, FITC wavelength (DiO), and combined brightfield/DiO (scale bar = 10 μm). (C) Percentage of BMDM cells that exhibited uptake of DiO-labeled apoptotic 3T3 fibroblasts on the different surfaces. Values have been normalized to the unstimulated BMDMs on maleimide. This value is representative of the propensity of the BMDM population for uptake on the different surfaces. (D) Mean fluorescence intensity of macrophages that exhibited uptake of DiO-labeled apoptotic cells. This metric is representative of the average amount of apoptotic cells taken up per BMDM (of the uptake positive BMDM population). Values have been normalized to unstimulated BMDMs on maleimide surfaces. (E) Normalized TNFα concentrations secreted by BMDMs that were stimulated with LPS/IFNγ, on the different surfaces, with and without apoptotic cells. For panels (C–E), values reported are average ± S.E.M., with N = 3 independent biological replicates, and the dots are individual data points. Statistical significance was determined by one-way ANOVA with Tukey's post hoc test (*$p < 0.05$, **$p < 0.01$, ***$p < 0.001$).

<u>Chapter 3.1b</u>: LAIR-1 KD BMDM Uptake Study

After observing the complex multifaceted immunomodulatory effects of the CLLP surfaces on various uptake behaviors exhibited by BMDMs of different phenotypes, it was important to investigate how the expression of LAIR-1, the target surface receptor for CLLP-conjugated surfaces, played a role in the observed increases in macrophage uptake. Particularly because of LAIR-1's reported role as an inhibitory receptor, it was critical to determine whether the observed effects on uptake were as a result of the complex multifaceted function of LAIR-1 or as a result of the complex multifaceted immunomodulatory properties of CLLP.

In order to investigate the contribution of LAIR-1 and CLLP interactions on the observed increase in uptake on CLLP surfaces, we examined the effects of knocking-down LAIR-1 gene expression on CLLP modulated uptake. Baseline expression, without gene knock-down, was first determined. Gene expression of LAIR-1 by BMDMs under each stimulation condition (M0, M1, M2), seeded on the CLLP and control surfaces, indicated that the expression of LAIR-1 was affected by surface material, as described earlier. Briefly, gene expression differences on the control surfaces (maleimide- and cysteine-functionalized) among the M0, M1, and M2 phenotypes were not observed to be statistically different, although M1 macrophages showed approximately half the average LAIR-1 gene expression of M0 and M2 macrophages on maleimide surfaces, and on cysteine-functionalized surfaces LAIR-1 expression on M1 and M2 macrophages were increased relative to M0 values. In contrast, on CLLP surfaces, LAIR-1 expression was doubled in M2 phenotypes relative to M0 macrophages ($p < 0.05$) (A.1.1.2).

LAIR-1 knockdown (KD) was effective and decreased LAIR-1 gene expression by 90% when compared to the non-target (NT) control (A.1.1.3). Uptake from these LAIR-1 KD cells were evaluated according to the MP uptake protocol, previously described (Figure 9A). The PLGA MP uptake system was chosen as the system to use in the knockdown study due to the consistent statistically significant results obtained when using the experimental system previously. LAIR-1 knockdown of unstimulated (M0) macrophages increased the average amount of PLGA MPs phagocytosed per BMDM on both maleimide (control) and CLLP-conjugated surfaces; in particular, the KD of LAIR-1 expression resulted in a significant ~35% increase in MFI on non-peptide surfaces, and a ~25% increase in uptake in cells cultured on CLLP surfaces (Figure 9B). The results also showed that CLLP induced significant increases of ~20% and ~30% in uptake per cell for both LAIR-1 KD and non-target (NT) BMDMs,

respectively (Figure 9B). The trends for all groups of both M1 and M2 phenotypes also supported the significant increases observed in the unstimulated M0 macrophages (Figure 9B). Decreasing the LAIR-1 gene expression abolished the previously observed decrease in the level of TNFα on CLLP surfaces for M1 (LPS/IFNγ) macrophages that were incubated with or without MPs (Figure 9E). However, the CLLP surface-induced decrease in TNFα (relative to the maleimide surface) that had previously been observed was conserved for the NT control group (Figure 9E). Interestingly, we observed that when LAIR-1 gene expression was decreased by KD, the expression of other receptors and molecules that have been implicated in cell uptake increased. Gene expression of CD36, SRA-1, integrin β2, and β-actin were examined, and all were significantly increased (Figure 10A). In contrast, F4/80, a surface marker for macrophages but which is not known to be linked to uptake, was the control used for this experiment and showed no increase in expression.

Overall, the LAIR-1 KD data showed that the higher expression of LAIR-1 decreased the average amount of cellular uptake on both control and CLLP surfaces (Figure 10B). These findings are consistent with published literature showing that knock-down LAIR-1 increased the uptake of lipids [94]. However, knocking down LAIR-1 expression arrested the anti-inflammatory effects (TNFα levels) of CLLP on M1-stimulated BMDMs, which is consistent with previously published results [72]. One explanation for the KD induced increase in uptake may be linked to the observation that decreasing the expression of LAIR-1 affected the expression of other receptors that are related to uptake; gene expression for CD36, SRA-1, and beta-2 integrin all significantly increased when LAIR-1 was knocked-down. These apparent correlations suggest that the expression of surface receptor LAIR-1 and its interaction with CLLP is not responsible for the increase in uptake observed on CLLP-coated surfaces, and that

competitive binding of CLLP may exist between LAIR-1 and other collagen-recognizing surface receptors. Several cell surface receptors, such as beta-2 integrin, CD36, LRP-1, and CR3 bind to collagen and/or collagen-like domains and have been implicated in upregulation of various mechanisms of cellular uptake [95-98]. It was hypothesized, based on literature and observed experimental results, that some of these collagen-recognizing surface receptors involved in uptake may also be binding CLLP. Furthermore, my data may suggest a correlation with non-collagen binding proteins that are associated with uptake as well; the expression of scavenger receptor SRA-1, a receptor critical in macrophage uptake[99, 100] and of beta-actin, which is involved in cell uptake, were also increased in the LAIR-1 KD macrophages. We hypothesized that the increase of SRA-1, beta-actin and other non-collagen binding proteins associated with uptake, in LAIR-1 KD BMDMs, could explain the observed increase in uptake of LAIR-1 KD BMDMs on maleimide surfaces when compared to NT BMDMs. Furthermore, the statistically significant increase in MP uptake between KD and NT BMDMs on CLLP provides further evidence that LAIR-1: CLLP interactions inhibit the increasing effect of CLLP on macrophage uptake (Figure 9B). The overall interpretation of the results of these LAIR-1 knockdown BMDM MP uptake experiments were to confirm that it was in fact the complex and multifaceted immunomodulatory properties of CLLP responsible for the observed effect on uptake and provided further evidence of LAIR-1's inhibitory nature.

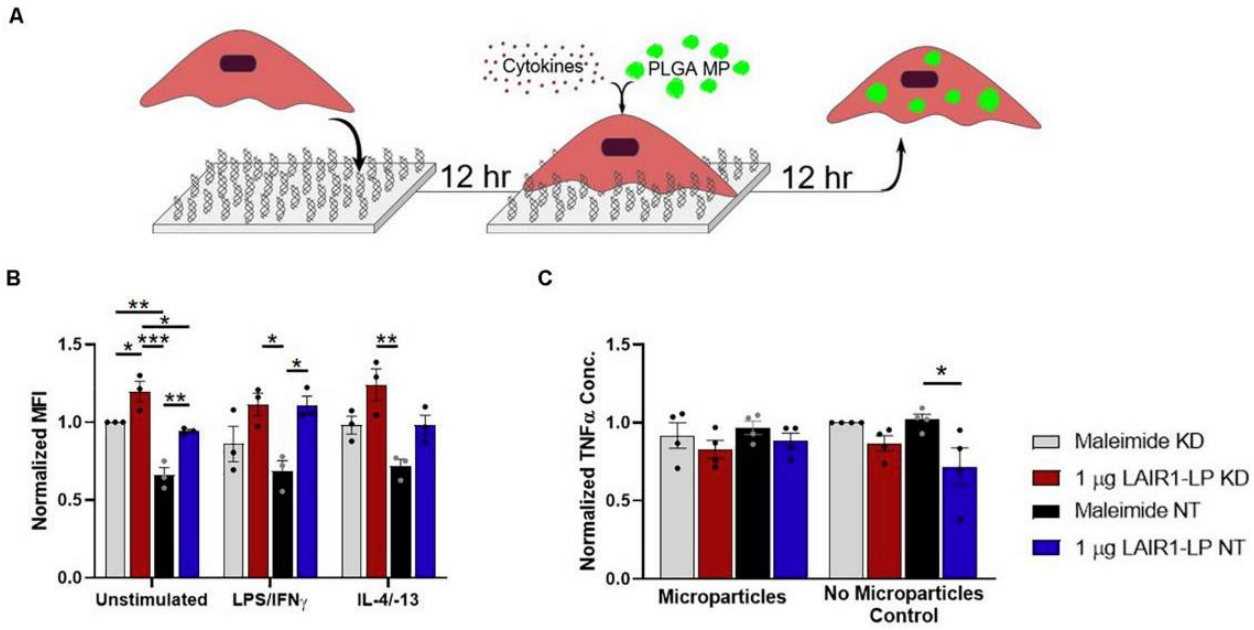

Figure 9: Effects of LAIR-1 expression on CLLP-conjugated surface-mediated uptake of PLGA MPs by BMDMs. (A) Diagram depicting the experimental conditions and experimental timeline used to investigate the effects of LAIR-1 expression on uptake of PLGA MP. (B) Mean fluorescence intensity of BODIPY-labeled PLGA MPs, in macrophages with internalized particles. LAIR-1 expression was decreased by knockdown (KD) of the LAIR-1 gene, compared to the non-targeted (NT) control. Values were normalized to unstimulated control KD BMDMs on maleimide surfaces. Values reported are average ± SEM, with N = 3 independent biological replicates, and a two-tailed unpaired t-test was used (*$p < 0.05$, **$p < 0.01$, ***$p < 0.001$). (C) Normalized ELISA data depicting the average TNFα concentration of LPS/IFNγ stimulated BMDMs (with LAIR-1 KD and NT) on surfaces with and without CLLP, incubated with and without PLGA MPs. Values reported are average ± S.E.M., with N = 3 independent biological replicates, and the dots are individual data points. Statistical significance was determined by one-way ANOVA with Tukey's post hoc test (*$p < 0.05$, **$p < 0.01$, ***$p < 0.001$).

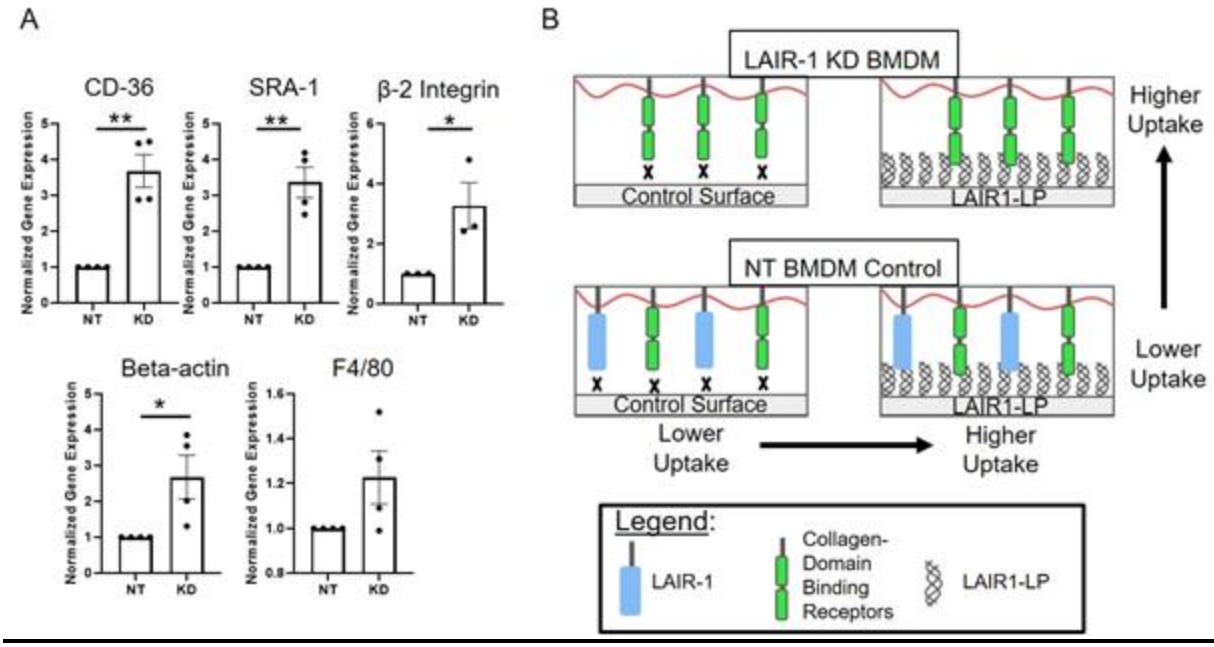

Figure 10: LAIR-1 knockdown affects uptake receptor expression (A) Relative gene expression of receptors involved in uptake. Cd36, SRA-1(Msr-1), and beta 2 integrin (Itgb2), were analyzed via qPCR, along with structural protein beta-actin (Actb) and F4/80 (Adgre1) which were used as controls. Gene expression is normalized to non-targeted (NT) polystyrene condition. Data presented as mean ± S.E.M. N of 3 or more independent biological replicates, and the dots are individual data points. *$p < 0.05$, **$p < 0.01$, ***$p < 0.001$, assessed by two-tailed Student's t-test. (B) Diagram depicting a proposed model consistent with gene expression data from LAIR-1 KD (top) and NT (bottom) BMDMs and cultured on control surfaces (left) and CLLP functionalized surfaces (right).

Chapter 3.2: Effects of CLLP Surfaces on BMDC Uptake

In order to fully understand the immunomodulatory effect of CLLP on the natural process of clearance and uptake, it was necessary to investigate dendritic cells, another innate immune cell type that plays a significant role in uptake. Furthermore, uptake is only the first step in a

critical innate immune response, carried out predominantly by dendritic cells, known as antigen presentation. As previously described, uptake by dendritic cells results in the internal processing of proteins into recognizable fragments, that are then presented on the surface of DCs by specific surface receptors that can then, in turn, be read by other immune cells, like T cells, which triggers and/or directs immune responses, particularly in the adaptive arm of the immune system. This process of uptake and antigen presentation is one of the main modes of communication between the innate and adaptive immune systems, is critical in maintaining homeostatic control over the body and is a process that has been implicated in development of multiple disease states as well as potential therapeutics. Therefore, it was important to investigate the immunomodulatory effects of CLLP on BMDC antigen presentation as well as uptake, not only for its prevalence in therapeutics and medical applications but also to more accurately characterize the biological role of collagen and LAIR-1 in the full natural context of uptake as it pertains to antigen presenting monocyte derived cells.

Chapter 3.2a: Effects of CLLP Surfaces on BMDC Uptake of Microparticles & Nanoparticles

In previous studies, we observed that macrophages cultured on CLLP-functionalized surfaces increased their uptake [76], and we were therefore interested if such behavior is also observed for BMDCs. Using methods described in the appendix (A.2.2.0) (A.2.2.1)(A.2.2.2)(A.2.2.3), we examined the effects of CLLP-functionalized surfaces on nanoparticle (NP) and microparticle (MP) uptake. As the model NP, we used the E2 protein NP, which is 25-nm in diameter and has been investigated as a delivery vehicle for drug molecules [101, 102] and antigens for vaccines [103-106]. For MPs, we used PLGA MPs, as they have utility in a wide variety of dendritic cell-targeted biomedical applications, from antigen-based

vaccines to delivery vehicles for DNA and anti-inflammatory drugs [107-110]. PLGA MPs were incubated with cells for 12 hours (A.2.2.3), however due to the rapid rate of clearance of nanoparticles, E2 uptake was saturated for all cells at 12 hours (A.2.2.4), thus a shorter timepoint (of 20 minutes) was used to see the effects of CLLP on NP uptake.

The results of this study showed BMDCs culture on CLLP surfaces alone (with no LPS stimulation) had no effect on nanoparticle uptake compared to cells cultured on control surfaces (Figures 11B,C). However, both F4/80+ and F4/80- BMDCs experienced significant increases in NP uptake of ~30% (Figure 11B) and ~40% (Figure 11C), respectively, on CLLP surfaces when stimulated with LPS. In contrast, for PLGA MPs, unstimulated BMDCs cultured on CLLP surfaces experience a statistically significant (~34%) increase in MP uptake, when compared to cells on control surfaces, but no differences were observed for LPS-stimulated (A.2.2.5). (I was unable to perform BMDC subpopulation analysis for MPs, due to extensive non-specific antibody binding to MPs.) Together, these results show that collagen-mimetic materials engineered with LAIR-1 ligands are capable of eliciting increased uptake of particles by BMDCs.

<u>Chapter 3.2b</u>: LAIR-1 KD Bolstered the Increases in Uptake on CLLP Surfaces for F4/80+ BMDCs and Had No Effect on the Increase in Uptake Experienced by F4/80- BMDCs on CLLP Surfaces

To further examine whether the CLLP-induced increase in uptake was due to LAIR-1, experiments were repeated using LAIR-1 knockdown cells (Figure 11A). BMDCs with knocked-down LAIR-1 expression showed an increase in uptake on CLLP surfaces compared to control surfaces, in both F4/80+ and F4/80- BMDC populations, with and without LPS stimulation

(Figure 11D,E). Unstimulated and LPS stimulated F4/80+ LAIR-1 KD BMDCs experienced an increase of ~17% and ~19% in uptake of E2 NP, respectively, on CLLP surfaces compared to the LAIR-1 KD cells on control surfaces (Figure 11D). For the F4/80- population, LPS-stimulated LAIR-1 KD BMDCs showed a ~30% increase in NP uptake on CLLP surfaces, compared to KD BMDCs on control surfaces (Figure 11E). Similarly for MP uptake, we observed that both non-target (NT) and LAIR-1 KD cells exhibited ~ 1.5-fold increase in uptake when cultured on CLLP surfaces (A.2.2.5).

Knocking down LAIR-1 expression did not abrogate CLLP-induced NP or MP uptake, suggesting that these increases are not the result of CLLP engagement with LAIR-1 (Figure 11D,E) (A.2.2.5). In fact, knockdown of LAIR-1 enhanced uptake in F4/80+ BMDCs on CLLP surfaces (by ~15% and ~24% in unstimulated and LPS-stimulated, respectively) when compared to the non-target (NT) controls, suggesting that LAIR-1 may in fact be inhibitory to the CLLP-induced increase in uptake (Figure 11D). While non-target siRNA treated cells showed modest increases in average E2 uptake, these trends were not statistically significant (Figure 11D,E). This was in contrast with the untreated wild type cells that showed significant CLLP-induced increases in uptake, likely because siRNA treatment itself has some nonspecific effects on particle uptake and overall cell function. Nevertheless, together these studies suggest that engineering collagen-mimetic materials with LAIR-1 ligands provides immunomodulation of BMDCs towards increased uptake, through means separate from (but not completely unaffected by) LAIR-1 engagement.

These findings were consistent with my previous work demonstrating that CLLP surfaces enhanced the uptake of a range of different materials by macrophages [76]. Using siRNA to knock-down LAIR-1 expression in macrophages, we also reported that reducing LAIR-1

expression enhanced the CLLP-induced increase in uptake, similar to the findings reported here for F4/80+ BMDCs [76](Figure 11D). Together, these studies illuminate the potential of utilizing collagen-mimetic surface materials to elicit increased uptake and clearance in monocyte-derived phagocytic cells, a critical step in the resolution of inflammation and initiation of healing [13, 111, 112]. Furthermore, increases in protein NP uptake highlight a potential application of CLLP engineered materials in vaccine delivery.

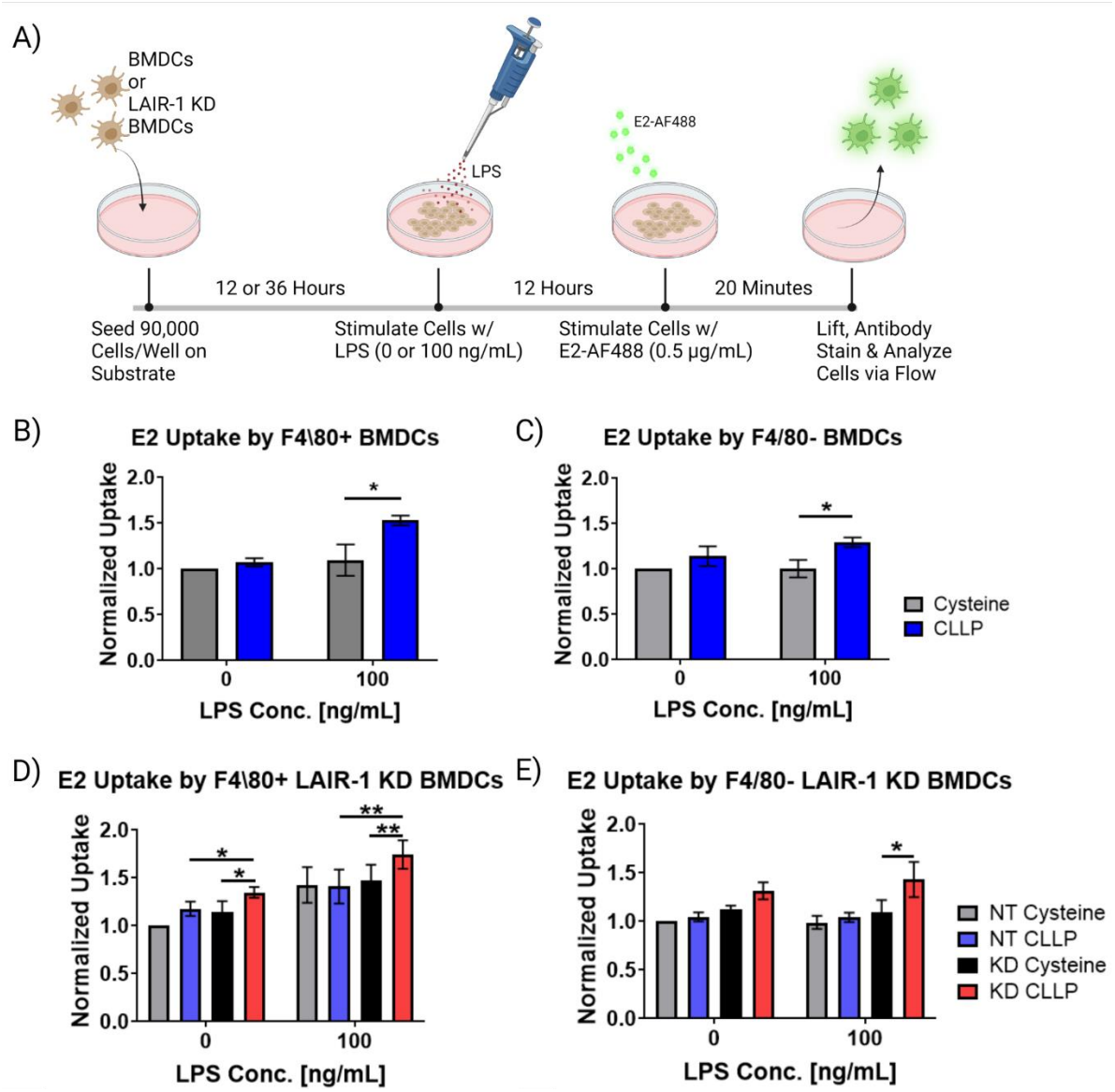

Figure 11: CLLP Surfaces Increase the Uptake of E2 Protein NPs by BMDCs, and LAIR-1 KD Further Increased Uptake on CLLP Surfaces A) Experimental timeline used to study the immunomodulatory effects of CLLP surfaces on protein nanoparticle uptake by BMDCs and LAIR-1 KD BMDCs. BMDCs are incubated for 12 hours, and KD BMDCs are incubated for 36 hours, prior to LPS stimulation. B) Normalized uptake MFI of AlexaFluor488 (AF488)-conjugated E2 protein nanoparticles by LAIR-1 expressing F4/80+ BMDCs on experimental surfaces, with and without LPS, determined via flow cytometry. C) Normalized uptake MFI of AF488-conjugated E2 protein nanoparticles by F4/80- BMDCs, which have little to no LAIR-1 expression, on CLLP-conjugated and cysteine-conjugated (control) surfaces. D) Normalized uptake MFI of AF488-conjugated E2 protein nanoparticles by both LAIR-1 KD and non-target F4/80+ BMDCs on experimental surfaces, with and without LPS, determined via flow cytometry. E) Normalized uptake MFI of AF488-conjugated E2 protein nanoparticles by both LAIR-1 KD and non-target F4/80- BMDCs on experimental surfaces, with and without LPS. Values reported are average ± S.E.M., with N = 3 independent biological replicates. Statistical significance was determined by two-way ANOVA with Bonferroni's post hoc test (*$p < 0.05$, **$p < 0.01$)

Chapter 3.2c: CLLP Surfaces Increased the SIINFEKL Antigen Display of F4/80- BMDCs when SIINFEKL was Delivered via NPs

I then examined whether the increase in NP uptake by BMDCs on CLLP surfaces, could translate to increased antigen presentation, if the antigen was delivered via NPs. We functionalized the E2 protein nanoparticles with the ovalbumin antigen SIINFEKL using published protocols [103](A.2.2.6)(A.2.2.7)(A.2.2.8) and incubated BMDCs that were seeded on

CLLP or control surfaces with either E2-SIINFEKL or soluble SIINFEKL. Antigen display was then measured by quantifying MHC I bound to SIINFEKL (A.2.2.9)(Figure 12A).

When SIINFEKL was conjugated to and delivered by the NPs (E2-SIINFEKL), a ~2-fold increase in antigen display was observed on F4/80- BMDCs that were seeded on CLLP surfaces compared to cells seeded on control surfaces, regardless of LPS stimulation condition (Figure 12C). However, when SIINFEKL was delivered to BMDCs in its soluble form, CLLP surfaces did not affect the overall antigen displayed by cells (A.2.2.10), suggesting that the increase in SIINFEKL display by NP delivery was a result of CLLP-induced increases in particle uptake. Although increases in average antigen display were observed for F4/80+ BMDCs on CLLP surfaces, they were not statistically significant (Figure 12B).

Chapter 3.2d: LAIR-1 KD Led to CLLP-induced Increases in SIINFEKL Antigen Display by F4/80+ BMDCs and Did Not Affect the CLLP-induced Increases in SIINFEKL Display by F4/80- BMDCs

To examine the role of LAIR-1 in antigen display, SIINFEKL-E2 delivery experiments were repeated using LAIR-1 knockdown cells (Figure 12A). We observed that when LAIR-1 expression was reduced, there was a ~50% increase in SIINFEKL display in F4/80+ BMDCs on CLLP surfaces when stimulated with LPS (Figure 12D). F4/80- LAIR-1 knockdown BMDCs also experienced an ~80% increase in SIINFEKL display when seeded onto CLLP surfaces relative to control surface, although only in the unstimulated condition (Figure 12E). The observation that knockdown of LAIR-1 rescues the CLLP-induced antigen display for F4/80+ BMDCs suggests that LAIR-1 may be inhibitory to the increase in uptake of E2-SIINFEKL facilitated by CLLP surfaces, which is also supported by the NP uptake data (Figure 11D).

Trends of increased SIINFEKL display were observed for both unstimulated non-target siRNA-treated cells and LPS-stimulated F4/80- LAIR-1 KD BMDCs (Figure 12E); however the differences were not statistically significant.

These results are consistent with my previous study, where we showed that knocking down LAIR-1 in macrophages enhanced CLLP-induced uptake [76]. This may be advantageous for vaccine design, where others have reported that the targeted delivery of vaccines to dendritic cells and increased antigen display may result in more robust adaptive immune responses, increasing the efficacy of the vaccines [113, 114]. For example, Bonifaz et al., found that in vivo targeting of antigens to maturing dendritic cells via the DEC-205 receptor increases the efficiency of vaccination for T cell immunity, including systemic and mucosal resistance in disease models [115]. Together, the results of the E2-SIINFEKL antigen delivery studies suggest that engineering LAIR-1 ligands into collagen-mimetic materials may provide a biomaterial strategy to increase vaccine efficacy through increases in vaccine uptake and antigen display by dendritic cells.

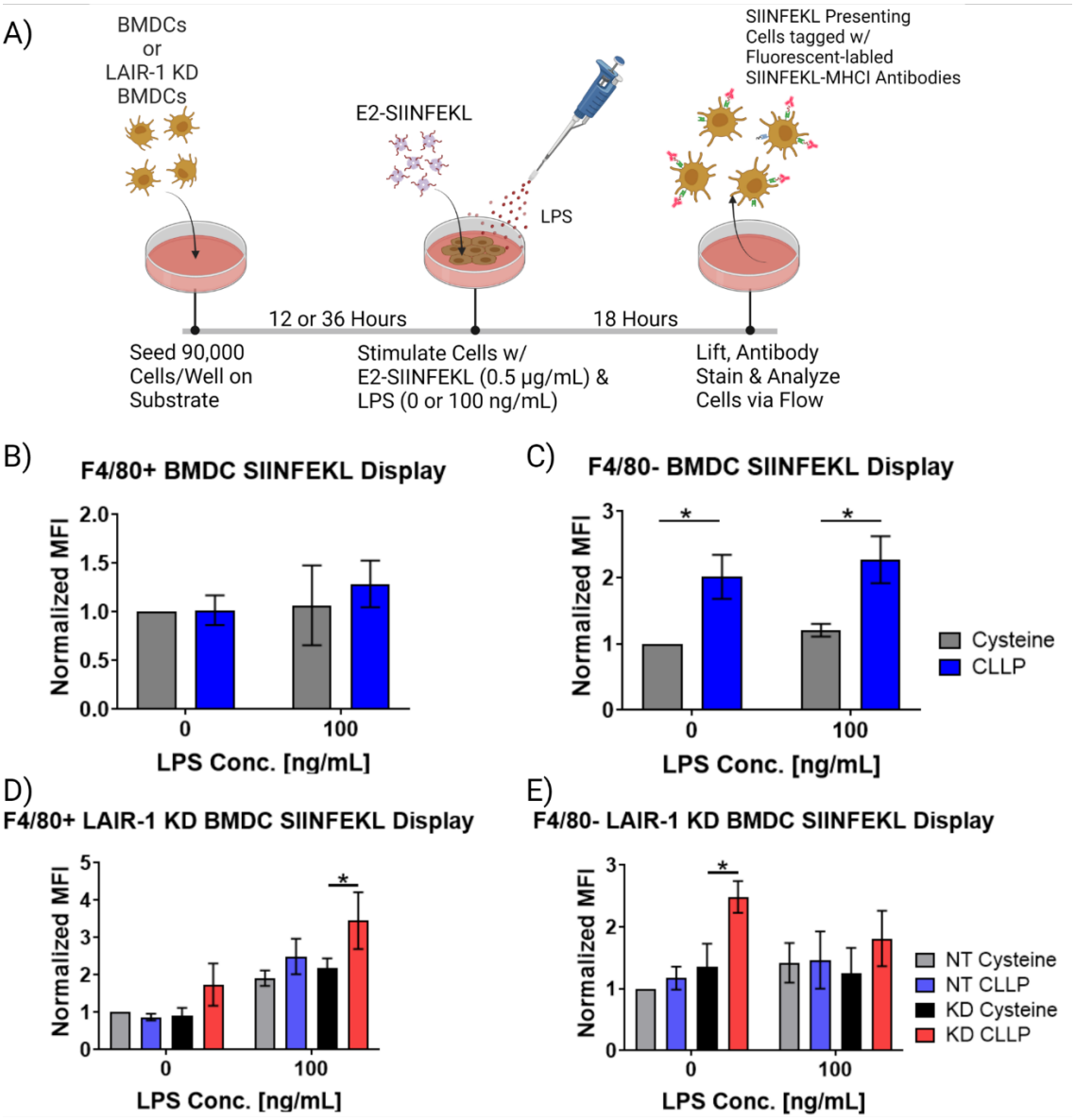

Figure 12: CLLP Surfaces Increase the SIINFEKL display of F4/80- BMDCs when SIINFEKL is delivered via E2 NPs. A) Experimental timeline of E2-SIINFEKL delivery to BMDCs and LAIR-1 KD BMDCs. BMDCs are incubated for 12 hours, and KD BMDCs are incubated for 36 hours, prior to LPS stimulation. B) Normalized MFI of MHC I-SIINFEKL display by LAIR-1 expressing F4/80+ cells, determined by antibody staining and flow cytometry. C) Normalized MFI of MHC I-SIINFEKL display by low LAIR-1 expressing F4/80- BMDCs. D) Normalized MFI of MHCI-SIINFEKL display by LAIR-1 knockdown (KD) and non-target (NT) F4/80+

BMDCs, determined by antibody staining and flow cytometry. E) Normalized MFI of MHCI-SIINFEKL display by naturally low LAIR-1 expressing F4/80- BMDCs treated with LAIR-1 siRNA or non-target siRNA, extent of SIINFEKL display was determined by antibody staining and flow cytometry. Values reported are average ± S.E.M., with N=4 independent biological replicates. Statistical significance was determined by two-way ANOVA with Bonferroni's post hoc test (*$p < 0.05$).

Chapter 3.3: Conclusion

The results of the experiments discussed in chapter 3 strongly support the conclusion that CLLP functionalized surfaces increase uptake by both BMDMs and BMDCs. This chapter also introduces the multifaceted immunomodulatory effect of CLLP and provides evidence that CLLP functionalized surfaces can modulate phagocyte behavior through pathways separate from (but not unaffected by) LAIR-1. Furthermore, experiments in this chapter suggest LAIR-1 engagement is inhibitory to uptake. Figure 13 is a graphical representation of the conclusions from chapter 3.

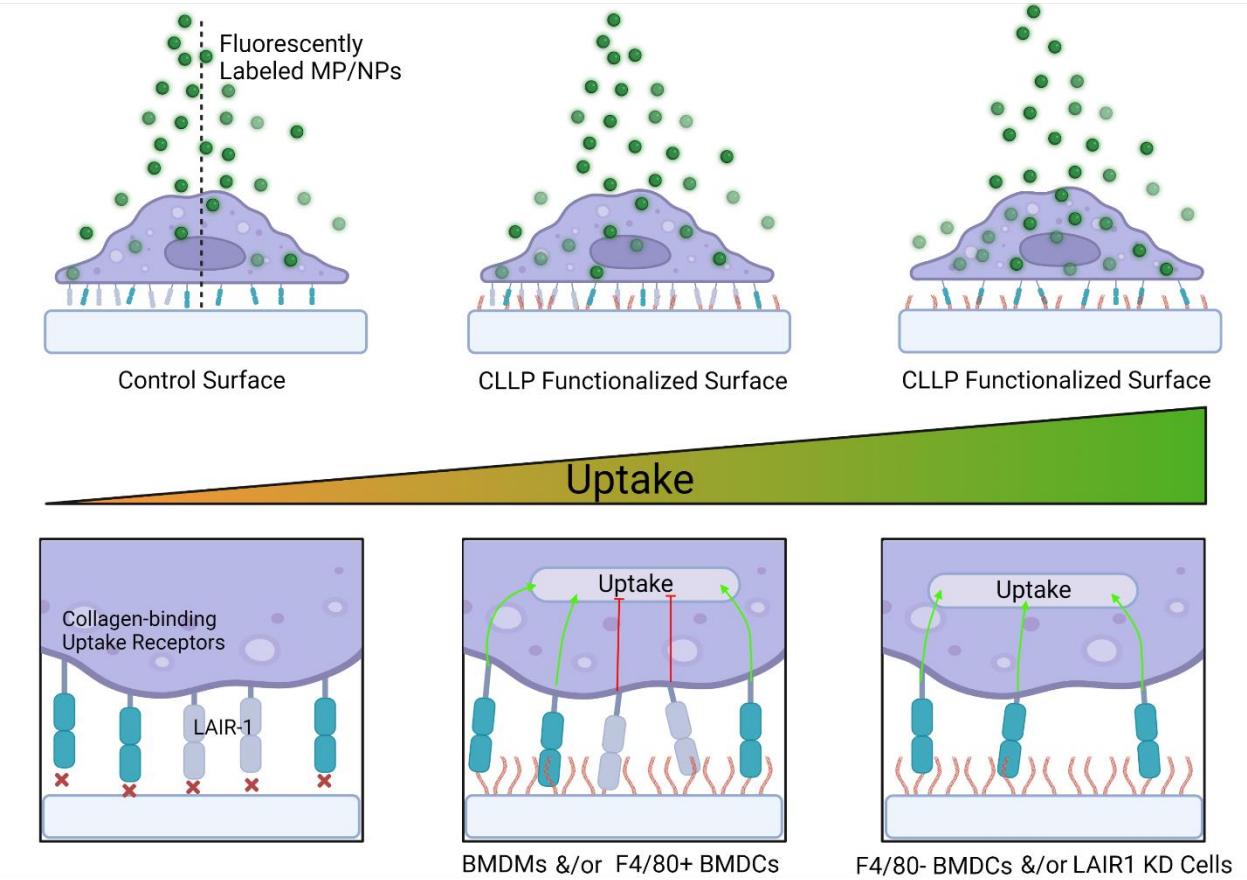

Figure 13: Graphical abstract summarizing the conclusions of chapter three, functionalizing cell culture surfaces with collagen mimetic high affinity LAIR-1 ligand peptides (CLLPs) increases the extent of uptake in murine bone marrow monocyte derived macrophages and dendritic cells, separately from the target receptor LAIR-1.

Chapter 4: Immunomodulatory Effects of NP Delivered CLLP

Scope of Chapter 4: Investigate the applications of CLLP functionalization and viability of NP delivered CLLP. Using CLLP conjugated E2 nanoparticles in vitro, examine the extent of immunomodulation induced via particle-delivered-CLLP.

- **4.1**: CLLP functionalized particles
  - 4.1a: BMDM Uptake of CLLP functionalized particles
  - 4.1b: BMDC Uptake of CLLP functionalized particles
- **4.2**: Chapter 4 conclusion

Chapter 4: Immunomodulatory Effects of NP Delivered CLLP

Chapter 4.1: Functionalizing the Exterior Surface of E2 Nanoparticle with CLLP

After characterizing the immunomodulatory effects of CLLP functionalized surfaces in vitro, we were curious to see if CLLP could be delivered to cells in vivo. In order to study the ability of particle delivered CLLP to effect immune cell behavior, it was decided that E2 protein nanoparticle would be used as the model delivery vehicle for CLLP. First the D381C mutant of E2 was internally functionalized with Alexa Fluor 488 fluorescent tags using thiol chemistry as previously described in the E2 nanoparticle uptake experiments (A.2.2.1). Next the native lysine's on the exterior of the internally loaded D381C E2 was reacted with a sulfo-SMCC linker, which in turn serves as the link binding CLLP to the surface of the E2 nanoparticle (A.3.1.0). The final conjugation efficiency of CLLP peptides to E2 subunits was 0.77 peptides per subunit, and the final size of the CLLP-E2-AF488 NP was 39.6 nm with a PDI of 0.19 (A.3.1.1)(A.3.1.2). The experimental protocol utilized to investigate CLLP's ability to maintain it previously reported immunomodulatory function when chemically conjugated to and delivered by nanoparticles is described in the appendix (A.3.1.3).

Chapter 4.1a: Functionalizing E2 Nanoparticles with CLLP Reduced BMDM Uptake

The results of the CLLP NP uptake experiments were in stark contrast to the results of surface functionalized CLLP experiments. BMDMs were seeded on cysteine conjugated surfaces as previously described (A.3.1.3), differentiated into different phenotypes using cytokines and stimulated with either E2 or CLLP-E2 NPs (Figure 14A). Functionalizing the surface of E2 with CLLP drastically reduced the uptake of the particle by BMDMs, nearly a 3-fold significant

reduction in uptake was observed in every BMDM phenotype investigated (Figure 14B). When analyzing the production of TNFα by activated BMDMs, cells that were incubated with CLLP-E2 experienced ~50% reduced TNFα production compared to cells incubated with E2 (Figure 14C). The presence of nanoparticles significantly increased the inflammatory activation of BMDMs when compared to cells on cysteine surfaces without nanoparticles (Figure 12C), however E2-CLLP nanoparticles reduced the TNFα production to the level of cells stimulated without nanoparticles. In fact, cells that were incubated with E2-CLLP on cysteine surfaces had non-significant differences compared to cells on CLLP surfaces without nanoparticles (Figure 12C).

The conclusion of this study provided evidence that functionalizing CLLP to the surfaces of E2 nanoparticles significantly reduced the uptake of the said particles compared to unfunctionalized E2. Secondly it was observed that CLLP delivered to BMDMs via nanoparticles successfully inhibited the inflammatory activation of BMDMs to an extent similar to that of CLLP functionalized surfaces. The reduction of TNFα by E2-CLLP strongly suggest LAIR-1 engagement. We further hypothesized that the observed decrease in E2-CLLP uptake may be a result of targeted LAIR-1 interactions (as previously described LAIR-1 was determined to be inhibitory to macrophage uptake). In order to indirectly study the role of LAIR-1 in E2-CLLP uptake, BMDC uptake of E2-CLLP was studied.

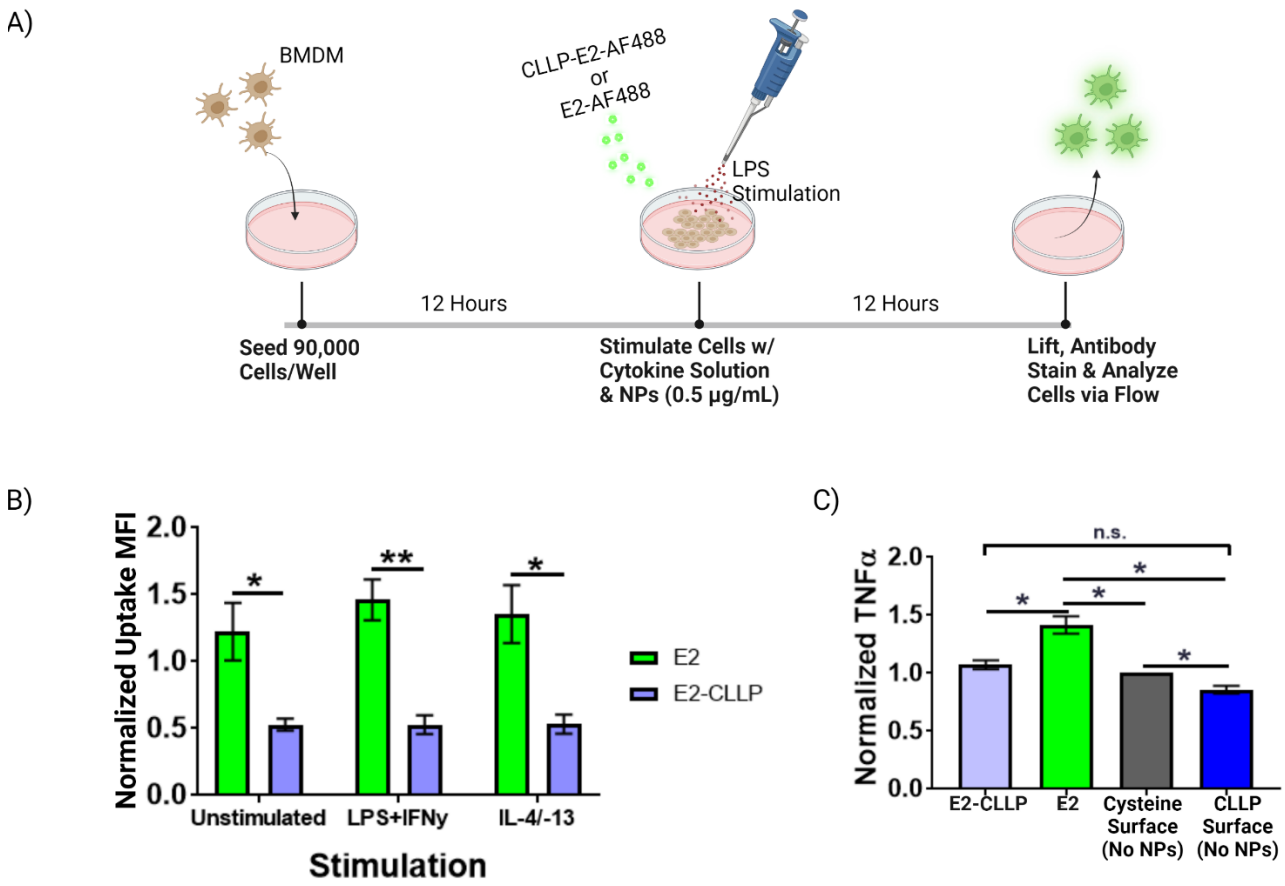

Figure 14: Functionalizing E2 with CLLP reduces uptake and TNFα production by BMDMs A) Experimental timeline used to study the immunomodulatory effects of CLLP functionalization on protein nanoparticle uptake by BMDMs. BMDMs are incubated for 12 hours, prior to cytokine and nanoparticle stimulation. Cells were then allowed to incubate for an additional 12 hours before being analyzed for extent of uptake via flow cytometry. B) Normalized uptake MFI of AlexaFluor488 (AF488)-conjugated E2 protein nanoparticles functionalized with and without CLLP by LAIR-1 expressing BMDMs determined via flow cytometry. C) Normalized TNFα produced by BMDMs when stimulated with pro-inflammatory compounds and either incubated with E2-CLLP, unfunctionalized E2 or no nanoparticles at all. Cells that received no nanoparticles were either seeded on cysteine surfaces or CLLP functionalize surfaces.

<u>Chapter 4.1b</u>: Functionalizing E2 Nanoparticles with CLLP Reduced F4/80+ BMDC but Not F4/80- BMDC Uptake

After observing a reduction in uptake by BMDMs when E2 was functionalized with CLLP, we were interested in analyzing the effect of particle delivered CLLP on BMDCs, particularly because of the heterogeneous LAIR-1 expression in BMDC subpopulations. We hypothesized that LAIR-1 expression would affect the way cells responded to CLLP-E2. BMDCs were seeded onto control surfaces stimulated with LPS and incubated with either E2 or CLLP-E2 as previously described (A.3.1.3) (Figure 15A).

The results of the CLLP-E2 uptake experiments in BMDCs were in part consistent with BMDM experiments and support the hypothesis that LAIR-1 expression affects the way cells respond to CLLP-E2. It was observed that F4/80+ BMDCs experienced a significant reduction in uptake of NPs when incubated with CLLP-E2 compared to E2 controls (Figure 15B). In contrast F4/80- BMDCs experienced no change in uptake of CLLP-E2 compared to E2 controls (Figure 15C). The results of these CLLP-E2 uptake experiments in BMDCs suggest that CLLP-E2 uptake is inhibited via LAIR-1. As previously mentioned F4/80+ BMDCs have a significantly higher LAIR-1 expression than F4/80- BMDCs, which have little to no LAIR-1 expression.

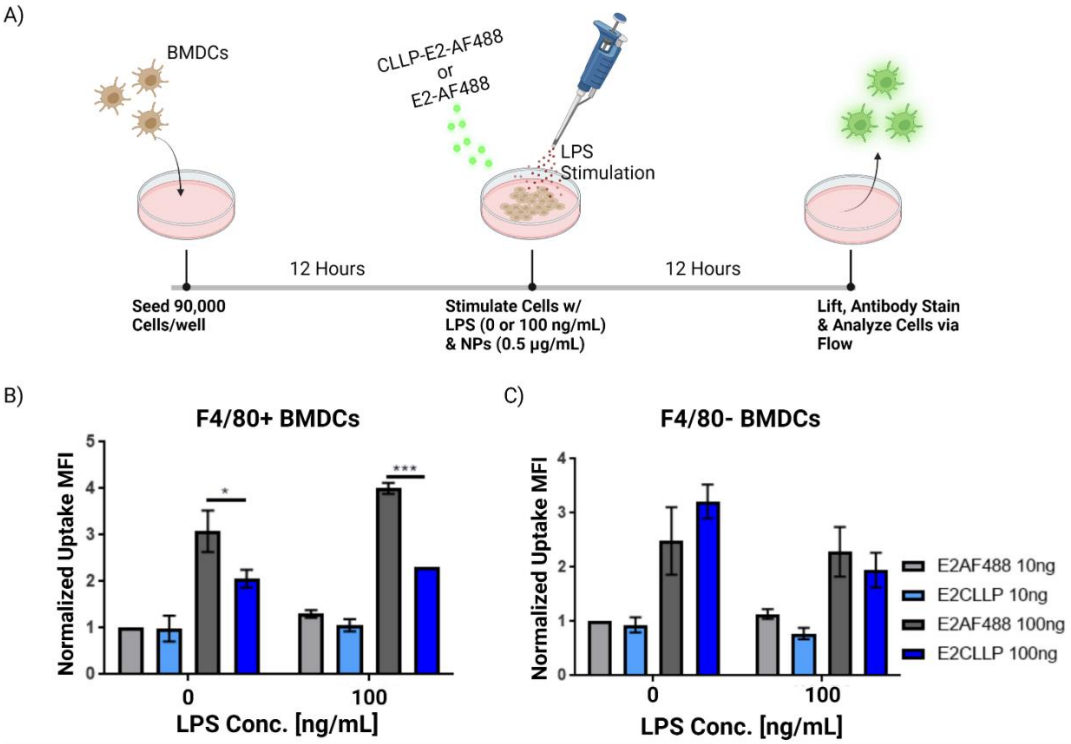

Figure 15: Functionalizing E2 with CLLP reduces uptake by F4/80+ BMDCs but not F4/80- BMDCs A) Experimental timeline used to study the immunomodulatory effects of CLLP functionalization on protein nanoparticle uptake by BMDCs. BMDCs are incubated for 12 hours, prior to LPS stimulation and Nanoparticle stimulation and then allowed to incubate for an additional 12 hours before being analyzed for extent of uptake via flow cytometry. B) Normalized uptake MFI of AlexaFluor488 (AF488)-conjugated E2 protein nanoparticles functionalized with and without CLLP by LAIR-1 expressing F4/80+ BMDCs (stimulated with and without LPS) determined via flow cytometry. C) Normalized uptake MFI of AlexaFluor488 (AF488)-conjugated E2 protein nanoparticles functionalized with and without CLLP by F4/80- BMDCs, which have little to no LAIR-1 expression, cysteine-conjugated surfaces.

Chapter 4.2: Conclusion

The experiments in chapter 4 demonstrate the ability of CLLP functionalized particles to successfully inhibit BMDM activation in vitro (Figure 14C). In contrast to CLLP functionalized surfaces, functionalizing nanoparticles with CLLP significantly reduced the uptake of the particle only by LAIR-1 expressing phagocytes such as BMDMs and F4/80+ BMDCs (Figure 14B) (Figure 15B) but not F4/80- BMDCs (Figure 15C). It was hypothesized based on the trends of uptake in the BMDC subpopulations that the uptake of E2-CLLP was being reduced via LAIR-1. These interesting results allude to another potential application of CLLP particles. Peripheral macrophage and monocyte uptake of nanoparticle delivered drugs remains a significant barrier to targeted nanoparticle therapeutics [116, 117]. Reducing the uptake by macrophage and macrophage-like cells could potentially increase the bioavailability of nanoparticle therapeutics. Furthermore, F4/80- BMDCs (cells that more closely resemble dendritic cells in vivo) did not experience significant reduction in uptake (Figure 15C). Meaning that by reducing macrophage uptake of nanoparticles, CLLP functionalization may be able to increase targeted delivery and uptake by dendritic cells, which would potentially increase the effectiveness of targeted dendritic cell therapies such as vaccines [113, 114, 118]. Overall, more research is needed on the potential applications of CLLP functionalized nanoparticles, particularly in vivo research.

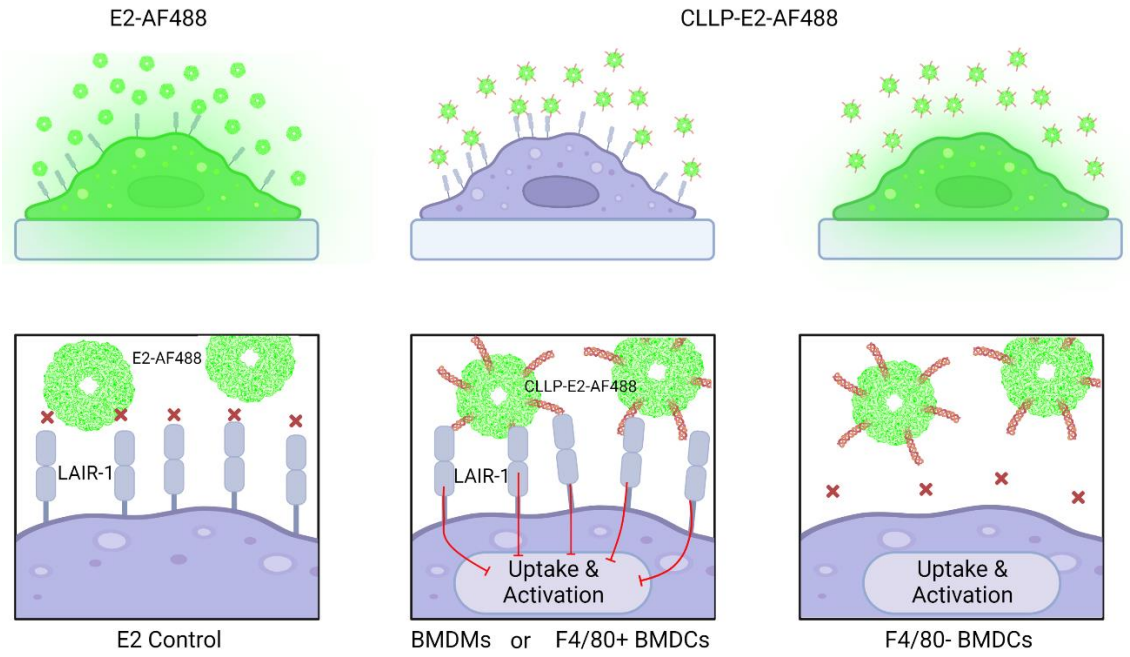

Figure 16: **G**raphical abstract summarizing the conclusions of chapter four. Functionalizing E2 nanoparticles with CLLP reduced the uptake of the particle by BMDMs and F4/80+ BMDCs, but not F4/80- BMDCs. Furthermore, delivering CLLP via nanoparticles successfully reduced the production of TNFα by inflamed BMDMs. Chapter four demonstrates some of the potential of nanoparticle functionalized CLLP as a deliverable anti-inflammatory therapy and postulates at further potential applications.

Chapter 5: Future Directions & Conclusion

Scope of Chapter 5: Discuss possible future directions of research and concluding remarks on the observed immunomodulatory effects of CLLP.

Chapter 5.1: Investigate the effects of CLLP functionalization on NP bioavailability and biodistribution *in vivo*

Chapter 5.2: Unanswered questions in need of research

Chapter 5.3: Conclusion

Chapter 5.1: Effect of CLLP Functionalization on NP Bioavailability & Biodistribution *in Vivo*

As previously mentioned, peripheral macrophage and monocyte uptake of nanoparticle delivered drugs remains a significant barrier to targeted nanoparticle therapeutics [116, 117]. Reducing the uptake by LAIR-1 expressing macrophage and macrophage-like cells could potentially increase the bioavailability of nanoparticle therapeutics. In order to provide evidence towards this hypothesis bioavailability experiments should be conducted in the future. For example, E2-AF488 could be functionalized with CLLP as previously described and injected into mice, via different injection routes, in order to study how CLLP functionalization affects the trafficking of NPs in the body.

To determine the differences in bioavailability and biodistribution between E2-AF488 and E2-AF488-CLLP, mice would be sacrificed at different time points and analyzed using microscopy and flow cytometry. Depending on the method of injection various points of interest would be analyzed using different techniques. For intravenous injection organs of interest, such as lymph nodes, liver, spleen, etc., will be harvested and analyzed for fluorescent signal using microscopy. Afterwards cells will be separated from tissue/organs, stained with cell-type markers and analyzed for NP uptake via flow cytometry. Peripheral blood will also be collected at different time points in order to determine circulating NP concentration via flow cytometry. Analysis of other injection routes, such as subcutaneous or intramuscular, should be analyzed in the same way as previously described for intravenous injection. Additionally, these more local injection routes should also be analyzed via tissue sectioning, staining and microscopy at the site

of injection, in order to study the effect of CLLP functionalization on NP uptake by tissue resident immune cells, such as macrophages. Figure 17 demonstrates a potential experimental timeline designed to analyze the difference in NP bioavailability and biodistribution caused by CLLP functionalization (Figure 17).

From the conclusions made in chapters 3 and 4, that LAIR-1 is inhibitory to uptake and functionalizing NPs with CLLP reduced uptake by LAIR-1 expressing cells in vitro, it was hypothesized that functionalizing NPs with CLLP would affect both the bioavailability and biodistribution of NPs *in vivo*. Specifically, it was hypothesized that reduced uptake by macrophages and macrophage-like cells would lead to increased bioavailability in the tissue microenvironment for local injections such as intramuscular or subcutaneous, and increased free NP concentration in peripheral circulation for intravenous injection. Increases in NP bioavailability, caused by a reduction in non-specific uptake, may potentially lead to more efficient and effective drug delivery to intended targets, effectively changing the biodistribution of the particle. Further supported by the conclusion in chapter 4, that F4/80- BMDCs did not experience decreases in uptake when NPs were functionalized by CLLP, it was postulated that decreasing uptake by macrophages and macrophage-like cells may increase the NP concentration accessible to resident dendritic cells for uptake. It was hypothesized that increasing effective delivery of CLLP NPs to dendritic cells may significantly increase the trafficking of NPs to organs such as the lymph nodes. As previously mentioned, increasing delivery of NPs to dendritic cells, by increasing the bioavailability of NPs via CLLP functionalization, potentially could increase the effectiveness of targeted dendritic cell therapies such as vaccines [113, 114, 118].

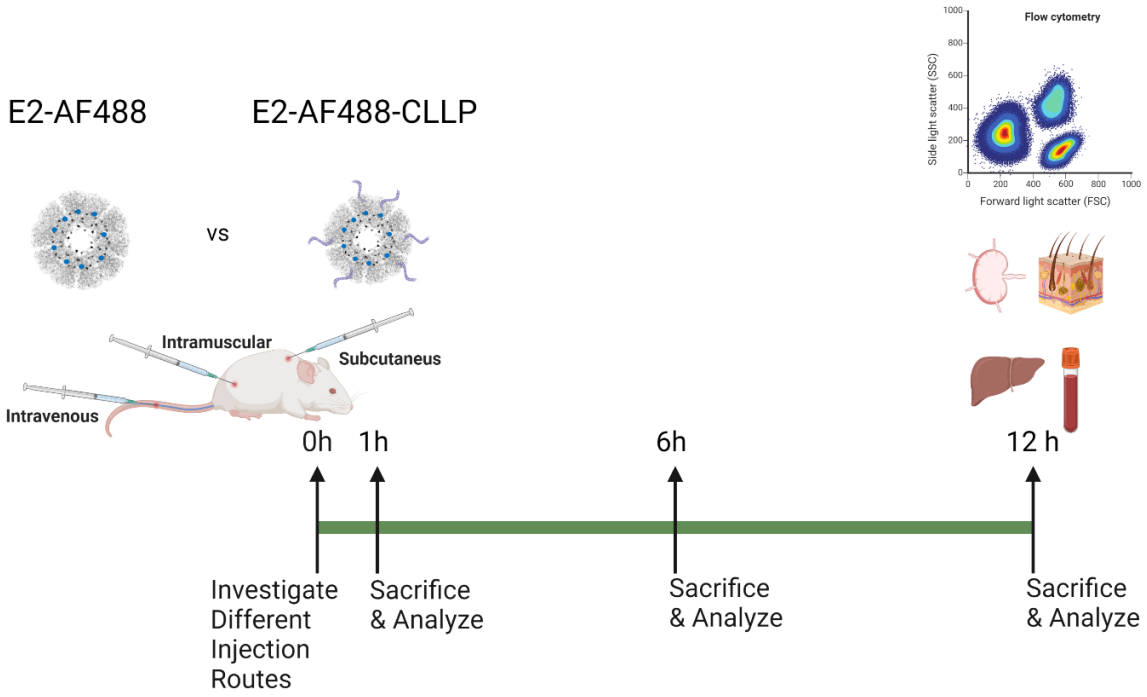

Figure 17: Potential experimental timeline designed to study the effects of CLLP functionalization on NP bioavailability and biodistribution via different injection routes. Image in part done in collaboration with Enya Li.

Chapter 5.2: Unanswered Questions in Need of Research

One of the most pressing questions that arose from the experiments conducted in this thesis is why does the method of CLLP delivery (i.e. surface functionalized CLLP, compared to NP functionalized CLLP) drastically change the immunomodulatory effect of CLLP on uptake? As chapter 3 showed, surface functionalized CLLP significantly increased uptake by BMDMs and BMDCs, independently of the target receptor LAIR-1. On the other hand, the conclusion from chapter 4 clearly showed functionalizing NPs with CLLP drastically reduced uptake, seemingly through LAIR-1 signaling, as supported by the fact that F4/80- BMDCs experienced no inhibition of uptake due to CLLP functionalized NPs (Figure 15). In order to begin to make sense of these seemingly contrasting results, it is important to remember the context of collagen

LAIR-1 ligands in vivo and how they function to transition inflammation towards resolution, as well as initiate clearance.

A traditional signal that the transition away from acute inflammation has begun is the deposition of collagen. As previously mentioned during resolution macrophages direct surrounding cells to deposit collagen, and over time as resolution of inflammation progresses the extent of collagen deposition and cross-linking (aka stiffening) increases [4][10]. Initially the newly deposited collagen is not extensively crosslinked and thus remains physiologically soft, during this time the main function of macrophages is to transition away from inflammation towards anti-inflammatory phenotypes [4]. At the end of resolution, marked by the clearance of apoptotic cells, the newly deposited collagen is much stiffer than the collagen deposited during early on in resolution [10]. The stiffer collagen environment that is temporally associated with an increase clearance of apoptotic cells in the inflammatory response, is much like a CLLP functionalized surface (when compared to the soft newly deposited collagen at the beginning of resolution). While the softer uncross-linked collagen proteins may be better represented by CLLP functionalized NPs. It was hypothesized that stiffness, and/or mechanotransduction, may play a role in how the immunomodulatory effects of CLLP are experienced by cells. Mechanotransduction is defined as the ability of a cell to actively sense, integrate, and convert mechanical stimuli into biochemical signals that result in intracellular changes, such as ion concentrations, activation of signaling pathways and transcriptional regulation. It has been shown in literature that the stiffness of a collagen material can affect the way a cell behaves [119]. It was postulated that over time the stiffening of collagen in the cellular microenvironment may help transition inhibited, anti-inflammatory macrophages, towards uptake and clearance. Therefore, it was hypothesized that functionalizing materials of different stiffness with CLLP

may alter the way CLLP affects uptake by macrophages and dendritic cells.

Chapter 5.3: Conclusion

Overall, the studies covered in this dissertation demonstrate the potential of collagen-mimetic LAIR-1 ligand peptides as a deliverable anti-inflammatory biomaterial with uniquely advantageous immunomodulatory effects on phagocyte uptake. It was determined that CLLP inhibits inflammatory activation via the target receptor LAIR-1. CLLP functionalized surfaces were found to increase the uptake by both macrophages and dendritic cells in a way independent of LAIR-1. F4/80- dendritic cells also experienced increased antigen display on CLLP surfaces when antigens were delivered to cells via nanoparticles. Moreover, the knockdown experiments performed in this dissertation provided evidence that LAIR-1 is inhibitory towards uptake. Which was further supported by the observed decrease in E2-CLLP uptake by LAIR-1 expressing phagocytes and the significant decrease in inflammatory activation of macrophages incubated with E2-CLLP. Not only does this dissertation provide potential applications of CLLP it also illuminates a nexus of regulatory control over innate immune function governed by LAIR-1 expression and the presence of LAIR-1 ligands (such as collagen) in the surrounding microenvironment. More research is needed to implement the potential applications of CLLP functionalized materials, as well as understand how the context of LAIR-1 ligands changes the overall immunomodulatory response to them.

References:

[1] J.R. Dunkelberger, W.C. Song, Complement and its role in innate and adaptive immune responses, Cell Res 20(1) (2010) 34-50.

[2] I. Aukhil, Biology of wound healing, Periodontol 2000 22 (2000) 44-50.

[3] M.E. Kotas, R. Medzhitov, Homeostasis, inflammation, and disease susceptibility, Cell 160(5) (2015) 816-827.

[4] C.N. Serhan, J. Savill, Resolution of inflammation: the beginning programs the end, Nat Immunol 6(12) (2005) 1191-7.

[5] E.E. Tuppo, H.R. Arias, The role of inflammation in Alzheimer's disease, Int J Biochem Cell Biol 37(2) (2005) 289-305.

[6] D. Furman, J. Campisi, E. Verdin, P. Carrera-Bastos, S. Targ, C. Franceschi, L. Ferrucci, D.W. Gilroy, A. Fasano, G.W. Miller, A.H. Miller, A. Mantovani, C.M. Weyand, N. Barzilai, J.J. Goronzy, T.A. Rando, R.B. Effros, A. Lucia, N. Kleinstreuer, G.M. Slavich, Chronic inflammation in the etiology of disease across the life span, Nat Med 25(12) (2019) 1822-1832.

[7] P. Hunter, The inflammation theory of disease. The growing realization that chronic inflammation is crucial in many diseases opens new avenues for treatment, EMBO Rep 13(11) (2012) 968-70.

[8] Y. Araki, T. Mimura, The Mechanisms Underlying Chronic Inflammation in Rheumatoid Arthritis from the Perspective of the Epigenetic Landscape, J Immunol Res 2016 (2016) 6290682.

[9] Y.C. Liu, X.B. Zou, Y.F. Chai, Y.M. Yao, Macrophage polarization in inflammatory diseases, Int J Biol Sci 10(5) (2014) 520-9.

[10] T.J. Koh, L.A. DiPietro, Inflammation and wound healing: the role of the macrophage, Expert Rev Mol Med 13 (2011).

[11] C.L. Bennett, A. Misslitz, L. Colledge, T. Aebischer, C.C. Blackburn, Silent infection of bone marrow-derived dendritic cells by Leishmania mexicana amastigotes, Eur J Immunol 31(3) (2001) 876-883.

[12] C. Bogdan, U. Schleicher, Comment on "TLR9-Dependent Activation of Dendritic Cells by DNA from Leishmania major Favors Th1 Cell Development and the Resolution of Lesions", J Immunol 183(11) (2009) 6859-6859.

[13] B.A. Imhof, M. Aurrand-Lions, Adhesion mechanisms regulating the migration of monocytes, Nat Rev Immunol 4(6) (2004) 432-444.

[14] A. Koutoulaki, M. Langley, A.J. Sloan, D. Aeschlimann, X.Q. Wei, TNF alpha and TGF-beta 1 influence IL-18-induced IFN gamma production through regulation of IL-18 receptor and T-bet expression, Cytokine 49(2) (2010) 177-184.

[15] N. Yamashita, H. Tashimo, Y. Matsuo, H. Ishida, K. Yoshiura, K. Sato, N. Yamashita, T. Kakiuchi, K. Ohta, Role of CCL21 and CCL19 in allergic inflammation in the ovalbumin-specific murine asthmatic model, J Allergy Clin Immun 117(5) (2006) 1040-1046.

[16] S.E. Adamson, N. Leitinger, The role of pannexin1 in the induction and resolution of inflammation, Febs Lett 588(8) (2014) 1416-1422.

[17] P. Blanco, A.K. Palucka, V. Pascual, J. Banchereau, Dendritic cells and cytokines in human inflammatory and autoimmune diseases, Cytokine Growth F R 19(1) (2008) 41-52.

[18] E. Vivier, M. Daeron, Immunoreceptor tyrosine-based inhibition motifs, Immunol Today 18(6) (1997) 286-91.

[19] T.A. Steevels, R.J. Lebbink, G.H. Westerlaken, P.J. Coffer, L. Meyaard, Signal inhibitory receptor on leukocytes-1 is a novel functional inhibitory immune receptor expressed on human phagocytes, J Immunol 184(9) (2010) 4741-8.

[20] T.A.M. Steevels, L. Meyaard, Immune inhibitory receptors: Essential regulators of phagocyte function, Eur J Immunol 41(3) (2011) 575-587.

[21] L. Meyaard, The inhibitory collagen receptor LAIR-1 (CD305), J Leukocyte Biol 83(4) (2008) 799-803.

[22] M. Daeron, S. Jaeger, L. Du Pasquier, E. Vivier, Immunoreceptor tyrosine-based inhibition motifs: a quest in the past and future, Immunol Rev 224 (2008) 11-43.

[23] A. Verbrugge, E.S. Rijkers, T. de Ruiter, L. Meyaard, Leukocyte-associated Ig-like receptor-1 has SH2 domain-containing phosphatase-independent function and recruits C-terminal Src kinase, Eur J Immunol 36(1) (2006) 190-8.

[24] U. Lorenz, SHP-1 and SHP-2 in T cells: two phosphatases functioning at many levels, Immunol Rev 228(1) (2009) 342-59.

[25] T.V. Nguyen, Y. Ke, E.E. Zhang, G.S. Feng, Conditional deletion of Shp2 tyrosine phosphatase in thymocytes suppresses both pre-TCR and TCR signals, J Immunol 177(9) (2006) 5990-6.

[26] L.M. Chow, M. Fournel, D. Davidson, A. Veillette, Negative regulation of T-cell receptor signalling by tyrosine protein kinase p50csk, Nature 365(6442) (1993) 156-60.

[27] Z. Honda, T. Suzuki, N. Hirose, M. Aihara, T. Shimizu, S. Nada, M. Okada, C. Ra, Y. Morita, K. Ito, Roles of C-terminal Src kinase in the initiation and the termination of the high affinity IgE receptor-mediated signaling, J Biol Chem 272(41) (1997) 25753-60.

[28] T. Vang, H. Abrahamsen, S. Myklebust, J. Enserink, H. Prydz, T. Mustelin, M. Amarzguioui, K. Tasken, Knockdown of C-terminal Src kinase by siRNA-mediated RNA interference augments T cell receptor signaling in mature T cells, Eur J Immunol 34(8) (2004) 2191-9.

[29] R.M. Thomas, C. Schmedt, M. Novelli, B.K. Choi, J. Skok, A. Tarakhovsky, J. Roes, C-terminal SRC kinase controls acute inflammation and granulocyte adhesion, Immunity 20(2) (2004) 181-91.

[30] L. Meyaard, G.J. Adema, C. Chang, E. Woollatt, G.R. Sutherland, L.L. Lanier, J.H. Phillips, LAIR-1, a novel inhibitory receptor expressed on human mononuclear leukocytes, Immunity 7(2) (1997) 283-90.

[31] R.J. Lebbink, T. de Ruiter, J. Adelmeijer, A.B. Brenkman, J.M. van Helvoort, M. Koch, R.W. Farndale, T. Lisman, A. Sonnenberg, P.J. Lenting, L. Meyaard, Collagens are functional, high affinity ligands for the inhibitory immune receptor LAIR-1, J Exp Med 203(6) (2006) 1419-1425.

[32] R.J. Lebbink, T. de Ruiter, G.J. Kaptijn, D.G. Bihan, C.A. Jansen, P.J. Lenting, L. Meyaard, Mouse leukocyte-associated Ig-like receptor-1 (mLAIR-1) functions as an inhibitory collagen-binding receptor on immune cells, Int Immunol 19(8) (2007) 1011-9.

[33] R.J. Lebbink, N. Raynal, T. de Ruiter, D.G. Bihan, R.W. Farndale, L. Meyaard, Identification of multiple potent binding sites for human leukocyte associated Ig-like receptor LAIR on collagens II and III, Matrix Biology 28(4) (2009) 202-210.

[34] Y. Zhang, K. Lv, C.M. Zhang, B.Q. Jin, R. Zhuang, Y. Ding, The role of LAIR-1 (CD305) in T cells and monocytes/macrophages in patients with rheumatoid arthritis, Cell Immunol 287(1) (2014) 46-52.

[35] V.V. Agashe, E. Jankowska-Gan, M. Keller, J.A. Sullivan, L.D. Haynes, J.F. Kernien, J.R. Torrealba, D. Roenneburg, M. Dart, M. Colonna, D.S. Wilkes, W.J. Burlingham, Leukocyte-Associated Ig-like Receptor 1 Inhibits Th1 Responses but Is Required for Natural and Induced Monocyte-Dependent Th17 Responses, J Immunol 201(2) (2018) 772-781.

[36] L.A. Casciola-Rosen, G. Anhalt, A. Rosen, Autoantigens targeted in systemic lupus erythematosus are clustered in two populations of surface structures on apoptotic keratinocytes, J Exp Med 179(4) (1994) 1317-30.

[37] D. Mevorach, J.O. Mascarenhas, D. Gershov, K.B. Elkon, Complement-dependent clearance of apoptotic cells by human macrophages, J Exp Med 188(12) (1998) 2313-20.

[38] D. Mevorach, J.L. Zhou, X. Song, K.B. Elkon, Systemic exposure to irradiated apoptotic cells induces autoantibody production, J Exp Med 188(2) (1998) 387-92.

[39] N.M. Thielens, F. Tedesco, S.S. Bohlson, C. Gaboriaud, A.J. Tenner, C1q: A fresh look upon an old molecule, Mol Immunol 89 (2017) 73-83.

[40] S.S. Bohlson, D.A. Fraser, A.J. Tenner, Complement proteins C1q and MBL are pattern recognition molecules that signal immediate and long-term protective immune functions, Mol Immunol 44(1-3) (2007) 33-43.

[41] D.A. Fraser, S.S. Bohlson, N. Jasinskiene, N. Rawal, G. Palmarini, S. Ruiz, R. Rochford, A.J. Tenner, C1q and MBL, components of the innate immune system, influence monocyte cytokine expression, J Leukoc Biol 80(1) (2006) 107-16.

[42] M.E. Benoit, E.V. Clarke, A.J. Tenner, C1q Binding to and Uptake of Apoptotic Lymphocytes by Human Monocyte-derived Macrophages, Bio Protoc 3(17) (2013).

[43] M.E. Benoit, E.V. Clarke, P. Morgado, D.A. Fraser, A.J. Tenner, Complement protein C1q directs macrophage polarization and limits inflammasome activity during the uptake of apoptotic cells, J Immunol 188(11) (2012) 5682-93.

[44] J. Hughes, Y. Liu, J. Van Damme, J. Savill, Human glomerular mesangial cell phagocytosis of apoptotic neutrophils: mediation by a novel CD36-independent vitronectin receptor/thrombospondin recognition mechanism that is uncoupled from chemokine secretion, J Immunol 158(9) (1997) 4389-97.

[45] V.A. Fadok, P.P. McDonald, D.L. Bratton, P.M. Henson, Regulation of macrophage cytokine production by phagocytosis of apoptotic and post-apoptotic cells, Biochem Soc Trans 26(4) (1998) 653-6.

[46] V.A. Fadok, D.L. Bratton, A. Konowal, P.W. Freed, J.Y. Westcott, P.M. Henson, Macrophages that have ingested apoptotic cells in vitro inhibit proinflammatory cytokine production through autocrine/paracrine mechanisms involving TGF-beta, PGE2, and PAF, J Clin Invest 101(4) (1998) 890-8.

[47] M. Son, B. Diamond, B.T. Volpe, C.B. Aranow, M.C. Mackay, F. Santiago-Schwarz, Evidence for C1q-mediated crosslinking of CD33/LAIR-1 inhibitory immunoreceptors and biological control of CD33/LAIR-1 expression, Sci Rep-Uk 7 (2017).

[48] M. Son, A. Porat, M.Z. He, J. Suurmond, F. Santiago-Schwarz, U. Andersson, T.R. Coleman, B.T. Volpe, K.J. Tracey, Y. Al-Abed, B. Diamond, C1q and HMGB1 reciprocally regulate human macrophage polarization, Blood 128(18) (2016) 2218-2228.

[49] X. Tang, L. Tian, G. Esteso, S.C. Choi, A.D. Barrow, M. Colonna, F. Borrego, J.E. Coligan, Leukocyte-associated Ig-like receptor-1-deficient mice have an altered immune cell phenotype, J Immunol 188(2) (2012) 548-58.

[50] T. Carvalheiro, S. Garcia, M.I. Pascoal Ramos, B. Giovannone, T. Radstake, W. Marut, L. Meyaard, Leukocyte Associated Immunoglobulin Like Receptor 1 Regulation and Function on Monocytes and Dendritic Cells During Inflammation, Front Immunol 11 (2020) 1793.
[51] X.L. Kang, J. Kim, M. Deng, S. John, H.Y. Chen, G.J. Wu, H. Phan, C.C. Zhang, Inhibitory leukocyte immunoglobulin-like receptors: Immune checkpoint proteins and tumor sustaining factors, Cell Cycle 15(1) (2016) 25-40.
[52] X.L. Kang, Z.G. Lu, C.H. Cui, M. Deng, Y.Q. Fan, B.J. Dong, X. Han, F.C. Xie, J.W. Tyner, J.E. Coligan, R.H. Collins, X.S. Xiao, M.J. You, C.C. Zhang, The ITIM-containing receptor LAIR1 is essential for acute myeloid leukaemia development, Nat Cell Biol 17(5) (2015) 665-U286.
[53] J.E. Park, D.D. Brand, E.F. Rosloniec, A.K. Yi, J.M. Stuart, A.H. Kang, L.K. Myers, Leukocyte-associated immunoglobulin-like receptor 1 inhibits T-cell signaling by decreasing protein phosphorylation in the T-cell signaling pathway, J Biol Chem 295(8) (2020) 2239-2247.
[54] S. Kim, E.R. Easterling, L.C. Price, S.L. Smith, J.E. Coligan, J.E. Park, D.D. Brand, E.F. Rosloniec, J.M. Stuart, A.H. Kang, L.K. Myers, The Role of Leukocyte-Associated Ig-like Receptor-1 in Suppressing Collagen-Induced Arthritis, J Immunol 199(8) (2017) 2692-2700.
[55] I. Bonaccorsi, C. Cantoni, P. Carrega, D. Oliveri, G. Lui, R. Conte, M. Navarra, R. Cavaliere, E. Traggiai, M. Gattorno, A. Martini, M.C. Mingari, A. Moretta, G. Ferlazzo, The immune inhibitory receptor LAIR-1 is highly expressed by plasmacytoid dendritic cells and acts complementary with NKp44 to control IFNalpha production, PLoS One 5(11) (2010) e15080.
[56] L. Meyaard, LAIR and collagens in immune regulation, Immunol Lett 128(1) (2010) 26-28.
[57] T.H. Brondijk, T. de Ruiter, J. Ballering, H. Wienk, R.J. Lebbink, H. van Ingen, R. Boelens, R.W. Farndale, L. Meyaard, E.G. Huizinga, Crystal structure and collagen-binding site of

immune inhibitory receptor LAIR-1: unexpected implications for collagen binding by platelet receptor GPVI, Blood 115(7) (2010) 1364-73.

[58] T.P. Rygiel, E.H. Stolte, T. de Ruiter, M.L. van de Weijer, L. Meyaard, Tumor-expressed collagens can modulate immune cell function through the inhibitory collagen receptor LAIR-1, Mol Immunol 49(1-2) (2011) 402-6.

[59] L. Meyaard, LAIR and collagens in immune regulation, Immunol Lett 128(1) (2010) 26-8.

[60] K. Gelse, E. Poschl, T. Aigner, Collagens--structure, function, and biosynthesis, Adv Drug Deliv Rev 55(12) (2003) 1531-46.

[61] B. Leitinger, Transmembrane collagen receptors, Annu Rev Cell Dev Biol 27 (2011) 265-90.

[62] H. Xu, N. Raynal, S. Stathopoulos, J. Myllyharju, R.W. Farndale, B. Leitinger, Collagen binding specificity of the discoidin domain receptors: binding sites on collagens II and III and molecular determinants for collagen IV recognition by DDR1, Matrix Biol 30(1) (2011) 16-26.

[63] A.T. Rowley, R.R. Nagalla, S.W. Wang, W.F. Liu, Extracellular Matrix-Based Strategies for Immunomodulatory Biomaterials Engineering, Advanced Healthcare Materials 8(8) (2019).

[64] T.D. Zaveri, J.S. Lewis, N.V. Dolgova, M.J. Clare-Salzler, B.G. Keselowsky, Integrin-directed modulation of macrophage responses to biomaterials, Biomaterials 35(11) (2014) 3504-3515.

[65] C.D. Reyes, A.J. García, α2β1 integrin-specific collagen-mimetic surfaces supporting osteoblastic differentiation, Journal of Biomedical Materials Research Part A 69A(4) (2004) 591-600.

[66] I. Boraschi-Diaz, J. Wang, J.S. Mort, S.V. Komarova, Collagen Type I as a Ligand for Receptor-Mediated Signaling, Front Phys-Lausanne 5 (2017).

[67] Z.H. Zhou, C.D. Ji, H.L. Xiao, H.B. Zhao, Y.H. Cui, X.W. Bian, Reorganized Collagen in the Tumor Microenvironment of Gastric Cancer and Its Association with Prognosis, J Cancer 8(8) (2017) 1466-1476.

[68] J. Helft, J. Bottcher, P. Chakravarty, S. Zelenay, J. Huotari, B.U. Schraml, D. Goubau, C. Reis e Sousa, GM-CSF Mouse Bone Marrow Cultures Comprise a Heterogeneous Population of CD11c(+)MHCII(+) Macrophages and Dendritic Cells, Immunity 42(6) (2015) 1197-211.

[69] K. Inaba, M. Inaba, N. Romani, H. Aya, M. Deguchi, S. Ikehara, S. Muramatsu, R.M. Steinman, Generation of Large Numbers of Dendritic Cells from Mouse Bone-Marrow Cultures Supplemented with Granulocyte Macrophage Colony-Stimulating Factor, J Exp Med 176(6) (1992) 1693-1702.

[70] Q. Cao, Y. Wang, X.M. Wang, J. Lu, V.W. Lee, Q. Ye, H. Nguyen, G. Zheng, Y. Zhao, S.I. Alexander, D.C. Harris, Renal F4/80+ CD11c+ mononuclear phagocytes display phenotypic and functional characteristics of macrophages in health and in adriamycin nephropathy, J Am Soc Nephrol 26(2) (2015) 349-63.

[71] A. Dos Anjos Cassado, F4/80 as a Major Macrophage Marker: The Case of the Peritoneum and Spleen, Results Probl Cell Differ 62 (2017) 161-179.

[72] Y.K. Kim, S.H. Chu, J.Y. Hsieh, C.M. Kamoku, A.J. Tenner, W.F. Liu, S.W. Wang, Incorporation of a Ligand Peptide for Immune Inhibitory Receptor LAIR-1 on Biomaterial Surfaces Inhibits Macrophage Inflammatory Responses, Adv Healthc Mater 6(24) (2017).

[73] B. Poudel, H.H. Ki, Y.M. Lee, D.K. Kim, Collagen I-induced dendritic cells activation is regulated by TNF-alpha production through down-regulation of IRF4, J Biosciences 40(1) (2015) 71-78.

[74] B. Poudel, D.S. Yoon, J.H. Lee, Y.M. Lee, D.K. Kim, Collagen I enhances functional activities of human monocyte-derived dendritic cells via discoidin domain receptor 2, Cell Immunol 278(1-2) (2012) 95-102.

[75] J.E. Lee, C.S. Kang, X.Y. Guan, B.T. Kim, S.H. Kim, Y.M. Lee, W.S. Moon, D.K. Kim, Discoidin domain receptor 2 is involved in the activation of bone marrow-derived dendritic cells caused by type I collagen, Biochem Bioph Res Co 352(1) (2007) 244-250.

[76] A.T. Rowley, V.S. Meli, N.J. Wu-Woods, E.Y. Chen, W.F. Liu, S.W. Wang, Effects of Surface-Bound Collagen-Mimetic Peptides on Macrophage Uptake and Immunomodulation, Front Bioeng Biotechnol 8 (2020) 747.

[77] X.Y. Sun, C. Xu, G. Wu, Q.S. Ye, C.N. Wang, Poly(Lactic-co-Glycolic Acid): Applications and Future Prospects for Periodontal Tissue Regeneration, Polymers-Basel 9(6) (2017).

[78] Z. Liu, W. Jiang, J. Nam, J.J. Moon, B.Y.S. Kim, Immunomodulating Nanomedicine for Cancer Therapy, Nano Lett 18(11) (2018) 6655-6659.

[79] H.M. Abdelaziz, M. Gaber, M.M. Abd-Elwakil, M.T. Mabrouk, M.M. Elgohary, N.M. Kamel, D.M. Kabary, M.S. Freag, M.W. Samaha, S.M. Mortada, K.A. Elkhodairy, J.Y. Fang, A.O. Elzoghby, Inhalable particulate drug delivery systems for lung cancer therapy: Nanoparticles, microparticles, nanocomposites and nanoaggregates, J Control Release 269 (2018) 374-392.

[80] C.Y. Wong, H. Al-Salami, C.R. Dass, Microparticles, microcapsules and microspheres: A review of recent developments and prospects for oral delivery of insulin, Int J Pharm 537(1-2) (2018) 223-244.

[81] K. Dua, V. Malyla, G. Singhvi, R. Wadhwa, R.V. Krishna, S.D. Shukla, M.D. Shastri, D.K. Chellappan, P.K. Maurya, S. Satija, M. Mehta, M. Gulati, N. Hansbro, T. Collet, R. Awasthi, G.

Gupta, A. Hsu, P.M. Hansbro, Increasing complexity and interactions of oxidative stress in chronic respiratory diseases: An emerging need for novel drug delivery systems, Chem Biol Interact 299 (2019) 168-178.

[82] D.J. McClements, Advances in nanoparticle and microparticle delivery systems for increasing the dispersibility, stability, and bioactivity of phytochemicals, Biotechnol Adv 38 (2020) 107287.

[83] Y. Yang, N. Bajaj, P. Xu, K. Ohn, M.D. Tsifansky, Y. Yeo, Development of highly porous large PLGA microparticles for pulmonary drug delivery, Biomaterials 30(10) (2009) 1947-1953.

[84] M. Yoshida, J.E. Babensee, Molecular aspects of microparticle phagocytosis by dendritic cells, Journal of Biomaterials Science, Polymer Edition 17(8) (2006) 893-907.

[85] Y.P. Jiao, F.Z. Cui, Surface modification of polyester biomaterials for tissue engineering, Biomed Mater 2(4) (2007) R24-R37.

[86] T.G. Kim, T.G. Park, Biomimicking extracellular matrix: Cell adhesive RGD peptide modified electrospun poly(D,L-lactic-Co-glycolic acid) nanofiber mesh, Tissue Eng 12(2) (2006) 221-233.

[87] N. Brandhonneur, F. Chevanne, V. Vie, B. Frisch, R. Primault, M.F. Le Potier, P. Le Corre, Specific and non-specific phagocytosis of ligand-grafted PLGA microspheres by macrophages, Eur J Pharm Sci 36(4-5) (2009) 474-485.

[88] D. Bobo, K.J. Robinson, J. Islam, K.J. Thurecht, S.R. Corrie, Nanoparticle-Based Medicines: A Review of FDA-Approved Materials and Clinical Trials to Date, Pharm Res 33(10) (2016) 2373-87.

[89] A.I. Skorobogatova, O.A. Terent'eva, V.A. Vainshtein, S.V. Okovityi, E.V. Flisyuk, I.A. Narkevich, Targeted Transport as a Promising Method of Drug Delivery to the Central Nervous System (Review), Pharmaceutical Chemistry Journal 53(9) (2019) 845-851.

[90] R. Nicolete, D.F. dos Santos, L.H. Faccioli, The uptake of PLGA micro or nanoparticles by macrophages provokes distinct in vitro inflammatory response, Int Immunopharmacol 11(10) (2011) 1557-1563.

[91] F. Yang, Y. He, Z. Zhai, E. Sun, Programmed Cell Death Pathways in the Pathogenesis of Systemic Lupus Erythematosus, J Immunol Res 2019 (2019) 3638562.

[92] J. Savill, Apoptosis in resolution of inflammation, J Leukocyte Biol 61(4) (1997) 375-380.

[93] V.A. Fadok, D.L. Bratton, A. Konowal, P.W. Freed, J.Y. Westcott, P.M. Henson, Macrophages that have ingested apoptotic cells in vitro inhibit proinflammatory cytokine production through autocrine/paracrine mechanisms involving TGF-beta, PGE2, and PAF, J Clin Invest 101(4) (1998) 890-898.

[94] X. Yi, J. Zhang, R. Zhuang, S. Wang, S. Cheng, D. Zhang, J. Xie, W. Hu, X. Liu, Y. Zhang, Y. Ding, Y. Zhang, Silencing LAIR-1 in human THP-1 macrophage increases foam cell formation by modulating PPARgamma and M2 polarization, Cytokine 111 (2018) 194-205.

[95] J. Herz, D.K. Strickland, LRP: a multifunctional scavenger and signaling receptor, J Clin Invest 108(6) (2001) 779-84.

[96] M. Lahti, J. Heino, J. Käpylä, Leukocyte integrins αLβ2, αMβ2 and αXβ2 as collagen receptors—Receptor activation and recognition of GFOGER motif, The International Journal of Biochemistry & Cell Biology 45(7) (2013) 1204-1211.

[97] B.T. Edelson, T.P. Stricker, Z. Li, S.K. Dickeson, V.L. Shepherd, S.A. Santoro, M.M. Zutter, Novel collectin/C1q receptor mediates mast cell activation and innate immunity, Blood 107(1) (2006) 143-50.

[98] S.L. Newman, M.A. Tucci, Regulation of human monocyte/macrophage function by extracellular matrix. Adherence of monocytes to collagen matrices enhances phagocytosis of opsonized bacteria by activation of complement receptors and enhancement of Fc receptor function., J Clin Invest 86(3) (1990) 703-714.

[99] Y. Yamada, T. Doi, T. Hamakubo, T. Kodama, Scavenger receptor family proteins: roles for atherosclerosis, host defence and disorders of the central nervous system, Cell Mol Life Sci 54(7) (1998) 628-640.

[100] V. Terpstra, N. Kondratenko, D. Steinberg, Macrophages lacking scavenger receptor A show a decrease in binding and uptake of acetylated low-density lipoprotein and of apoptotic thymocytes, but not of oxidatively damaged red blood cells, Proc Natl Acad Sci U S A 94(15) (1997) 8127-31.

[101] J.L.S. Milne, D. Shi, P.B. Rosenthal, J.S. Sunshine, G.J. Domingo, X.W. Wu, B.R. Brooks, R.N. Perham, R. Henderson, S. Subramaniam, Molecular architecture and mechanism of an icosahedral pyruvate dehydrogenase complex: a multifunctional catalytic machine, Embo J 21(21) (2002) 5587-5598.

[102] D. Ren, F. Kratz, S.W. Wang, Protein nanocapsules containing doxorubicin as a pH-responsive delivery system, Small 7(8) (2011) 1051-60.

[103] N.M. Molino, A.K.L. Anderson, E.L. Nelson, S.W. Wang, Biomimetic Protein Nanoparticles Facilitate Enhanced Dendritic Cell Activation and Cross-Presentation, Acs Nano 7(11) (2013) 9743-9752.

[104] N.M. Molino, M. Neek, J.A. Tucker, E.L. Nelson, S.W. Wang, Viral-mimicking protein nanoparticle vaccine for eliciting anti-tumor responses, Biomaterials 86 (2016) 83-91.

[105] M. Neek, T.I. Kim, S.W. Wang, Protein-based nanoparticles in cancer vaccine development, Nanomedicine-Uk 15(1) (2019) 164-174.

[106] M. Neek, J.A. Tucker, N. Butkovich, E.L. Nelson, S.W. Wang, An Antigen-Delivery Protein Nanoparticle Combined with Anti-PD-1 Checkpoint Inhibitor Has Curative Efficacy in an Aggressive Melanoma Model, Adv Ther (Weinh) 3(12) (2020).

[107] C. Wischke, H.H. Borchert, J. Zimmermann, I. Siebenbrodt, D.R. Lorenzen, Stable cationic microparticles for enhanced model antigen delivery to dendritic cells, J Control Release 114(3) (2006) 359-368.

[108] S. Jilek, H. Zurkaulen, J. Pavlovic, H.P. Merkle, E. Walter, Transfection of a mouse dendritic cell line by plasmid DNA-loaded PLGA microparticles in vitro, Eur J Pharm Biopharm 58(3) (2004) 491-499.

[109] S. Jhunjhunwala, G. Raimondi, A.W. Thomson, S.R. Little, Delivery of rapamycin to dendritic cells using degradable microparticles, J Control Release 133(3) (2009) 191-197.

[110] M.H. Liu, D.D. Feng, X.Y. Liang, M. Li, J. Yang, H. Wang, L.Y. Pang, Z.M. Zhou, Z.M. Yang, D.L. Kong, C. Li, Old Dog New Tricks: PLGA Microparticles as an Adjuvant for Insulin Peptide Fragment-Induced Immune Tolerance against Type 1 Diabetes, Molecular Pharmaceutics 17(9) (2020) 3513-3525.

[111] A.C. Doran, A. Yurdagul, I. Tabas, Efferocytosis in health and disease, Nat Rev Immunol 20(4) (2020) 254-267.

[112] A. Zhang, A. Lacy-Hulbert, S. Anderton, C. Haslett, J. Saville, Apoptotic Cell-Directed Resolution of Lung Inflammation Requires Myeloid alpha v Integrin-Mediated Induction of Regulatory T Lymphocytes, Am J Pathol 190(6) (2020) 1224-1235.

[113] K. Sehgal, K.M. Dhodapkar, M.V. Dhodapkar, Targeting human dendritic cells in situ to improve vaccines, Immunol Lett 162(1 Pt A) (2014) 59-67.

[114] L.J. Cruz, P.J. Tacken, F. Rueda, J.C. Domingo, F. Albericio, C.G. Figdor, Targeting nanoparticles to dendritic cells for immunotherapy, Methods Enzymol 509 (2012) 143-63.

[115] L.C. Bonifaz, D.P. Bonnyay, A. Charalambous, D.I. Darguste, S. Fujii, H. Soares, M.K. Brimnes, B. Moltedo, T.M. Moran, R.M. Steinman, In vivo targeting of antigens to maturing dendritic cells via the DEC-205 receptor improves T cell vaccination, J Exp Med 199(6) (2004) 815-24.

[116] E. Blanco, H. Shen, M. Ferrari, Principles of nanoparticle design for overcoming biological barriers to drug delivery, Nat Biotechnol 33(9) (2015) 941-51.

[117] J.A. Finbloom, F. Sousa, M.M. Stevens, T.A. Desai, Engineering the drug carrier biointerface to overcome biological barriers to drug delivery, Adv Drug Deliv Rev 167 (2020) 89-108.

[118] K. Sasaki, Y. Sato, K. Okuda, K. Iwakawa, H. Harashima, mRNA-Loaded Lipid Nanoparticles Targeting Dendritic Cells for Cancer Immunotherapy, Pharmaceutics 14(8) (2022).

[119] V.S. Meli, A. T. Rowley, P.K. Veerasubramanian, S.E. Heedy, A.F. Yee, W.F. Liu, and S-W Wang, Role of Substrate Stiffness and Collagen Interactions in Macrophage Immunomodulation, in preparations for Biomaterials Science., 2022

Appendix:

(A.1.0.1) Maleimide Well Surface Functionalization Protocol: Cysteine or CLLP was suspended in an endotoxin-free binding buffer (0.1 M sodium phosphate, 0.15 M sodium chloride, 10 mM EDTA; pH of 7.2) to facilitate thiol bonding to maleimide-activated clear 8-well strip plate (Pierce™) surfaces. Tris(2-carboxyethyl)phosphine (TCEP, 20 mM) in HEPES (50 mM) was added to achieve a final concentration of 2 mM (100x molar excess to the peptide) in order to prevent peptide-to-peptide disulfide bond formation. A final functionalization solution was made of 2 µM CLLP and 2 mM TCEP in binding buffer. The solution was allowed to react at room temperature for 20 minutes, added to wells at either 0.2 µM or 0.02 µM of CLLP, along with binding buffer stock to achieve a 100 µL total volume, and then allowed to react in the wells overnight at 4°C. The wells were then washed 3x with sterile PBS. Final amounts of CLLP reacted were 100 ng and 1 µg per well (or 1ug/mL and 10ug/ml respectively).

(**A.1.0.2) Triple Helical Structure of CLLP Confirmed by CD Scan:** Circular Dichroism Scan characterizing the triple helical suprastructure of CLLP, signal is normalized to the number of peptide bonds in CLLP, the X axis describes the wavelength of polarized light interacting with the peptide and the Y axis is a metric describing the extent of the elliptical nature of a structure derived from the absorbance value of the reflected polarized light.

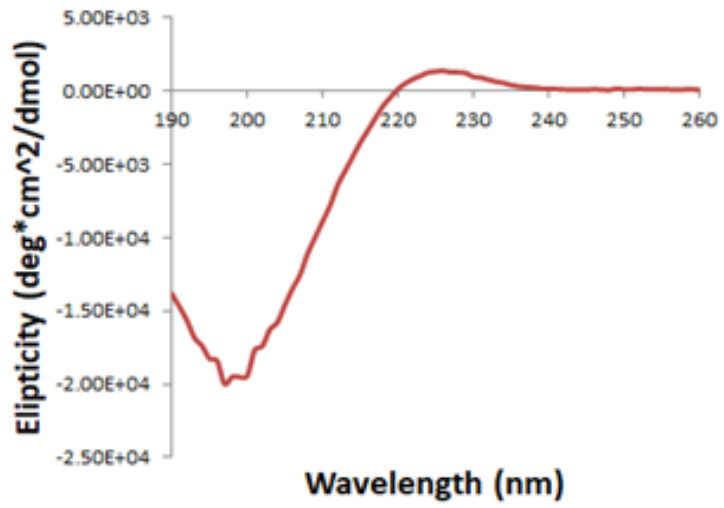

(A.1.0.3) <u>Determining Surface Saturation Using Biotinylated CLLP and Streptavidin-HRP</u>:

A CLLP peptide biotinylated at the C-terminus was used to quantify the extent of surface functionalization; streptavidin-horseradish peroxidase (HRP) was reacted in 100x molar excess of surface-conjugated CLLP for 1 hour, washed, and incubated with tetramethylbenzidine (TMB), and the absorbance was measured to quantify the CLLP surface concentration using a standard curve. Values reported are average ± S.E.M., with N=3 independent replicates, and the dots are individual data points. **Work done in collaboration with Dr. Esther Chen**

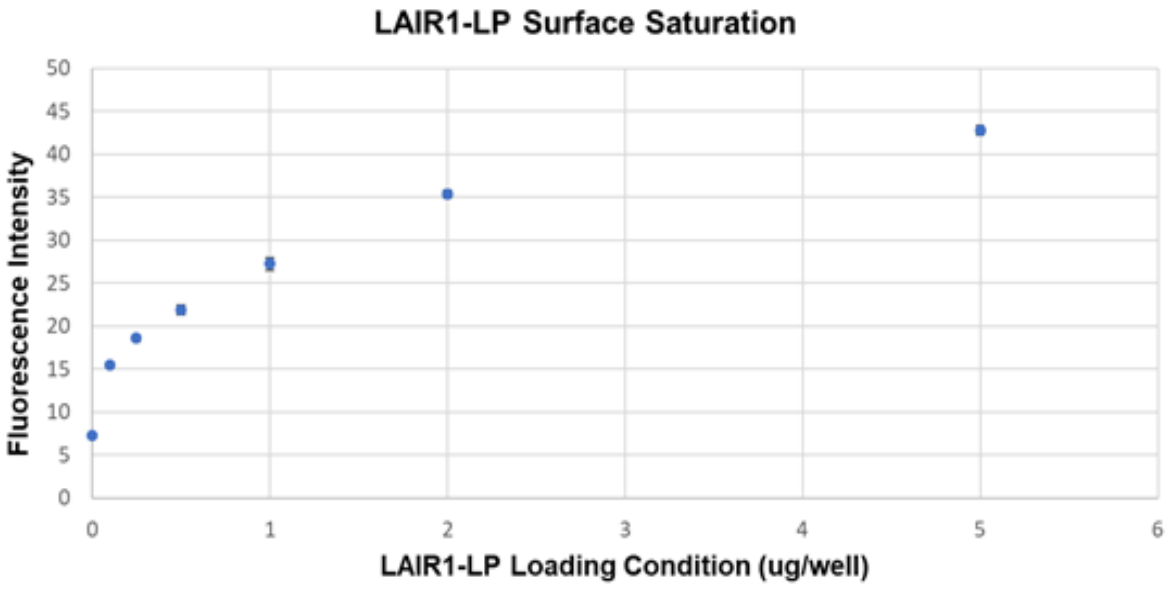

(A.1.0.4) <u>Confirming Surface Saturation of CLLP via Extent of TNFα Reduction</u>: Using TNFα as a metric to describe the extent of LPS induced activation of BMDMs seeded on control surfaces and CLLP surfaces, conjugated with different concentrations of CLLP in the initial functionalization reaction, the observed data provides evidence that functional surface saturation, in terms of inhibition, is reached at 1ug CLLP. Values reported are average ± S.E.M., with N=3 independent biological replicates, and the dots are individual data points. Statistical significance was determined by one-way ANOVA with Tukey's post hoc test (*p < 0.05, **p < 0.01, ***p < 0.001). **Work done in collaboration with Dr. Esther Chen**

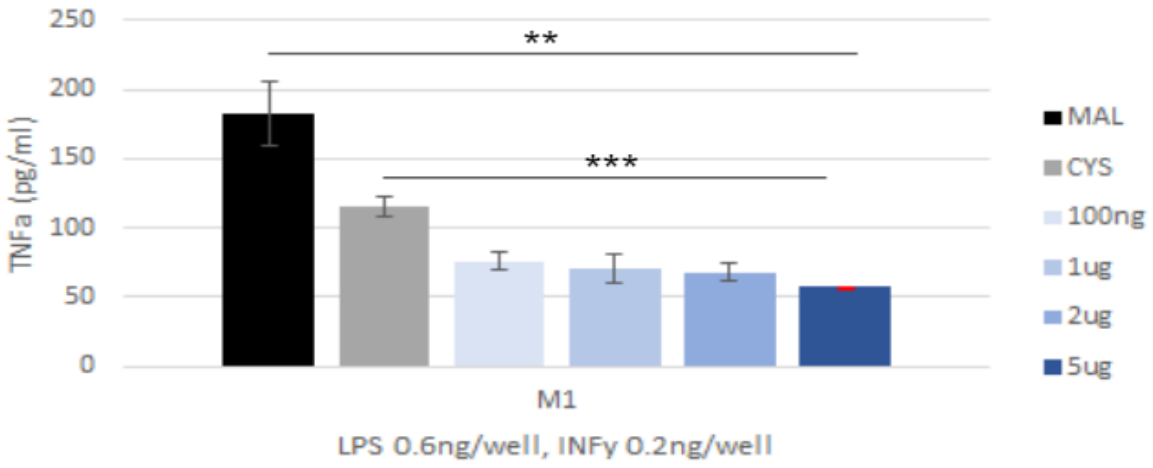

(A.1.0.5) <u>LPS Activation Study BMDM/DC Protocol</u>: Day 7 BMDM/DC culture cells were lifted from culture plates and seeded onto experimental surfaces (either CLLP functionalized, or cysteine functionalized or non-functionalized maleimide 96-well plates) in 100 µL of D-10 media for 12 hours. After the 12-hour seeding period BMDMs on experimental surfaces were either stimulated with 0.3 ng/mL LPS and 0.3 ng/mL IFNγ or equal volume of D-10 media (non-activated control group). BMDMs were then allowed to incubate with the stimulation solution

for 12 hours, before the supernatant was collected and cytokines were analyzed by ELISA and/or multiplex array analysis. BMDCs were stimulated with either 100 ng/mL LPS or equal volume BMDC media, allowed to incubate for 12 hours before being lifted, stained with fluorescently tagged antibodies and analyzed for inflammatory markers via flow cytometry. **Work done in collaboration with Dr. Esther Chen**

(A.1.0.6) <u>Bone Marrow Monocyte Culture & Differentiation Protocol</u>: All procedures requiring animal tissues were carried out in accordance with protocols approved by the Institutional Animal Care and Use Committee (IACUC) at the University of California, Irvine. Femurs were harvested from C57BL/6J mice (Jackson Laboratory), and bone marrow from each bone was flushed with either sterile PBS or sterile Dulbecco's Modified Eagle's medium (DMEM) supplemented with 10% heat-inactivated fetal bovine serum (FBS) and then centrifuged to pellet cells. The cell pellet was resuspended in ammonium-chloride-potassium (ACK) lysis buffer (Thermo Fisher) to lyse red blood cells, centrifuged, and then resuspended and cultured either in D-10 macrophage media or DC growth media. D-10 macrophage media consists of high-glucose DMEM supplemented with 10% heat-inactivated FBS, 2 mM L-glutamine, 100 U/ml penicillin, 100 µg/ml streptomycin (Thermo Fisher), and 10% conditioned media from CMG 14–12 cell expressing recombinant mouse macrophage colony stimulating factor (M-CSF). Cells were cultured for 7 days on non-tissue culture treated polystyrene plates, in 10 mL of D-10 macrophage media (media replaced on day 3 and day 6) to induce differentiation to bone marrow derived macrophages (BMDMs). DC growth media is composed of Corning™ RPMI 1640 Medium (Mod.) 1X without L-Glutamine supplemented with, 10% heat-inactivated FBS, 2 mM L-glutamine (Corning™), 100 U/ml penicillin, 100 µg/ml streptomycin (Thermo Fisher), 1 mM sodium pyruvate (HyClone™), 1x NEAA (Lonza™

BioWhittaker™ MEM Eagle Nonessential Amino Acid Solution 100X), 50 microMolar 2β-Mercaptoethanol. In order to differentiate BMDCs, cells were cultured on non-tissue culture treated polystyrene plates, in 10 mL of DC growth media for 7-8 days (media replaced on day 3 and 6) and were stimulated with 20 ng/ml of GM-CSF on days 0, 3 and 6. For all experiments BMDMs and/or BMDCs were lifted from culture plates and allowed to seed on CLLP functionalized well surfaces for at least 12 hours before beginning any experiments.

(A.1.1.0) <u>LAIR-1 Knock Down BMDM/DC Protocol:</u> Briefly, $0.5x10^6$ freshly isolated day 6 BMDMs/DCs were transfected with 100 nM of LAIR-1 siRNA or non-target siRNA in 20 µl of nucleofection solution. After nucleofection, cells were recovered in respective cell media and seeded on both 1 µg CLLP surfaces and maleimide control surfaces for 36 hours, to ensure sufficient knockdown, before beginning the stimulation steps of experiments as described in this appendix. **Work done in collaboration with Dr. Vijaykumar Meli**

(A.1.1.1) <u>Determining Gene Expression Protocol</u>: Cells were lysed directly on the culture dish using TRI Reagent, and chloroform was added to the lysate. The samples were vortexed vigorously for 15 sec and allowed to stand at RT for 10 min. Then, the mixture was centrifuged at 12,000 g for 15 min at 4°C. The upper aqueous phase that contains RNA was separated carefully to a new tube and 0.5 ml of 2-propanol per ml of TRI Reagent used was added. Then the samples were allowed to stand at RT for 10 min and further centrifuged at 12,000 g for 10 min at 4°C. The RNA pellet was washed with 1 ml of 75% ethanol per 1 ml of TRI Reagent used in sample preparation. The pellet was briefly air-dried, and the RNA was dissolved in DEPC-treated water. The cDNA was made using High-Capacity cDNA Reverse Transcription Kit (Applied Biosystems). 1 µg of total RNA was used to synthesize cDNA using random primers provided in the kit following the manufacturer's protocol. Once the cDNA was made, it was

diluted 10 times with ultrapure water and used for qPCR. Quantabio's PerfeCTa SYBR Green FastMix was used for real-time PCR. Briefly, for every 25 ul reaction, 12.5 µl of the PerfecCTa SYBR Green Fastmix, 2 µl of diluted cDNA and 1 µl (500 nM) of each forward and reverse primers and 8.5 µl of ultrapure water was used. A total of 40 cycles were performed on Bio-Rad's CFX-96 real-time PCR system. Further the relative gene expression was analyzed by 2-ΔΔCT method (Livak and Schmittgen, 2001). **Work done in collaboration with Dr. Vijaykumar Meli**

(A.1.1.2) <u>Effects of Seeding Surface on LAIR-1 Expression in Different BMDM Phenotypes</u>: Gene expression data depicting the effects of experimental and control surfaces on LAIR-1 expression in the three predetermined phenotypes (The three BMDM phenotypes are described here as; M0 meaning no stimulation, M1 meaning 0.1 ng/mL LPS and 0.3 ng/mL IFNy, and M2 meaning 3 ng/mL of IL-4/-13). Data is normalized to unstimulated BMDMs on each surface. Values reported are average ± S.E.M., with N≥3 independent biological replicates, and the dots are individual data points. Statistical significance was determined by one-way ANOVA with Tukey's post hoc test (*p < 0.05, **p < 0.01, ***p < 0.001) **Work done in collaboration with Dr. Vijaykumar Meli**

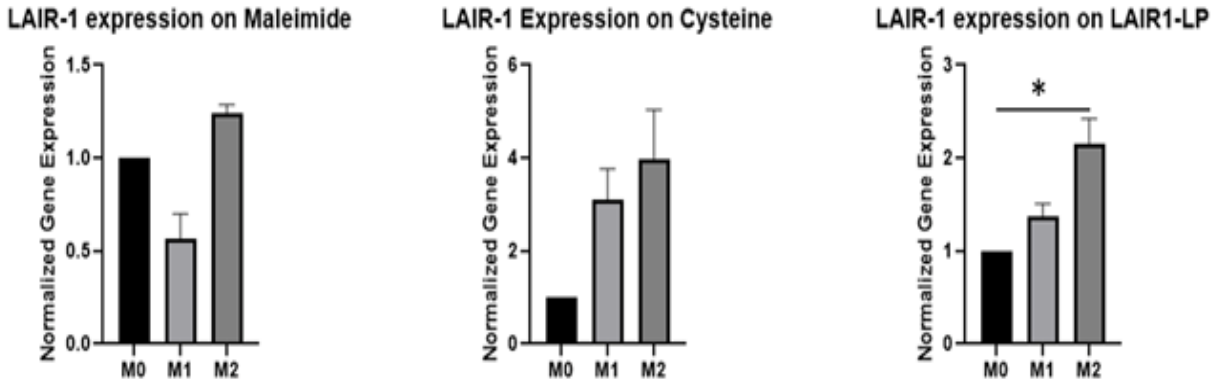

(A.1.1.3) <u>Extent of LAIR-1 KD in BMDMs</u>: Gene expression displaying the extent of LAIR-1 knockdown. Values reported are average ± S.E.M., with N=4 independent biological replicates, and the dots are individual data points. Statistical significance was determined by one-way ANOVA with Tukey's post hoc test (*p < 0.05, **p < 0.01, ***p < 0.001). **Work done in collaboration with Dr. Vijaykumar Meli**

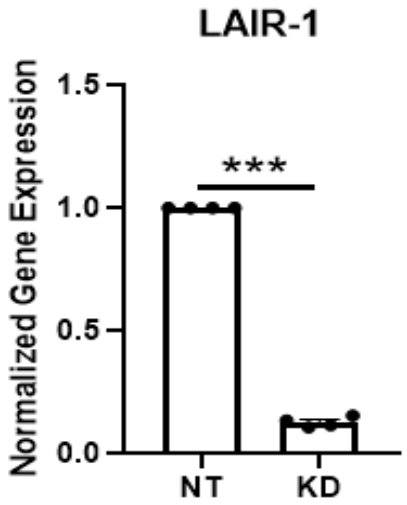

(A.1.2.0) <u>Extent of LAIR-1 KD in BMDCs</u>: Representative data of the extent of LAIR-1 KD analyzed via fluorescently tagged LAIR-1 antibodies and Flow cytometry. Cell Only controls refer to cells without the LAIR-1 antibody stain. Significant reduction of average LAIR-1 expression in BMDCs was observed after 36 hours incubation with siRNA.

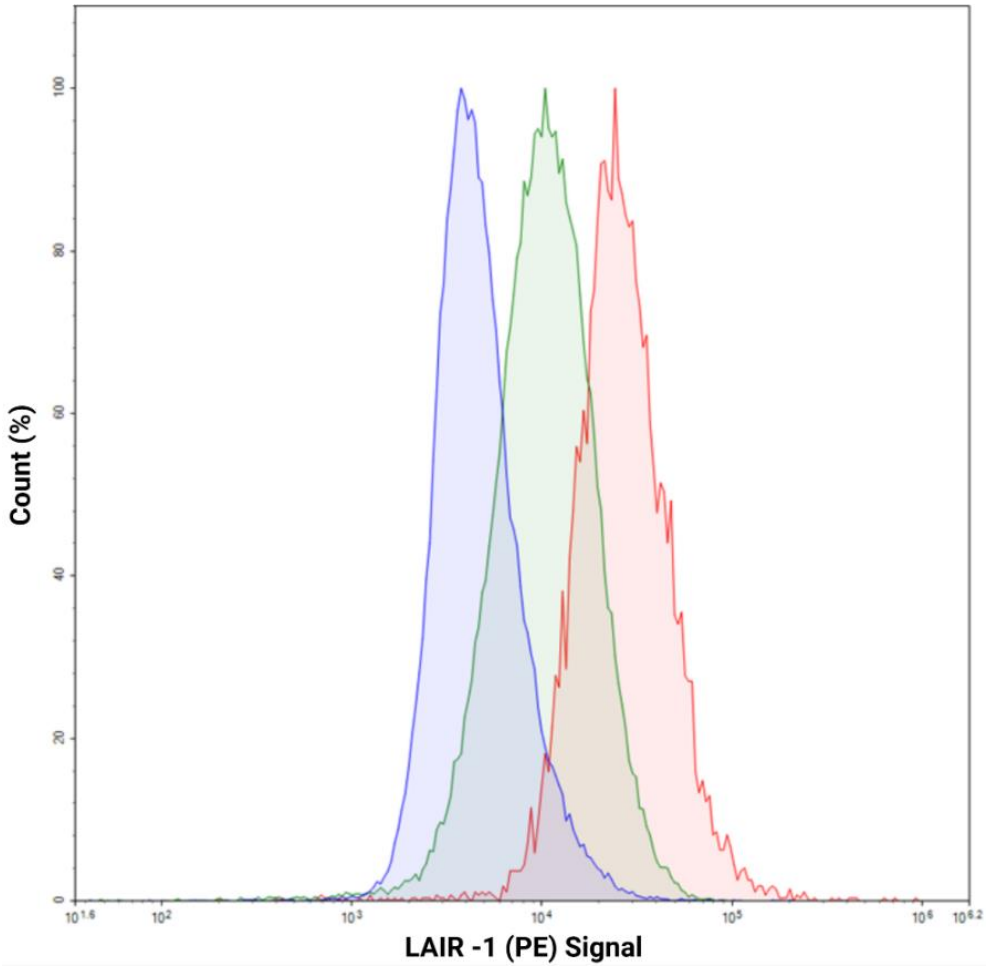

(A.2.1.0) <u>PLGA Microparticle Synthesis Protocol</u>: 20 mg of PLGA (Resomer RG 504H, Poly(D,L-lactide-co-glycolide), and 20 µL BODIPY (1 mg/mL) were dissolved in 1 mL DMC (dimethyl chloride). Mixture was vortexed and dropwise precipitated into 30 mL 1% PVA (poly(vinyl alcohol), 87-90% hydrolyzed, average MW 30,000-70,000). Solution was mixed using a point-arm sonicator at low speed for 5 minutes. PLGA was pelleted by spinning at 4200 rpm for 5 minutes. Particles were then vacuum filtered, washed with Milli-Q water, and then filtered using 1 µm and 10 µm sieves to achieve particles with 1-10 µm diameter. After pelleting, particles were stored dry at 4°C for use the next day.

(A.2.1.1) <u>BMDM PLGA Microparticle Uptake Study Protocol:</u> Day 7 BMDMs were seeded in 96-well maleimide surfaces and surfaces functionalized with cysteine or LAIR1-LP as described above for 12 h, and then incubated with stimulation solution and PLGA MPs (150,000 particles/well) for an additional 12 h. Final concentrations of stimulation solution per well were as follows: 0.08 ng/ml of LPS and 0.26 ng/ml IFNγ in D10 media (inflammatory M1 phenotype), or 2.6 ng/ml IL-4/13 in D10 media (resolution M2 phenotype), or unstimulated groups received only D10 media (naive M0 phenotype). After 12 h of incubation with the particles and cytokines, cell supernatant was removed for cytokine analysis via ELISA, wells were then washed with PBS, and BMDMs were lifted for flow cytometry analysis. Four replicate wells were combined for each condition for each n, and the experiment was repeated with cells from multiple mice, n ≥ 3. **Work done in collaboration with Natalie Wu-Woods**

(A.2.1.2) <u>PLGA Nanoparticle Synthesis Protocol</u>: 20 mg of PLGA (Resomer RG 504H, Poly(D,L-lactide-co-glycolide) and 20 µL BODIPY (1mg/mL) were dissolved in 1.33 mL of acetone and vortexed. 0.67 mL of methanol was immediately added to the solution and vortexed again. Mixture was dropwise precipitated into 18 mL of 5% Pluronic F-68 in MilliQ water (Gibco Pluronic F-68) with stirring on a stir plate for 2 h covered at room temperature. PLGA was pelleted by spinning at 14,000 rpm for 5 min. Particles were characterized using dynamic light scattering (DLS; Malvern Zetasizer ZS) and stored dry at 4°C for use the next day. **Work done in collaboration with Natalie Wu-Woods**

(A.2.1.3) <u>Size of PLGA NPs Determined via DLS</u>: Representative Dynamic Light Scattering analysis showing the distribution of PLGA NP diameter. The average PLGA NP diameter was determined to be 214 ± 51 nm with an average PDI of 0.035 (n = 4). **Work done in collaboration with Natalie Wu-Woods**

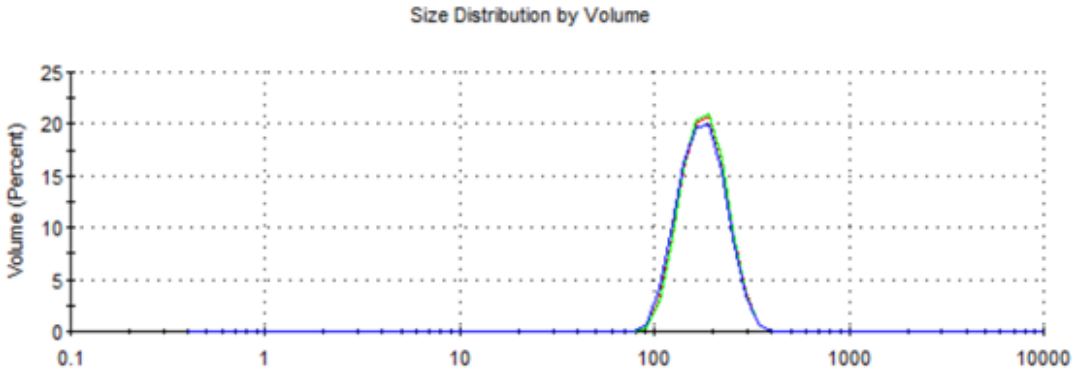

(A.2.1.4) <u>BMDM PLGA Nanoparticle Uptake Study Protocol:</u> Day 7Bone marrow derived macrophages were seeded in 96-well maleimide plates on various functionalized surfaces (maleimide, cysteine, and 100 ng or 1 μg CLLP surfaces) at ~30,000 cells/well for 12 h. Due to the rapid uptake of nanoparticles, co-stimulation with cytokines and nanoparticles was not possible. In order to assess the effects of CLLP on nanoparticle uptake of the various stimulated phenotypes, a pre-stimulation timeline was used. Cells were incubated with cytokines at the concentrations previously mentioned (A.2.1.1) for a 12-h incubation period before adding fluorescently dyed PLGA nanoparticles (approximately 250 nm in diameter) in excess. In order to add consistent NP concentration across experiments, NPs were pelleted, weighed and diluted to the same density, and then added at 0.001 mg/ml to each well. Uptake was allowed to occur for only 1 h, after which, cells were washed in PBS, lifted with scraping and analyzed by flow cytometry as previously described. Supernatant was again saved for cytokine analysis via

ELISA. Four replicate wells were combined for each condition for each N and the experiment was repeated with multiple mice (n = 3). **Work done in collaboration with Natalie Wu-Woods**

(A.2.1.5) <u>BMDM Particle Uptake Saturation:</u> Percentage of BMDMs exhibiting "saturated" uptake of PLGA MPs after a 12-hour incubation period (top) and NPs after a 1-hour incubation period (bottom). Saturated condition is defined as the percentage of unstimulated BMDMs exhibiting uptake on average is greater than 80% on all surfaces.

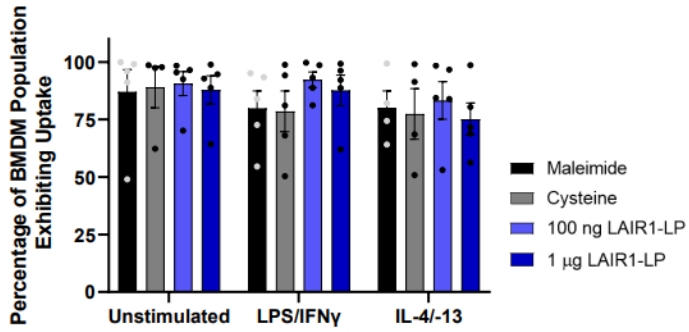

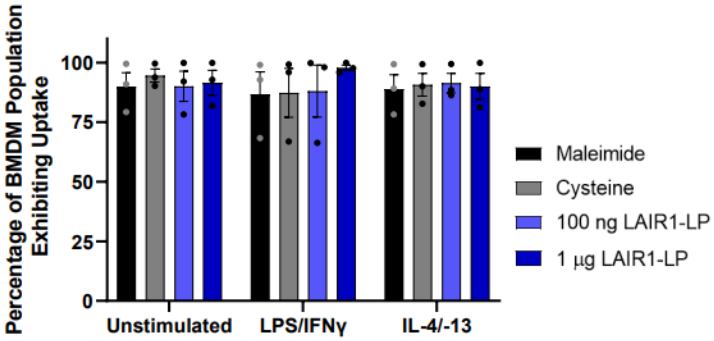

(A.2.1.6) <u>Induction of Apoptosis in 3T3 Fibroblasts Protocol</u>: Briefly, apoptotic 3T3 fibroblasts were derived as follows. NIH/3T3 (ATCC CRL-1658) mouse embryonic fibroblast line was first grown to confluence in DMEM complete media (10% FBS, +100 μg/ml (1%) penicillin/streptomycin/glutamine) on polystyrene tissue culture flasks. Fibroblast cells were then lifted, counted and 3 million 3T3 fibroblasts were dyed with DiO by incubating at 37°C for 30

minutes with DiO. Fluorescently dyed cells were then resuspended in 5 mL of fresh warmed DMEM complete and seeded on polystyrene cell culture dishes. An additional 5 mL of warmed DMEM complete was then added to the culture dish and cells were allowed to seed for 12 hours before being stimulated with 1 μg/ml ionomycin to induce apoptosis. Cells were incubated for an additional 12 hours with ionomycin, to ensure complete apoptosis, before being lifted, spun down and then resuspended in 1 mL of warmed D10. **Work done in collaboration with Dr. Raji Nagalla**

(A.2.1.7) BMDM Apoptotic Cell Uptake Study Protocol: Bone marrow derived macrophages were seeded onto experimental surfaces (maleimide, cysteine, as well as unsaturated and saturated LAIR1-LP surfaces) at ~30,000 BMDMs/well as previously discussed. BMDMs were seeded for 12 h, and cells were stimulated with their respective stimulation solutions as previously mentioned (A.2.1.1) and incubated for an additional 12 h. Apoptotic 3T3s were seeded for 12 h, lifted, and resuspended thoroughly in D10 media at a concentration of ~3 million cells/ml (based on seeding density). BMDMs were co-incubated with ~35,0000 apoptotic 3T3 fibroblasts and allowed to incubate for 1 h before being washed with PBS and lifted for analysis by flow cytometry. TNFα in the supernatant was analyzed by ELISA. Four replicate wells were combined for each condition for each N and the experiment was independently repeated ($n \geq 3$ mice). For this experimental system apoptotic cells were not introduced in great excess since higher apoptotic cell to BMDM ratios caused aggregation and heterogeneous coverage of the surfaces.

(A.2.1.8) Trends at Unsaturated PLGA MP Uptake by BMDMs: The effects of CLLP on the uptake of PLGA MPs, both percent population exhibiting uptake and on average uptake per

BMDM, at **unsaturated conditions** (i.e. when unstimulated BMDMs exhibiting uptake on average is <80%).

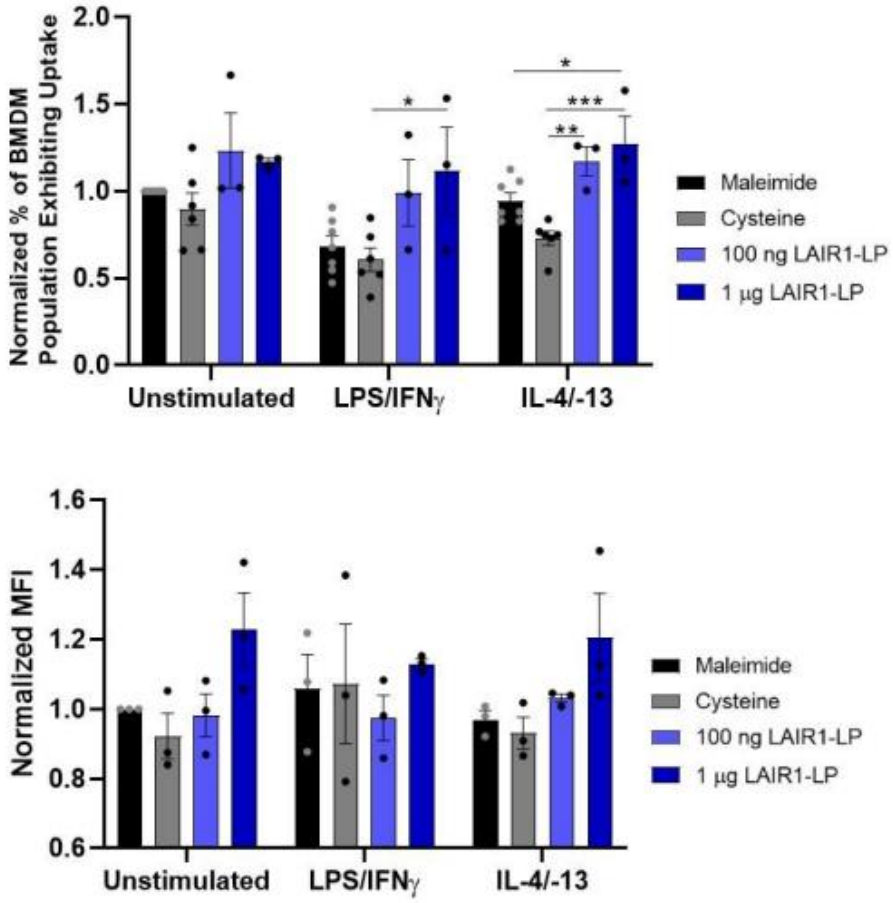

(A.2.2.0) **<u>BMDC E2 Nanoparticle Uptake Study Protocol:</u>** ~90,000 day 7 BMDCs per well were seeded on each experimental surface and incubated at 37°C and 5% CO2 for 12 hours. BMDCs were then stimulated with LPS at either 100 ng/mL or 0 ng/mL and allowed to incubate for another 12 hours. After incubation with the LPS, 0.05 μg of E2-AF448 nanoparticles were incubated with the cells for 20 minutes before experimental and control cells were lifted, washed, stained and analyzed via flow cytometry to determine the extent of uptake. 20 minutes of incubation was used due to the rapid clearance of E2 nanoparticles. Longer incubation periods

resulted in saturated uptake in all cell populations (A.2.2.4). Nonspecific staining with fluorescently tagged antibodies did not occur due to the rapid and complete internalization of E2 nanoparticles by BMDCs and the ease of separation of the remaining nanoparticles via centrifugation, allowing analysis of F4/80 subpopulations. Eight replicate wells were combined for each condition for each N and the experiment was repeated with multiple mice (N=3)

(A.2.2.1) <u>E2 AF488 Conjugation Protocol</u>: E2(D381C) was mixed with 8.5 molar equivalents of TCEP per E2(D381C) subunit for 1 h at room temperature to reduce the internal cysteines. 3 molar excess of Alexa Fluor 488 (AF488) per E2(D381C) was mixed with the reduced E2(D381C) for 2 h at room temperature, and 4 ºC overnight. Unreacted AF488 was removed with Zeba Spin Desalting Columns with 40K molecular weight cut-off (Thermo ScientificTM) to get the final product (E2-AF488). E2-AF488 nanoparticle size was then analyzed via dynamic light scattering (DLS, Malvern Zetasizer ZS) (A.2.2.2). E2-AF488 protein nanoparticles were also determined to be LPS free via LAL testing. **Work done in collaboration with Enya Li**

(A.2.2.2) <u>DLS of E2-AF488</u>: Dynamic Light Scattering data showing the average size of E2-AF488 after running 3 different reaction batches, post functionalization. The average of three E2-AF488 batches showed an average size of 36.5 nm and a PDI of 0.19.

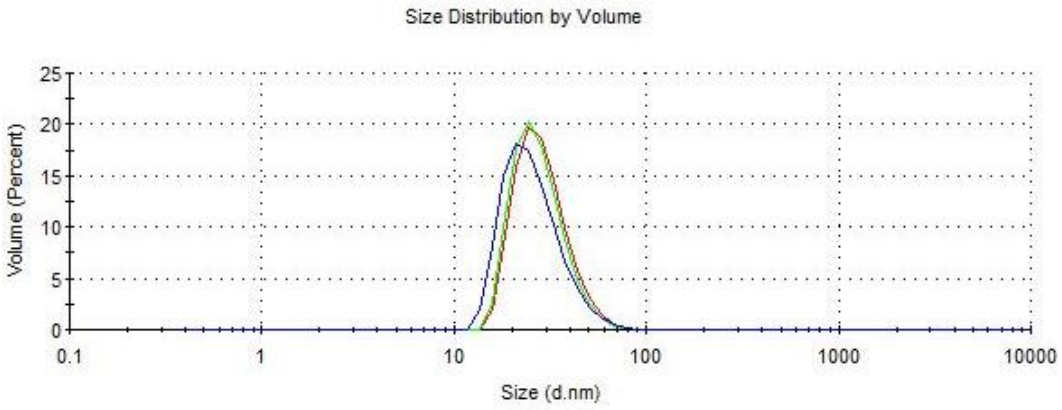

(A.2.2.3) <u>BMDC PLGA MP Uptake Study Protocol:</u> ~30,000 day 7 BMDCs per well were seeded on each experimental surface and incubated at 37°C and 5% CO2 for 12 hours. BMDCs were then stimulated with both fluorescently dyed PLGA MPs (Ratio 5:1, MPs:Cells) and LPS at either 100 ng/mL or 0 ng/mL and allowed to incubate for another 12 hours. Finally, experimental and control cells were lifted, washed, and analyzed via flow cytometry to determine the extent of uptake. Eight replicate wells were combined for each condition for each N and the experiment was repeated with multiple mice (N=3)

(A.2.2.4) <u>Saturated E2 Nanoparticle Uptake by BMDCs at 12 Hours:</u> BMDCs were seeded on control and experimental surfaces for 12 hours, then stimulated with both E2-AF488 and LPS, and further incubated for another 12 hours before being lifted and analyzed via flow cytometry. Normalized MFI ± SEM data describing average uptake of E2 NPs per cell for (A) F4/80+ BMDCs and (B) F4/80+ BMDCs

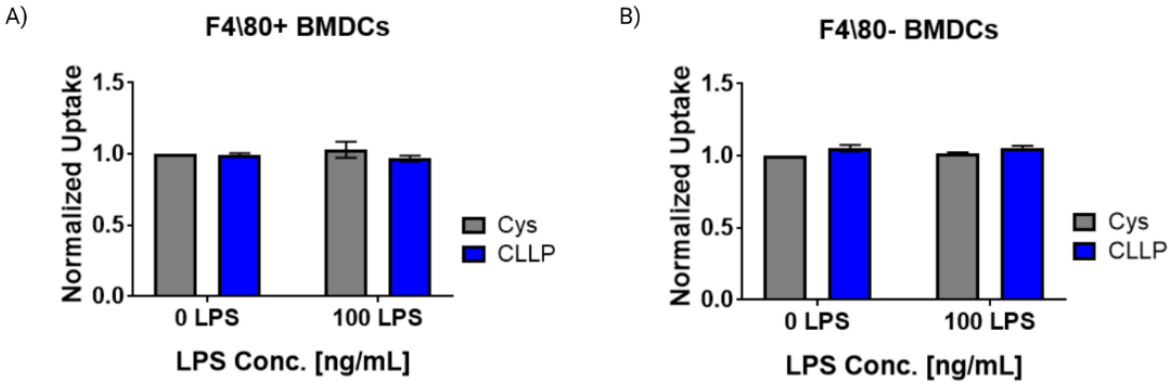

(A.2.2.5) <u>CLLP Surfaces Increase the Uptake of PLGA MPs by BMDCs & LAIR-1 Knockdown has No Observable effect on the CLLP Induced Increase in PLGA MP Uptake:</u> A) Experimental timeline of PLGA MP uptake studies using BMDCs with or without LPS stimulation on CLLP surfaces. B) Normalized MFI signal of fluorescently dyed PLGA MPs

taken up by BMDCs determined via flow cytometry. C) Experimental timeline used to investigate PLGA MP uptake by LAIR-1 knockdown BMDCs. D) Normalized MFI signal of fluorescently dyed PLGA MPs uptake by either LAIR-1 knockdown or non-target control BMDCs. Values reported are average ± S.E.M., with N = 3 independent biological replicates. Statistical significance was determined by two-way ANOVA with Bonferroni's post hoc test (*p < 0.05)

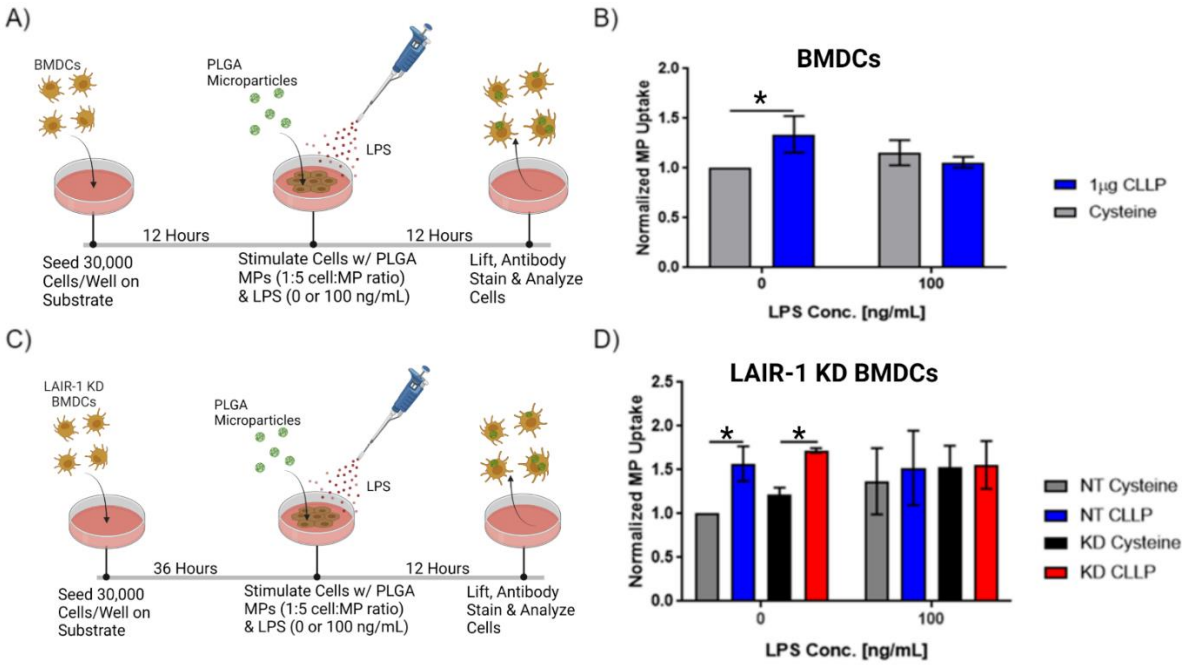

(A.2.2.6): <u>SIINFEKL conjugation to E2 Nanoparticle Protocol</u>: The E2 D381C protein was first incubated with sulfosuccinimidyl 4-(N-maleimidomethyl)cyclohexane-1-carboxylate (SMCC), at a 20-fold excess to the E2 protein monomer, for 30 min at room temperature. After 30 min incubation the unreacted linker was removed via desalting spin columns. SMCC-functionalized E2 was combined with a 10-fold excess (to E2 monomer) of the CSIINFEKL(Genemed Synthesis) (10x excess TCEP reduced) peptide for 2 h at RT. Excess peptide was removed by desalting spin columns. Efficiency of SIINFEKL conjugation to the E2

protein was assessed by SDS-PAGE and mass spectroscopy, while the final concentration of the E2-SIINFEKL nanoparticle was determined via BCA. Using the information obtained from both the BCA and the SDS-PAGE, the relative amount of E2-SIINFEKL needed to deliver the desired amount of SIINFEKL was determined. E2-SIINFEKL was determined to be LPS free via LAL testing. The final concentration of E2-SIINFEKL after functionalization was determined to be 1.09 mg/mL of 0.13 mg/mL (A.2.2.5). **Work done in collaboration with Aaron Ramirez**

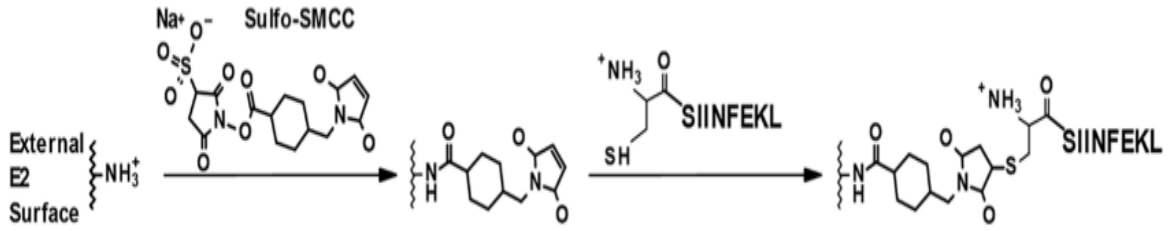

(A.2.2.7) **<u>Mass Spectroscopy of E2-SIINFEKL</u>**: Mass Spectroscopy analysis determining the relative efficiency of the SIINFEKL E2 conjugation reaction. The molecular weight of E2 is 28105, molecular weight of SMCC linker is 219 and the molecular weight of C-SIINFEKL was 1066. The peaks in the spectrum represent different combinations of E2 conjugated with various amounts of SMCC linker and SIINFEKL peptide. For example, the largest peak at 33716 represents E2 with 11 SMMC linkers and 3 SIINFEKL peptides conjugated. After analysis Mass spectroscopy indicated that the average amount of SIINFEKL peptide per E2 monomer was ~3.2, the final concentration of E2-SIINFEKL after functionalization was determined to be 1.09 mg/mL with a relative SIINFEKL concentration of 0.13 mg/mL. **Work done in collaboration with Aaron Ramirez**

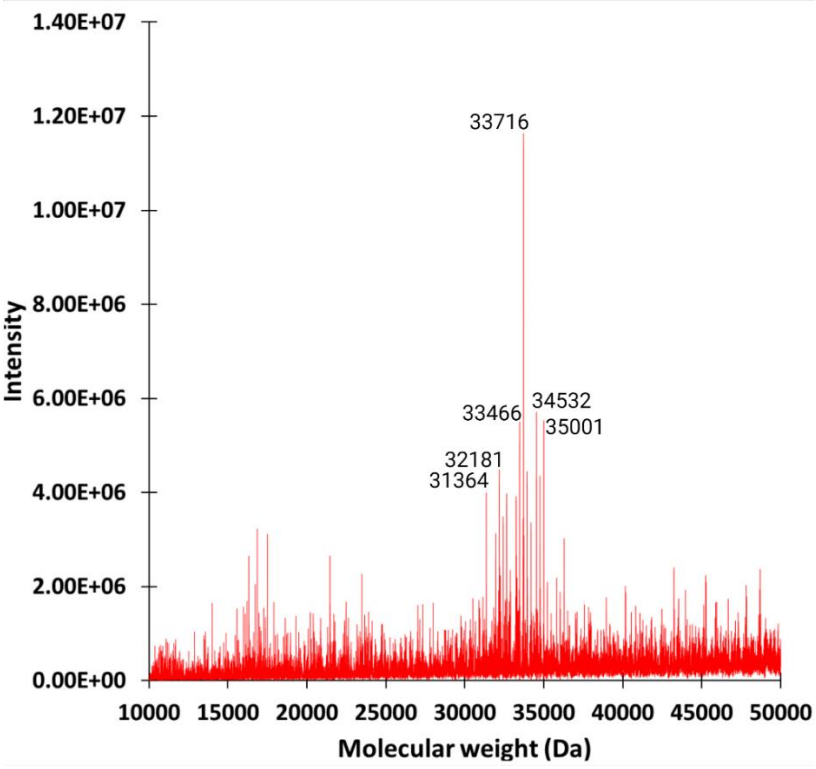

(A.2.2.8) **<u>Average Size of E2-SIINFEKL Determined by DLS</u>**: Dynamic Light Scattering data showing the average size of E2-SIINFEKL after running 3 different reaction batches, post functionalization. The average of three E2-SIINFEKL batches showed an average size of 50.2 nm and a PDI of 0.26. **Work done in collaboration with Aaron Ramirez**

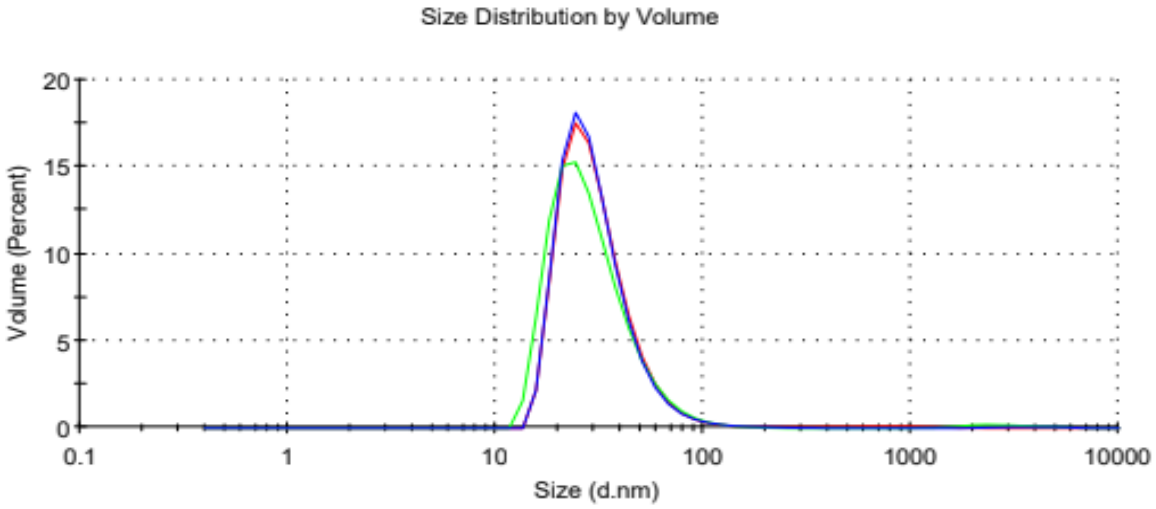

(A.2.2.9) <u>BMDCs E2-SIINFEKL Uptake & SIINFEKL Antigen Display Studies Protocols:</u>

~90,000 day 7 BMDCs per well were seeded on each experimental surface and incubated at 37°C and 5% CO2 for 12 hours. Then cells were stimulated with soluble or E2 functionalized with SIINFEKL (at either 0.05, 0.25, 1 µg/mL soluble SIINFEKL or ~0.065 µg/mL relative SIINFEKL delivered via E2) for each LPS stimulation condition (0, 100 ng/mL) for 18 hours. After incubating with the antigen for 18 hours, BMDCs were lifted and stained with both CD11c antibody (FITC) and MHC I presented SIINFEKL antibody in the context of H-2kb (APC), as well as, F4/80 (PE), and MHC II (PE-Cy7) antibodies. Extent of MHCI-SIINFEKL display by BMDCs was then analyzed using flow cytometry. Eight replicate wells were combined for each condition, for each N, and the experiment was repeated with multiple mice (N=4).

(A.2.2.10) <u>BMDCs Soluble SIINFEKL Display:</u> Normalized MFI ± SEM of SIINFEKL display on MHCI by (A) F480+ BMDCs and (B) F480- BMDCs when SIINFEKL is delivered in its soluble form to cells, on both CLLP and control surfaces. Extent of SIINFEKL display was determined by flow cytometry and a fluorescently labeled SIINFEKL-MHCI antibody. Values reported are average ± S.E.M., with N = 3 independent biological replicates. Statistical significance was determined by two-way ANOVA with Bonferroni's post hoc test (*$p < 0.05$, **$p < 0.01$)

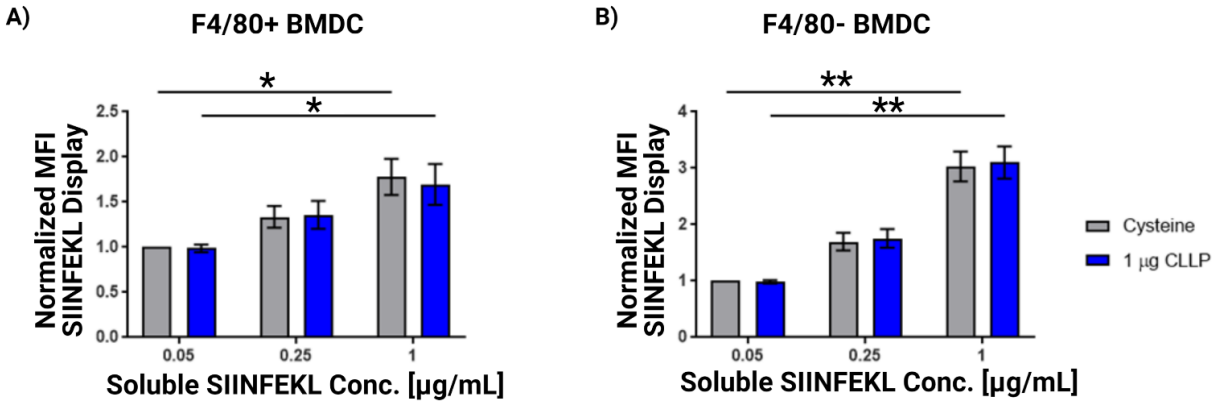

(A.3.1.0) <u>CLLP Conjugation to E2 Nanoparticle Protocol</u>: The E2-AF488 nanoparticle (A.2.2.1) was first incubated with sulfosuccinimidyl 4-(N-maleimidomethyl)cyclohexane-1-carboxylate (SMCC), at a 20-fold excess to the E2 protein monomer, for 30 min at room temperature. After 30 min incubation the unreacted linker was removed via desalting spin columns. SMCC-functionalized E2 was combined with a 5-fold excess (to E2 monomer) of the CLLP (Genemed Synthesis) (10x excess TCEP reduced) peptide for 2 h at RT and then overnight at 4°C. Excess peptide was removed by desalting spin columns. Efficiency of SIINFEKL conjugation to the E2 protein was assessed by SDS-PAGE (A.3.1.1) **Work done in collaboration with Enya Li**

(A.3.1.1) <u>CLLP-E2 SDS Page Gel:</u> The final conjugation efficiency of CLLP peptides to E2 subunits was determined via SDS page gel and densitometry. The efficiency of the functionalization reaction was determined to be 0.77 CLLP peptides per E2 subunit. **Work done in collaboration with Enya Li**

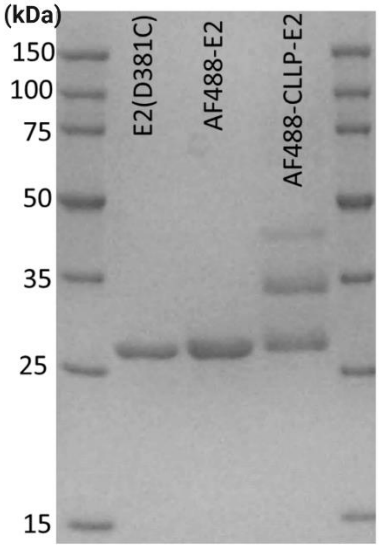

(A.3.1.2) <u>CLLP-E2 Dynamic Light Scattering:</u> Representative Dynamic Light Scattering analysis showing the distribution of CLLP-E2-AF488 diameter. The average CLLP-E2-AF488 diameter was determined to be 39.6 nm with an average PDI of 0.19 (n = 3). **Work done in collaboration with Enya Li**

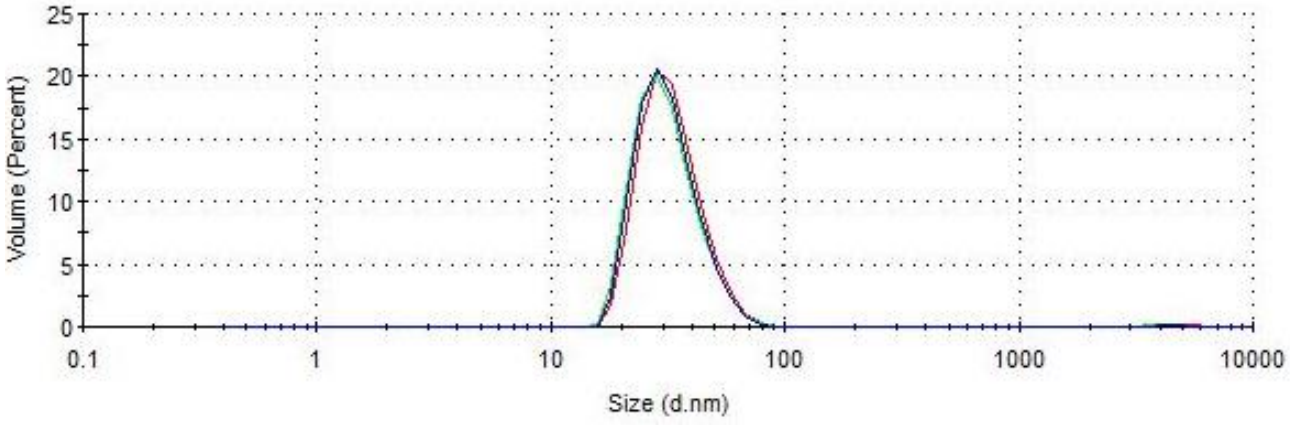

(A.3.1.3) <u>CLLP-E2 Uptake and Inhibition Studies Protocols</u>: ~90,000 day 7 BMDM/DCs per well were seeded on cysteine surfaces and incubated at 37°C and 5% CO2 for 12 hours. Then cells were stimulated with cytokine solutions (BMDMs)(A.2.1.1) or LPS stimulation condition (0, 100 ng/mL)(BMDCs) and either E2-AF488 or E2-AF488 functionalized with CLLP (at ~0.5 µg/mL) for 12 hours. After incubating for 12 hours, BMDM/DCs were lifted and analyzed via flow cytometry for extent of nanoparticle uptake. Supernatant from BMDM experiments was collected and analyzed for TNFα via ELISA. BMDCs were stained with both CD11c antibody (FITC) CD86 (APC), as well as, F4/80 (PE), and MHC II (PE-Cy7) antibodies and markers were analyzed via flow cytometry. Eight replicate wells were combined for each condition, for each N, and the experiment was repeated with multiple mice (N≥3).